

SYNTHESIS AND PRESUMPTIVE CROSSLINKING OF STIMULI-RESPONSIVE  
DIBLOCK POLYMER BRUSHES

A Dissertation

Presented to

The Graduate Faculty of The University of Akron

In Partial Fulfillment

of the Requirements for the Degree

Doctor of Philosophy

Brian Kenneth Mirous

May, 2006

SYNTHESIS AND PRESUMPTIVE CROSSLINKING OF STIMULI-RESPONSIVE  
DIBLOCK POLYMER BRUSHES

Brian Kenneth Mirous

Dissertation

Approved:

Accepted:

---

Advisor  
Dr. William J. Brittain

---

Department Chair  
Dr. Mark D. Foster

---

Committee Member  
Dr. Mark D. Foster

---

Dean of the College  
Dr. Frank N. Kelley

---

Committee Member  
Dr. Roderic P. Quirk

---

Dean of the Graduate School  
Dr. George R. Newkome

---

Committee Member  
Dr. Frank W. Harris

---

Date

---

Committee Member  
Dr. Michael J. Taschner

## ABSTRACT

The objective of this research was to create diblock polymer brushes containing a functional polymer as the bottom block and a polystyrene (PS) top block to obtain a “switchable surface” that displays a rearrangement into pinned micelles upon treatment with block selective solvents. The goal was also to crosslink these brushes to stabilize any changes in morphology and surface composition after rearrangement. Effectiveness of the presumed crosslinking was determined by further exposure of the brushes to solvent or thermal treatment.

Brushes of poly(*N,N*-dimethylaminoethyl methacrylate) (PDMAEMA) were prepared by an *in situ* surface-initiated polymerization from flat silicon substrates *via* atom transfer radical polymerization (ATRP). Reaction conditions were further optimized so that a sample could be removed from the polymerization solution, analyzed, and then subjected to a subsequent polymerization to prepare an additional PDMAEMA block of similar thickness, suggesting efficient re-initiation of chains. Styrene was polymerized from an optimized Si/SiO<sub>2</sub>//PDMAEMA brush to give a Si/SiO<sub>2</sub>//PDMAEMA-*b*-PS brush. This brush exhibited switching properties, as measured by water contact angles, when exposed to solvent or thermal treatment. No pinned micelles were observed; presumably the low glass transition temperature (19 °C) of the PDMAEMA prevented rough surface features at ambient temperature. Crosslinking was investigated by exposing the switched brush to an  $\alpha,\omega$ -dihaloalkane.

The presumptive crosslinking did not always make surface composition permanent, as evidenced by water contact angle changes upon further solvent or thermal treatment.

Similar experiments were done to prepare poly(2-hydroxyethyl methacrylate) (HEMA) and poly(glycidyl methacrylate) (PGMA) brushes. The brushes were extended with styrene to give Si/SiO<sub>2</sub>//PHEMA-*b*-PS and Si/SiO<sub>2</sub>//PGMA-*b*-PS brushes that again exhibited reversible switching properties. A pinned micelle morphology was not observed, and the surface roughness of the brushes in the extended and switched states was similar to that of Si/SiO<sub>2</sub>//PHEMA and Si/SiO<sub>2</sub>//PGMA homopolymer brushes. Crosslinking was investigated by exposing the switched Si/SiO<sub>2</sub>//PHEMA-*b*-PS and Si/SiO<sub>2</sub>//PGMA-*b*-PS brushes to a difunctional acyl chloride and multifunctional primary amines, respectively. In all cases the presumed crosslinking was relatively ineffective in preventing the brushes from further responding to solvent or thermal treatment, as measured by water contact angles.

## DEDICATION

To Mom and Dad:

Thank you for all your love and support—I couldn't have come this far without you.

## ACKNOWLEDGEMENTS

First and foremost, I would like to thank my advisor Dr. William Brittain for his advice and support—not only throughout the course of my graduate career, but during my two summers as an intern as well. Dr. B., it was through your encouragement that I made the decision to come to graduate school in the first place. I'd also like to thank all the group members that have taught and guided me along the way—especially postdoctoral associates Dr. Jude Rademacher, Dr. Stephen Boyes, and Dr. Neil Ayres. Thanks also go to Bulent Akgun and Stephanie Swearingen for performing AFM analysis.

I'd like to deeply thank Mom, Dad, and Elizabeth. Words cannot express how much I've always appreciated your love and support. To my amazing wife Heather who I met halfway through my time here in graduate school, thank you for brightening my days and for putting up with all my chemistry talk. GV, thanks for being there for me when I needed you most...I'll never forget our late night lab excursion. John, when grad school pushed me mentally, you went to the gym and pushed me physically. Thanks.

## TABLE OF CONTENTS

	Page
LIST OF TABLES.....	xi
LIST OF FIGURES.....	xiii
LIST OF SCHEMES.....	xv
CHAPTER	
I. INTRODUCTION.....	1
II. HISTORICAL BACKGROUND.....	7
2.1. Polymer Brushes.....	7
2.2. Preparation of Surface-Tethered Polymers.....	10
2.2.1. Physisorption Method.....	10
2.2.2. Covalent Attachment <i>via</i> “Grafting To”.....	13
2.2.3. Covalent Attachment <i>via</i> “Grafting From”.....	14
2.2.3.1. “Grafting From” Using Conventional Free Radical Polymerization.....	15
2.2.3.2. “Grafting From” Using Metathesis Polymerization.....	17
2.2.3.3. “Grafting From” Using Ionic Polymerization.....	18
2.2.3.4. “Grafting From” Using Controlled Radical Polymerization.....	19
2.3. Atom Transfer Radical Polymerization.....	26
2.3.1. General Background.....	26
2.3.2. Reaction Components.....	28

2.3.2.1. Monomers.....	28
2.3.2.2. Initiators.....	29
2.3.2.3. Transition Metal Catalysts.....	30
2.3.2.4. Ligands.....	31
2.3.2.5. Solvents.....	33
2.3.3. Surface-Initiated ATRP.....	33
III. EXPERIMENTAL.....	36
3.1. Materials.....	36
3.2. Characterization Methods.....	38
3.3. Synthesis and Preparation of Reagents.....	39
3.3.1. Initiator Synthesis.....	39
3.3.2. Purification of Copper Halides.....	40
3.3.3. Ligand Synthesis.....	41
3.4. Substrate Preparation.....	42
3.5. Surface Immobilization of Trichlorosilane ATRP Initiator.....	42
3.6. Synthesis of Block Copolymer Brushes <i>via</i> Surface-Initiated ATRP.....	43
3.6.1. Preparation of Si/SiO <sub>2</sub> //PDMAEMA Brushes.....	43
3.6.2. Preparation of Si/SiO <sub>2</sub> //PHEMA Brushes.....	44
3.6.3. Preparation of Si/SiO <sub>2</sub> //PGMA Brushes.....	45
3.6.4. Preparation of Si/SiO <sub>2</sub> //PS Brushes.....	46
3.6.5. Preparation of PS from Si/SiO <sub>2</sub> //PDMAEMA and Si/SiO <sub>2</sub> //PHEMA Brushes.....	46
3.6.6. Preparation of PS from Si/SiO <sub>2</sub> //PGMA Brushes.....	47

3.6.7. Preparation of PDMAEA from Si/SiO <sub>2</sub> //PS Brushes.....	48
3.7. Surface Rearrangement and Presumptive Crosslinking of Diblock Copolymer Brushes.....	49
3.7.1. Si/SiO <sub>2</sub> //PDMAEMA- <i>b</i> -PS.....	49
3.7.2. Si/SiO <sub>2</sub> //PS- <i>b</i> -PDMAEA.....	50
3.7.3. Si/SiO <sub>2</sub> //PHEMA- <i>b</i> -PS.....	50
3.7.4. Si/SiO <sub>2</sub> //PGMA- <i>b</i> -PS.....	51
IV. RESULTS AND DISCUSSION.....	52
4.1. Synthesis and Characterization of ATRP Initiator.....	52
4.2. Synthesis and Presumptive Crosslinking of Si/SiO <sub>2</sub> //PDMAEMA- <i>b</i> -PS.....	55
4.2.1. Si/SiO <sub>2</sub> //PDMAEMA Brushes <i>via</i> ATRP.....	55
4.2.2. Sequential Extension of Si/SiO <sub>2</sub> //PDMAEMA Brushes.....	57
4.2.3. Preparation of Si/SiO <sub>2</sub> //PDMAEMA- <i>b</i> -PS.....	61
4.2.4. Surface Rearrangement of Si/SiO <sub>2</sub> //PDMAEMA- <i>b</i> -PS.....	65
4.2.5. Presumptive Crosslinking of Si/SiO <sub>2</sub> //PDMAEMA- <i>b</i> -PS.....	71
4.3. Synthesis and Presumptive Crosslinking of Si/SiO <sub>2</sub> //PS- <i>b</i> -PDMAEA.....	75
4.3.1. Si/SiO <sub>2</sub> //PS- <i>b</i> -PDMAEA Brushes <i>via</i> ATRP.....	76
4.3.2. Surface Rearrangement and Presumptive Crosslinking of Si/SiO <sub>2</sub> //PS- <i>b</i> -PDMAEA.....	77
4.4. Synthesis and Presumptive Crosslinking of Si/SiO <sub>2</sub> //PHEMA- <i>b</i> -PS.....	80
4.4.1. Si/SiO <sub>2</sub> //PHEMA Brushes <i>via</i> ATRP.....	80
4.4.2. Sequential Extension of Si/SiO <sub>2</sub> //PHEMA Brushes.....	81
4.4.3. Preparation of Si/SiO <sub>2</sub> //PHEMA- <i>b</i> -PS.....	83
4.4.4. Surface Rearrangement of Si/SiO <sub>2</sub> //PHEMA- <i>b</i> -PS.....	86

4.4.5. Surface Modification of Si/SiO <sub>2</sub> //PHEMA.....	89
4.4.6. Presumptive Crosslinking of Si/SiO <sub>2</sub> //PHEMA- <i>b</i> -PS.....	95
4.5. Synthesis and Presumptive Crosslinking of Si/SiO <sub>2</sub> //PGMA- <i>b</i> -PS.....	96
4.5.1. Si/SiO <sub>2</sub> //PGMA Brushes <i>via</i> ATRP.....	96
4.5.2. Sequential Extension of Si/SiO <sub>2</sub> //PGMA Brushes.....	97
4.5.3. Preparation of Si/SiO <sub>2</sub> //PGMA- <i>b</i> -PS.....	99
4.5.4. Surface Rearrangement of Si/SiO <sub>2</sub> //PGMA- <i>b</i> -PS.....	101
4.5.5. Presumptive Crosslinking of Si/SiO <sub>2</sub> //PGMA and Si/SiO <sub>2</sub> //PGMA- <i>b</i> -PS.....	102
V. SUMMARY AND CONCLUSIONS.....	107
REFERENCES.....	111
APPENDIX.....	119

## LIST OF TABLES

Table	Page
4.1. Ellipsometric Measurements of Si/SiO <sub>2</sub> //PDMAEMA Brush Extension With Additional DMAEMA Monomer ( $\pm 0.5$ nm).....	60
4.2. Thickness of PS Extension from Si/SiO <sub>2</sub> //PDMAEMA ( $\pm 0.5$ nm).....	64
4.3. Solution GPC Data for Si/SiO <sub>2</sub> //PDMAEMA- <i>b</i> -PS Brush Synthesis.....	65
4.4. Surface Rearrangement of Si/SiO <sub>2</sub> //PDMAEMA- <i>b</i> -PS ( $\theta = \pm 3^\circ$ ).....	66
4.5. Presumptive Crosslinking of Si/SiO <sub>2</sub> //PDMAEMA- <i>b</i> -PS ( $\theta = \pm 3^\circ$ ).....	74
4.6. Solution GPC Data for Si/SiO <sub>2</sub> //PS- <i>b</i> -PDMAEA Brush Synthesis.....	77
4.7. Rearrangement and Presumptive Crosslinking of Si/SiO <sub>2</sub> //PS- <i>b</i> -PDMAEA ( $\theta = \pm 3^\circ$ ).....	79
4.8. Ellipsometric Measurements of Si/SiO <sub>2</sub> //PHEMA Brush Extension With Additional HEMA Monomer ( $\pm 0.5$ nm).....	82
4.9. Thickness of PS Extension from Si/SiO <sub>2</sub> //PHEMA ( $\pm 0.5$ nm).....	84
4.10. Solution GPC Data for Si/SiO <sub>2</sub> //PHEMA- <i>b</i> -PS Brush Synthesis.....	84
4.11. Surface Rearrangement of Si/SiO <sub>2</sub> //PHEMA- <i>b</i> -PS ( $\theta = \pm 3^\circ$ ).....	86
4.12. C-H Bond Stretching Intensities for Modified Si/SiO <sub>2</sub> //PHEMA.....	94
4.13. Presumptive Crosslinking of Si/SiO <sub>2</sub> //PHEMA- <i>b</i> -PS ( $\theta = \pm 3^\circ$ ).....	96
4.14. Ellipsometric Measurements of Si/SiO <sub>2</sub> //PGMA Brush Extension With Additional GMA Monomer ( $\pm 0.5$ nm).....	98
4.15. Surface Rearrangement of Si/SiO <sub>2</sub> //PGMA- <i>b</i> -PS ( $\theta = \pm 3^\circ$ ).....	101
4.16. Presumptive Crosslinking of Si/SiO <sub>2</sub> //PGMA- <i>b</i> -PS ( $\theta = \pm 3^\circ$ ).....	104

4.17. Presumptive Crosslinking of Si/SiO<sub>2</sub>//PGMA-*b*-PS ( $\theta = \pm 3^\circ$ ).....106

## LIST OF FIGURES

Figure	Page
2.1. Examples of Polymer Brushes in Bulk or Solution.....	8
2.2. Surface Tethered Polymer Brushes.....	8
2.3. Covalent Grafting Methods.....	9
2.4. Physisorbed Polymer Brushes.....	12
2.5. Common ATRP Initiators.....	30
2.6. Commonly Used ATRP Ligands.....	32
2.7. Surface-Initiated Polymerization Setup.....	34
4.1. Some Reaction Products of Trichlorosilanes with Silicon Substrates.....	54
4.2. ATR-FTIR Spectrum of the Surface Immobilized ATRP Initiator.....	55
4.3. ATR-FTIR Spectrum of Si/SiO <sub>2</sub> //PDMAEMA.....	57
4.4. Block Extension.....	59
4.5. ATR-FTIR Spectrum of Si/SiO <sub>2</sub> //PDMAEMA Brush Extension.....	61
4.6. ATR-FTIR Spectrum of Si/SiO <sub>2</sub> //PDMAEMA- <i>b</i> -PS.....	63
4.7. AFM Images of Si/SiO <sub>2</sub> //PDMAEMA- <i>b</i> -PS After (a) Thermal Annealing and (b) Methanol Treatment.....	70
4.8. Proposed Crosslinking of Pinned Micelles.....	71
4.9. ATR-FTIR Spectrum of Si/SiO <sub>2</sub> //PDMAEMA- <i>b</i> -PS After Presumptive Crosslinking.....	73
4.10. Possible Crosslinker Reactions With a Polymer Brush.....	74

4.11. ATR-FTIR Spectrum of Si/SiO <sub>2</sub> //PS- <i>b</i> -PDMAEA After Presumptive Crosslinking.....	80
4.12. ATR-FTIR Spectrum of Si/SiO <sub>2</sub> //PHEMA- <i>b</i> -PS.....	85
4.13. AFM Images of Si/SiO <sub>2</sub> //PHEMA- <i>b</i> -PS After (a) Cyclohexane Treatment and (b) Methanol Treatment.....	89
4.14. ATR-FTIR Spectrum of Si/SiO <sub>2</sub> //PHEMA Reactions.....	91
4.15. Acyl Chlorides.....	93
4.16. ATR-FTIR Spectrum of Modified Si/SiO <sub>2</sub> //PHEMA.....	94
4.17. ATR-FTIR Spectrum of Si/SiO <sub>2</sub> //PGMA- <i>b</i> -PS Reactions.....	100
4.18. ATR-FTIR Spectrum of Si/SiO <sub>2</sub> //PGMA Reactions.....	102
4.19. ATR-FTIR Spectrum of Si/SiO <sub>2</sub> //PGMA- <i>b</i> -PS After Presumptive Crosslinking.....	105
4.20. Primary Amine Crosslinker Molecules.....	105
A.1. GPC Chromatogram of PDMAEMA Synthesized Using the CuBr Catalyst System.....	119
A.2. GPC Chromatogram of PDMAEMA Synthesized Using the CuCl/CuCl <sub>2</sub> Catalyst System.....	120
A.3. GPC Chromatogram of PDMAEA.....	121
A.4. GPC Chromatogram of PHEMA Synthesized Using the CuCl Catalyst System.....	122
A.5. GPC Chromatogram of PHEMA Synthesized Using the CuCl/CuCl <sub>2</sub> Catalyst System.....	123

## LIST OF SCHEMES

Scheme	Page
1.1. The Persistent Radical Effect.....	4
2.1. Azo Initiator Immobilization and Polymerization.....	16
2.2. General Schemes for CRP Methods.....	21
2.3. Proposed Surface Rearrangement Mechanism for Si/SiO <sub>2</sub> //PS- <i>b</i> -PMMA.....	24
2.4. Si/SiO <sub>2</sub> //PS- <i>b</i> -PMMA Brush Synthesis Using Reverse ATRP.....	25
2.5. General ATRA Scheme.....	27
2.6. General ATRP Scheme.....	28
4.1. Synthesis and Surface Immobilization of [11-(2-bromo-2-methyl)propionyloxy]undecyltrichlorosilane.....	53
4.2. Si/SiO <sub>2</sub> //PDMAEMA Brush Synthesis.....	55
4.3. Si/SiO <sub>2</sub> //PDMAEMA- <i>b</i> -PS Brush Synthesis.....	62
4.4. Si/SiO <sub>2</sub> //PS- <i>b</i> -PDMAEA Brush Synthesis.....	76
4.5. Si/SiO <sub>2</sub> //PHEMA Brush Synthesis.....	80
4.6. Si/SiO <sub>2</sub> //PHEMA- <i>b</i> -PS Brush Synthesis.....	83
4.7. Si/SiO <sub>2</sub> //PGMA Brush Synthesis.....	97
4.8. Si/SiO <sub>2</sub> //PGMA- <i>b</i> -PS Brush Synthesis.....	99

## CHAPTER I

### INTRODUCTION

Polymer brushes have generated interest due to their ability to alter the surface properties of materials. This has led to applications such as stabilization of colloidal suspensions,<sup>1</sup> lubrication of surfaces,<sup>2</sup> microcontact printing,<sup>3</sup> bioactive surfaces,<sup>4</sup> and chemical gating for smart materials.<sup>5,6</sup> A polymer brush is defined as an assembly of polymer chains which are tethered by one end to a surface or interface where the grafting density is high enough such that the chains are forced to stretch away from the tethering site to avoid segmental overlap.<sup>7,8</sup> Brushes are unique when compared to other surface grafted polymer systems in that the stretched conformations of the chains in a polymer brush are under equilibrium conditions. Two properties that result from these confined geometries are the linear correlation of brush height to degree of polymerization<sup>9</sup> and a possible change in glass transition temperature when compared to bulk polymer films.<sup>10</sup>

There are generally two techniques used to tether polymer chains to a solid substrate—physisorption or covalent attachment.<sup>11</sup> A physisorbed brush typically consists of a diblock copolymer where one block strongly adheres to the surface and the other block stretches away from the surface.<sup>12</sup> A drawback to physisorbed brushes is that they are thermally and solvolytically unstable due to the relatively weak van der Waals forces or hydrogen bonding that anchors them to the surface. Alternatively, polymers can be anchored to a surface through covalent attachment by the “grafting to” or “grafting

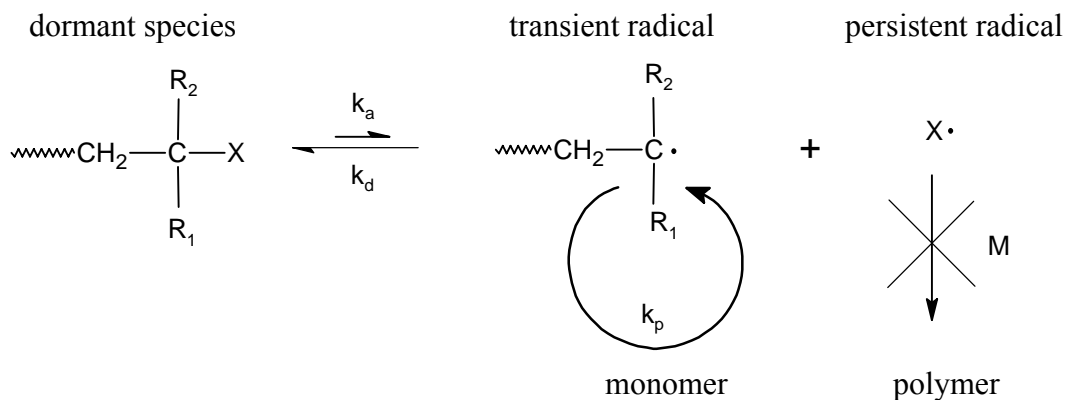
from” methods. In the “grafting to” method, pre-formed, end-functionalized chains are reacted with a chemically activated substrate to form a tethered polymer layer.<sup>13</sup> The covalent attachment makes the polymer layer relatively more thermally and solvolytically stable than physisorbed polymers. However, relatively low grafting densities are obtained because large polymer chains are not able to diffuse to reactive surface sites which are sterically hindered by surrounding grafted chains.

The “grafting from” approach creates covalently attached polymers with a higher grafting density. In the “grafting from” method, surface immobilized initiators are used to grow polymers *in situ* to generate a polymer brush.<sup>11</sup> Initiators have been introduced onto surfaces using plasma and glow-discharge treatment in the presence of a gas,<sup>6,14,15</sup> Langmuir-Blodgett film formation followed by chemical attachment,<sup>16</sup> or by the deposition of a self-assembled monolayer (SAM) containing surface anchoring groups.<sup>17</sup> Surface-initiated polymerization (SIP) from these immobilized initiators can then be used to grow polymer brushes.

A living polymerization is defined as a chain polymerization that proceeds without chain transfer or termination.<sup>18,19</sup> Living polymerization techniques can afford polymers with high levels of control over characteristics such as molecular weight, molecular weight distribution, chain architecture, chain end functionality, and copolymer composition. Because brush thickness is dependent on molecular weight, living SIP techniques may therefore be used to produce brushes with tunable film thicknesses and provide means for preparation of multi-block brushes through sequential monomer addition. Ionic, coordination, and ring-opening living polymerization methods have all been reported. However, these methods require stringent reagent purification, and are

sensitive to functional groups and impurities. By contrast, free radical polymerization is relatively tolerant of reaction impurities and allows for the use of functional monomers and solvents. This technique is constrained, however, by the existence of termination events which leads to a lack of precise control over molecular weight, molecular weight distribution, chain architecture, and end-group functionality.

Controlled radical polymerization (CRP) combines the control of a living polymerization with the more process-friendly conditions of a free radical polymerization. Otsu and coworkers<sup>20</sup> first described a model for living radical polymerization where a dormant chain end reversibly dissociates into a transient radical species and smaller persistent radicals, which are more stable and cannot initiate polymerization themselves. Both types of radical species are formed in equal amounts at the onset of polymerization. The persistent radicals cannot react among themselves, but combine with the transient species in the reverse reaction. However, the transient radicals can also undergo irreversible self-termination, which leads to an excess of the persistent species. The buildup of persistent radicals favors the crossreaction and inhibits (though never completely) the self-termination reaction. This Persistent Radical Effect<sup>21</sup> (PRE) (Scheme 1.1) minimizes irreversible termination during a radical polymerization by limiting the concentration of propagating radicals.



Scheme 1.1. The Persistent Radical Effect

The unstable transient radical can undergo propagation with monomer with a rate constant  $k_p$  or it can recombine with the persistent radical to reform the dormant species. If the rate constant for recombination ( $k_d$ ) is sufficiently large compared to the rate constant for dissociation ( $k_a$ ), the concentration of transient radicals present at any given time is low, thereby minimizing the possibility of two transient radicals coupling and undergoing permanent bimolecular termination. Fast recombination of the persistent radical with the transient radical would also limit the number of monomer units that can add to the chain during any one monomer addition cycle. However, the dissociation needs to be facile enough that addition cycles can occur to high conversion. A linear increase in molecular weight and a narrowing of molecular weight distribution with increasing monomer conversion are a consequence of the PRE during polymerization.<sup>21</sup>

Several different CRP methods have been developed.<sup>22</sup> Atom transfer radical polymerization (ATRP)<sup>23</sup> relies on a transition metal complex to catalyze reversible removal of a halogen atom from a dormant species to create a transient radical. Transient radicals are generated in reversible addition-fragmentation chain transfer (RAFT)<sup>24</sup>

polymerization by the reversible transfer of a thiocarbonyl thio group between an active and dormant species. In stable free radical polymerization (SFRP), transient radicals are generated by (for example) the thermal decomposition of an alkoxyamine end group<sup>25</sup> into transient and persistent radicals. All three CRP methods are governed by the equilibrium between activation and deactivation steps (with rate constants  $k_a$  and  $k_d$  respectively). The free radicals generated in each CRP process react with monomer with a rate constant  $k_p$  as they would in a conventional free radical process. Though bimolecular termination (with a rate constant of  $k_t$ ) is minimized due to the PRE, the formation of a small amount of unreactive polymer is unavoidable. As with other living polymerization techniques, CRP produces polymers with reactive end groups that can be chain extended to yield block copolymers.

Previously, Zhao and Brittain<sup>26</sup> reported the synthesis of a tethered polystyrene-*b*-poly(methyl methacrylate) brush from silicon substrates (Si/SiO<sub>2</sub>//PS-*b*-PMMA). A layer of cationic polymerization initiator was first immobilized onto a silicon surface. Cationic polymerization of styrene from the surface was performed, followed by ATRP of methyl methacrylate using the  $\omega$ -chloropolystyrene moieties to initiate polymerization to yield an AB diblock copolymer brush. This brush was found to undergo reversible surface rearrangement into micellar structures containing PMMA cores and PS shells in response to immersion in block-selective solvents.<sup>27</sup>

Zhao and Brittain<sup>27</sup> used (Si/SiO<sub>2</sub>//PS-*b*-PMMA) brushes to create pinned micelle patterned surfaces. Patterned organic films have found applications in cell growth control,<sup>28,29</sup> microelectronics,<sup>30</sup> and biomimetic materials fabrication.<sup>31</sup> Several methods for patterning polymer films on a surface include various methods of lithography, block

copolymer self-assembly, and microcontact printing.<sup>32</sup> Surface patterning *via* treatment of tethered diblock copolymer films with block selective solvents has been the subject of theoretical investigation.<sup>33,34</sup>

The research described herein uses ATRP as a controlled radical technique to prepare diblock polymer brushes from silicon substrates *via* sequential monomer addition. Previous diblock brushes made using ATRP were found to undergo stimuli-responsive surface rearrangement through solvent<sup>27,35,36</sup> as well as thermal<sup>36</sup> treatment. The goal of this project was to grow tethered AB diblock copolymer brushes where the tethered A block consists of poly(2-hydroxyethyl methacrylate) (PHEMA), poly(*N,N*-dimethylaminoethyl methacrylate) (PDMAEMA), or poly(glycidyl methacrylate) (PGMA) and the outer B block consists of polystyrene (PS), in hopes of observing similar stimuli-responsive rearrangement into pinned micelle patterned surfaces. The functionality of the micelle “shells” can then be exploited in crosslinking reactions to lock the surface morphology into place so it is no longer reversible.

## CHAPTER II

### HISTORICAL BACKGROUND

#### 2.1. Polymer Brushes

Polymer brushes have generated interest due to their unique properties and potential applications in modifying the surface properties of materials.<sup>2-6</sup> A polymer brush is an assembly of polymer chains which are tethered by one end to a surface or interface with a high enough grafting density that, under equilibrium conditions, the chains are forced to stretch away from the tethering site to avoid overlap.<sup>7,8</sup> Two unique properties that arise from the confined geometry of brushes are the linear correlation of brush height to the degree of polymerization<sup>9</sup> and a possible elevation of glass transition temperature.<sup>10</sup> Potential applications for polymer brushes include: lubrication,<sup>2</sup> microcontact printing,<sup>3</sup> bioactive surfaces,<sup>4</sup> and in chemical gating for smart materials.<sup>5,6</sup>

Some examples<sup>9</sup> of polymer brush systems in bulk or solution are shown in Figure 2.1. Brushes can be formed by diblock copolymers at the interface between two immiscible liquids where each block is preferentially solubilized by a different liquid. The junction points between blocks will be confined to the interface—forcing the blocks to stretch away from that interface. Examples of this type of polymer brush system are biphasic layers and polymer micelles. A similar situation may occur in the melt state where the microphase separation of block copolymers can form various ordered morphologies such as a lamellar structure.

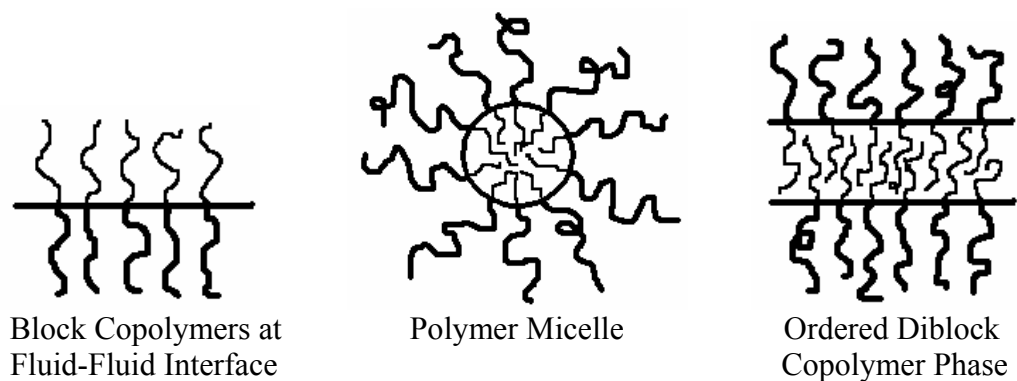


Figure 2.1. Examples of Polymer Brushes in Bulk or Solution

Polymer brushes can also be formed by tethering polymer chains to solid substrates. Tethering can be achieved by physisorption or through covalent attachment. A typical example of a physisorbed brush is shown in Figure 2.2 where one block of a diblock polymer is preferentially attracted to a surface, leaving the chains of the other block to stretch away from the surface. The relatively weak van der Waals forces or hydrogen bonding that anchors a physisorbed brush causes the brush to be unstable towards solvent or thermal treatment.

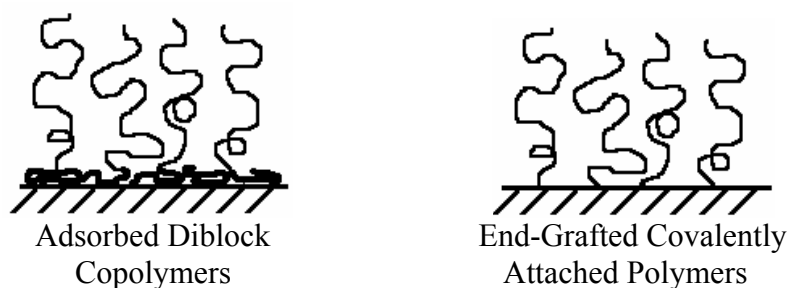


Figure 2.2. Surface Tethered Polymer Brushes

An alternative method of anchoring chains to a surface is through covalent attachment. Polymer films anchored in this manner are inherently more thermally and

solvolytically stable. There are two methods for chemically attaching polymer chains to a solid substrate: the “grafting to” and “grafting from” techniques (Figure 2.3).<sup>11</sup>

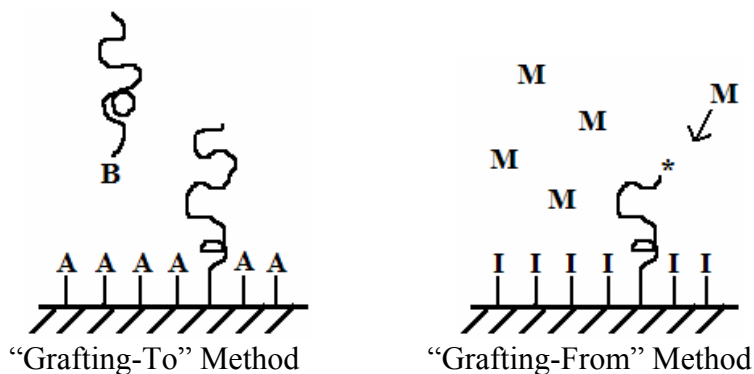


Figure 2.3. Covalent Grafting Methods

In the “grafting to” method, pre-formed, end-functionalized polymer chains are reacted with a chemically activated substrate. One advantage of this method is that polymer chains can be characterized before being attached to the substrate. The drawback, however, is that only relatively low grafting densities (and therefore thin polymer films) are obtained due to steric crowding of already attached chains on the surface that hinder diffusion of more chains to reactive sites. In the “grafting from” method, a surface immobilized initiator layer is covalently bonded to a substrate followed by an *in situ* surface-initiated polymerization (SIP). Thick brushes with a high graft density can be formed because monomer can easily diffuse to reactive sites of the growing polymer chains.

## 2.2. Preparation of Surface-Tethered Polymers

### 2.2.1. Physisorption Method

Polymer brushes which are physisorbed on a surface consist of two different components: an “anchor” end which is strongly adsorbed to the surface, and the “bouy,” or rest of the chain which forms the brush layer. Though end-functionalized polymer chains may form physisorbed brushes,<sup>37</sup> the anchoring end of a brush which is physisorbed to a surface is typically a specific block of a block copolymer. Physisorption of block or graft copolymers can be accomplished in the presence of a selective solvent or a selective surface.<sup>11</sup> The selective solvation method employs a solvent which is a precipitant for the “anchoring” block and a good solvent for the other block which forms the brush. Alternatively, the selective surface method directs physisorption by employing a surface which strongly prefers one block.

The selective solvent method has been used to anchor ionically synthesized polystyrene-*block*-poly(2-vinylpyridine) (PS-*b*-P2VP) on silicon oxide<sup>38,39</sup> and mica<sup>38,40</sup> surfaces. The samples were deposited using toluene, which is a good solvent for PS. The P2VP blocks were adsorbed to the surface while the PS chains formed the brush layer. Poly(4-*tert*-butylstyrene) brushes were also formed by the deposition of poly(4-*tert*-butylstyrene)-*block*-sodium poly(styrene-4-sulfonate) (PtBS-*b*-NaPSS) in an aqueous solution on mica.<sup>40</sup> In this case water was a good solvent for the NaPSS, allowing the PtBS to be anchored to the mica surface. The selective surface method has been used to make PS brushes by depositing polystyrene-*block*-poly(ethylene oxide) onto a variety of surfaces<sup>41-43</sup> using toluene, which is a good solvent for both the PS and PEO blocks. In

this case, the polar PEO block was more strongly attracted to the surface and became the anchor for the nonpolar PS block.

One disadvantage with adsorbing diblocks to a surface is that the blocks must be chemically different (i.e., nonpolar PS and polar P2VP or PEO) to be selectively attracted to a solvent or surface. This requirement limits the different types of diblock systems that can be used for physisorption. Another problem with adsorbing diblocks to a surface is that attachment of more polymer chains is hindered by a diffusion barrier created by already attached diblocks. In an effort to circumvent this second problem, Stöhr and Rühle<sup>44</sup> investigated a novel means of creating physisorbed diblock brushes using a physisorbed macroinitiator. A poly( $\epsilon$ -caprolactone) polymer containing azo free radical initiating groups (I-I) was physisorbed to silicon oxide substrates, followed by an *in situ* free radical polymerization of *n*-alkyl methacrylates. Figure 2.4(b) shows this process alongside the typical physisorption of a diblock polymer, (a).

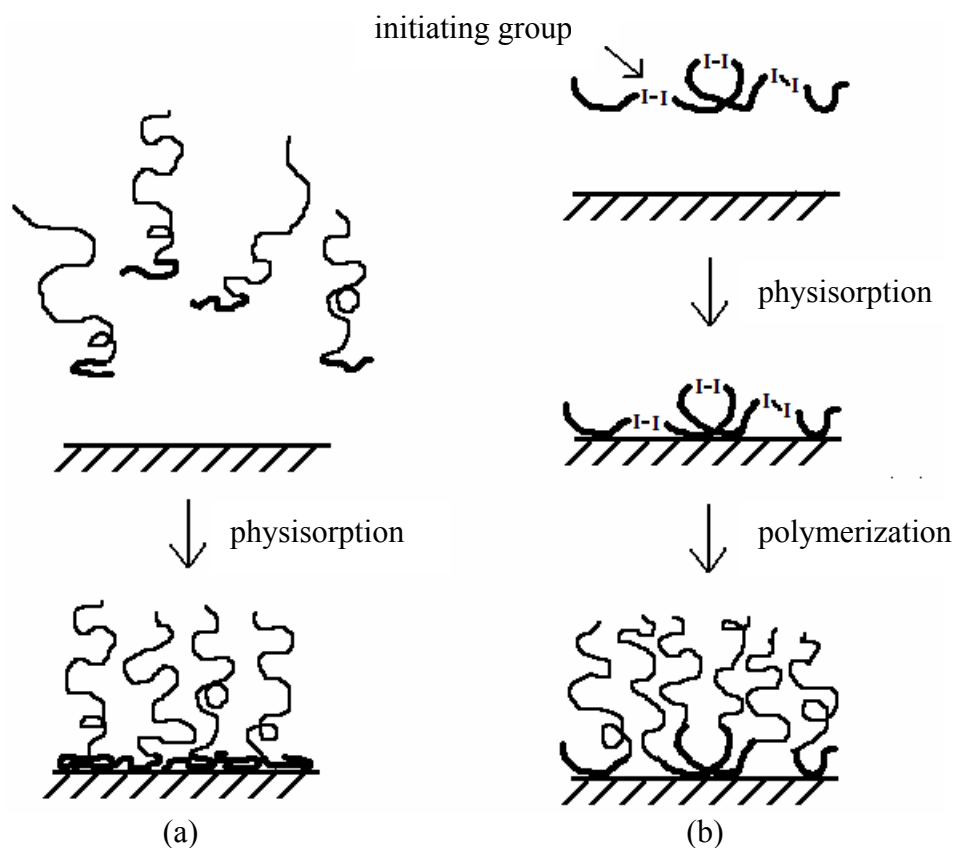


Figure 2.4. Physisorbed Polymer Brushes

Physisorbed polymer brushes are generally held to substrates through van der Waals forces or hydrogen bonding, and these relatively weak interactions render the brushes thermally and solvolytically unstable, resulting in desorption of the brushes upon exposure to good solvents for the anchoring moiety. Heating the brushes above the glass transition temperature or melting temperature may also cause dewetting of the substrate and formation of polymer droplets.<sup>11</sup> This desorption may be prevented by covalently bonding the chains to a surface.

### 2.2.2. Covalent Attachment *via* “Grafting To”

In the “grafting to” method, end-functionalized chains react with substrates to form covalently attached polymer brushes, making them more robust to solvent and thermal treatment. Controlled polymerization techniques have been used to synthesize chains of desired molecular weight and narrow molecular weight distribution, which can later be grafted to substrates. For example, Koutsos and coworkers<sup>45</sup> used anionic polymerization to synthesize variable length thiol-terminated polystyrenes and grafted them to gold substrates. Tran and Auroy<sup>46</sup> created PS brushes by grafting anionically synthesized polystyrenes with trichlorosilane endgroups to silanol (Si-OH) groups on the surface of silicon wafers. Later these brushes were sulfonated to create poly(styrene sulfonate) brushes. Yoshikawa and Tsubokawa<sup>47</sup> synthesized poly(isobutyl vinyl ether) (PIBVE) *via* cationic polymerization where the living PIBVE chain ends were grafted to modified carbon black surfaces containing nucleophilic amino, sodium phenolate, and sodium carboxylate groups.

Though surfaces may be modified by direct chemical reaction as in the previous example, self-assembled monolayers (SAMs) and other coupling agents may also be attached to surfaces to introduce chemical functionality. For example, Pruker and coworkers<sup>48</sup> first covered a silicon substrate with a monolayer of a photoreactive benzophenone derivative and then used ultraviolet light to immobilize layers of PS and poly(ethyloxazoline) (PEOX). Minko and coworkers<sup>49</sup> anchored carboxyl-terminated PS and P2VP to a silicon oxide surface by first modifying the surface with 3-glycidoxypropyl trimethoxysilane.

The covalent “grafting to” method offers several advantages over grafting brushes *via* physisorption. Covalently attached brushes are more robust in the presence of high temperatures or solvent treatment. The ability to functionalize substrates and polymer end-groups with relative ease eliminates the need to create chemically different diblock polymers for physical attachment. One problem with the covalent “grafting to” method, as with grafting diblock polymers to a surface *via* physisorption, is that only relatively low grafting densities and therefore relatively low film thicknesses are obtained. Reactive endgroups must diffuse through a barrier of existing polymer film to couple with functional groups on the surface and this diffusion barrier becomes more pronounced as more chains are attached. This effect was noticed by Yoshikawa and Tsubokawa<sup>47</sup> when it was discovered that the number of grafted chains decreased as the molecular weight of the chains increased. Though brushes have been prepared *via* the “grafting to” method,<sup>50</sup> more densely grafted brushes may be prepared by using the “grafting from” method to circumvent the diffusion barrier problem.

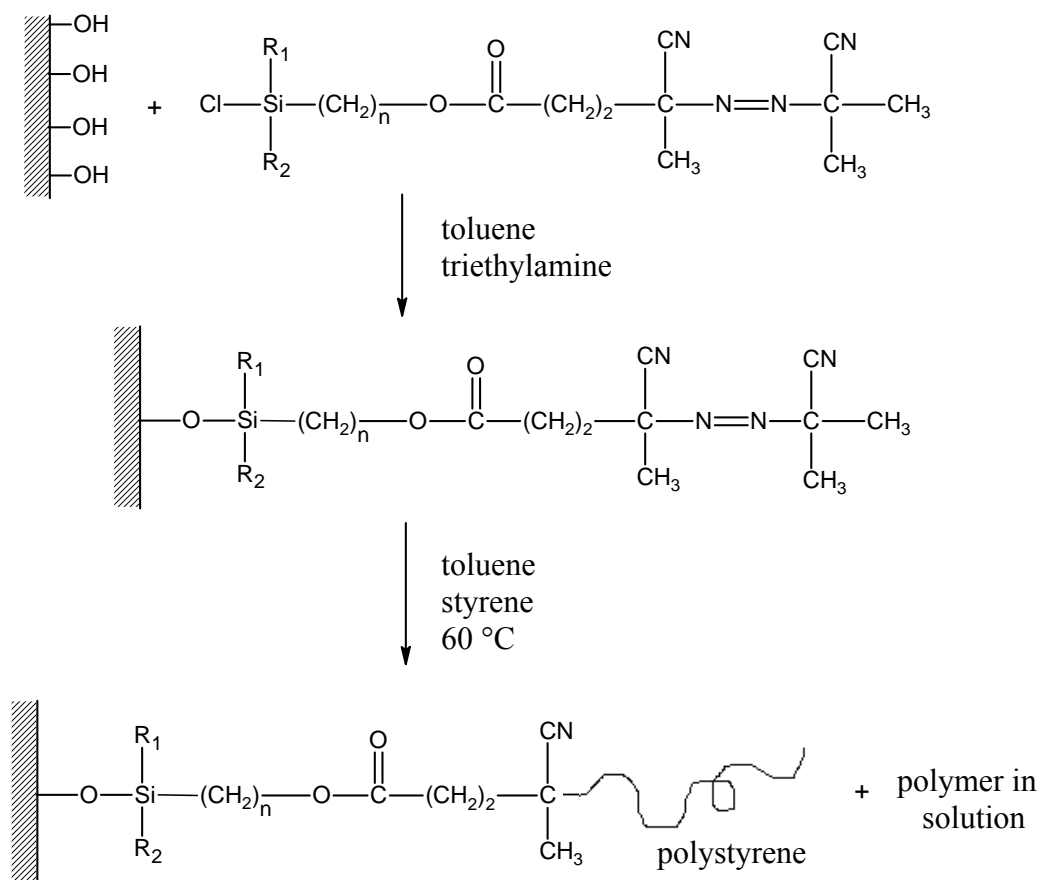
### 2.2.3. Covalent Attachment *via* “Grafting From”

The “grafting from” approach has become the method of choice to produce thick, densely grafted, covalently attached polymer brushes. A layer of polymerization initiator is first covalently attached to a substrate, followed by an *in situ* surface-initiated polymerization to produce the desired brush. Methods of introducing initiators onto a surface include using plasma and glow-discharge treatment, Langmuir-Blodgett techniques, or SAM deposition. A wide range of polymerization methods such as ionic,

radical, and ring-opening metathesis may then be used to grow brushes, depending on the initiating species.

#### 2.2.3.1. “Grafting From” Using Conventional Free Radical Polymerization

Prucker and R  he<sup>17</sup> reported the synthesis of an initiator molecule containing an azo headgroup, a cleavable ester bond, and a chlorosilane anchoring group. The chlorosilane endgroup, previously known to form self-assembled monolayers,<sup>51</sup> was used to anchor the molecule to silica gel. Heating the initiator-functionalized silica gel in a styrene solution led to the thermal decomposition of the azo moiety and subsequent free radical polymerization of styrene to produce PS brushes as well as polymer in solution (Scheme 2.1). The PS chains were later degrafted *via* cleavage of the ester bond for light scattering and GPC analysis.



Scheme 2.1. Azo Initiator Immobilization and Polymerization

Biesalski and coworkers<sup>52</sup> deposited the same initiator molecule on planar silicon substrates to prepare poly(4-vinylpyridine) (P4VP) brushes. The pendant pyridine groups were subsequently quaternized with iodomethane to produce polyelectrolyte brushes. Feng and coworkers<sup>53</sup> deposited a similar azo initiator functionalized with thiol end-groups onto gold substrates. A mixed brush was created by photoinitiation in the presence of styrene followed by further photoinitiation in a solution of methyl methacrylate.

The use of conventional free radical polymerization gave researchers little control over the ability to prepare brushes with predetermined molecular weights and narrow

molecular weight distributions. Controlled polymerization techniques such as ring-opening metathesis (ROMP), ionic, and controlled radical polymerization have therefore been used as methods to produce controlled molecular weight brushes. In addition, these techniques have been used to create end-functionalized and block copolymer brushes with relative ease.

#### 2.2.3.2. “Grafting From” Using Metathesis Polymerization

Juang and coworkers<sup>54</sup> prepared a polynorbornene (PNBE) brush through a ROMP mediated by Grubbs’ catalyst that had been anchored to a silicon surface. Brush thickness was controlled by varying the monomer concentration in the solution. Detrembleur and coworkers<sup>55</sup> grew PNBE brushes from steel electrodes by first grafting poly(norbornenylmethylene acrylate) (PNBE-A) from the electrodes through an electrografting process. The PNBE-A film was modified with a Grubbs’ catalyst and then exposed to a solution of NBE to grow the PNBE brushes. Liu and coworkers<sup>56</sup> polymerized norbornenyl-functionalized monomers from gold substrates patterned with a Grubbs’ catalyst. Moon and Swager<sup>57</sup> polymerized a norbornene end-capped poly(*p*-phenylene ethynylene) (PPE) macromonomer from a silicon surface functionalized with a Grubbs’ metathesis catalyst to create PPE brushes.

Harada and coworkers<sup>58</sup> deposited a mixture of 7-octenyltrichlorosilane and octyltrichlorosilane on hydroxyl functionalized silicon substrates *via* microcontact printing. The surface-anchored vinyl groups were then reacted with a Grubbs’ catalyst before ROMP was performed in a solution of 2,2,2-trifluoroethyl bicyclo[2.2.1]hept-2-ene-5-carboxylate. Though minimal brush growth was observed from surfaces

functionalized with 100% 7-octenyltrichlorosilane, a 40/60, *mol/mol* solution of 7-octenyltrichlorosilane/octyltrichlorosilane provided maximum brush thicknesses in this study. Presumably, lower surface coverage of the catalyst led to thicker brushes because reactions between adjacent ROMP catalyst groups were avoided.

### 2.2.3.3. “Grafting From” Using Ionic Polymerization

Zhou and coworkers<sup>59</sup> modified 1,1-diphenylethylene (DPE) with a quaternized amine anchoring group in order to attach it to clay particles. The surface bound DPE was derivatized with *n*-butyllithium and subsequently used to initiate the anionic polymerization of styrene. Advincula and coworkers<sup>60</sup> modified DPE with monochlorosilane and thiol anchoring groups to attach it to silicon and gold substrates, respectively. DPE substrates were derivatized with *sec*-butyllithium before initiating brush growth. Diblock brushes Si/SiO<sub>2</sub>//PS-*b*-polyisoprene (Si/SiO<sub>2</sub>//PS-*b*-PI) and Si/SiO<sub>2</sub>//polybutadiene-*b*-PS were synthesized *via* a one-pot sequential monomer addition method where the first polymerization was allowed to reach completion before a second monomer was added to the reaction.

Quirk and coworkers<sup>61</sup> also prepared diblock brushes from silicon substrates *via* anionic polymerization from a surface attached DPE initiator. However, a “macroinitiator” approach was used so that the first block (Si/SiO<sub>2</sub>//PI) was removed from the polymerization and characterized before immersion in a subsequent polymerization of ethylene oxide (EO) to produce Si/SiO<sub>2</sub>//PI-*b*-PEO. This group also prepared films of Si/SiO<sub>2</sub>//PI using the “grafting to” method. As expected, grafting

densities were found to be lower for the PI films made by the “grafting to” method than for those made by the “grafting from” method.

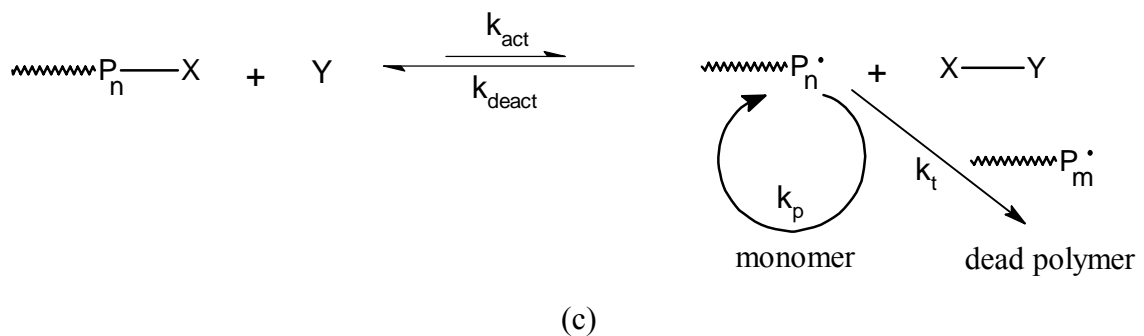
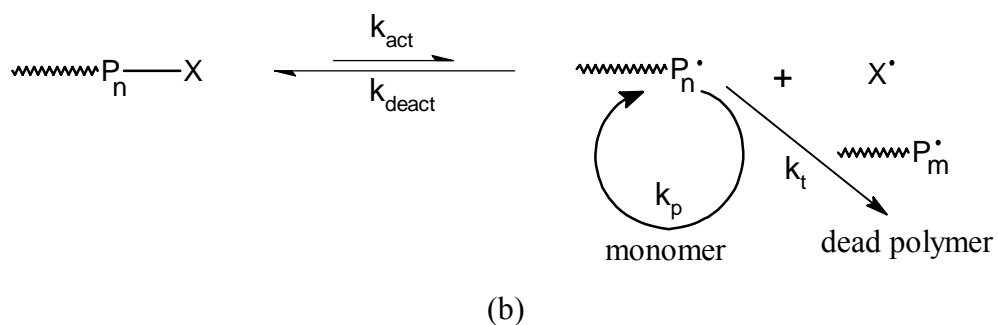
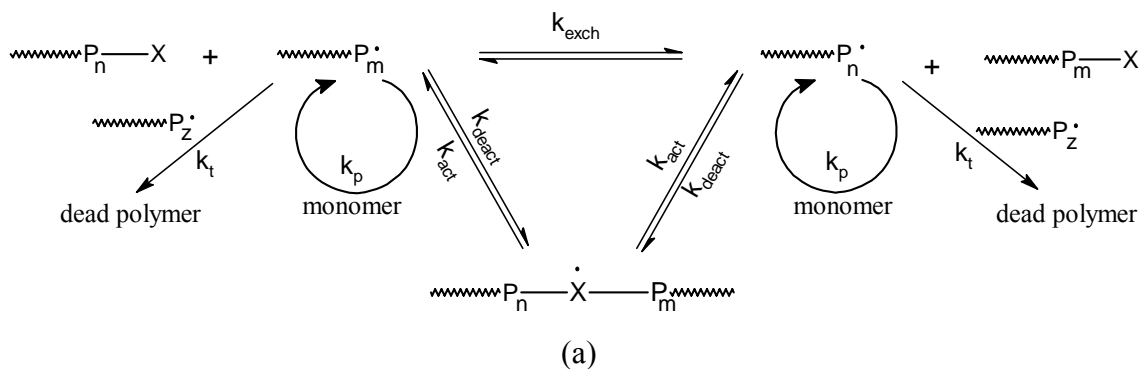
Polystyrene brushes have also been synthesized using cationic polymerization. Zhao and Brittain<sup>26</sup> used  $\text{TiCl}_4$  to initiate the cationic polymerization of styrene from silicon substrates functionalized with a cumyl ether compound. Interestingly, the cumyl ether contained a deuterated moiety which allowed the researchers to monitor the initiation efficiency by measuring the decrease in intensity of the C-D stretching vibration peak in the IR spectrum of the brush. An initiator efficiency of 7% was reported. The resulting Si/SiO<sub>2</sub>//PS brush was later used for the initiation of methyl methacrylate (MMA) under atom transfer radical polymerization (ATRP) conditions to produce the diblock Si/SiO<sub>2</sub>//PS-*b*-PMMA brush.

#### 2.2.3.4. “Grafting From” Using Controlled Radical Polymerization

Though ionic and metathesis polymerization techniques allow preparation of brushes with controlled molecular weight and narrow molecular weight distribution as well as the ability to functionalize end-groups and easily create diblocks, these methods are highly sensitive to water and oxygen contamination. Controlled radical polymerization (CRP) techniques combine the control of these living polymerization techniques with the wide range of monomers and tolerance of impurities that conventional free radical polymerization has to offer. A model for CRP<sup>20</sup> describes the generation of active propagating radicals and smaller persistent radicals from the reversible dissociation of a dormant chain end (see Scheme 1.1). The buildup of persistent radicals, caused by some active radical species undergoing bimolecular

termination, allows for an increasing amount of coupling between the active and persistent radicals and results in a self-regulating process of reversible termination.<sup>21</sup>

The three most studied CRP techniques are reversible addition fragmentation chain transfer (RAFT), nitroxide-mediated polymerization (NMP), and atom transfer radical polymerization (ATRP). All three methods depend on the equilibrium between the dormant and active radical species lying strongly towards the dormant state for control in the polymerization. In Scheme 2.2, the persistent radical (X) represents a chain transfer agent being transferred between two growing chains in a RAFT polymerization (a), an alkoxyamine radical in NMP (b), and a halogen atom in ATRP (c).<sup>23</sup> In all three methods a growing radical propagates with rate constant  $k_p$  and is terminated according to  $k_t$ . All three methods have been used to make polymer brushes.



Scheme 2.2. General Schemes for CRP Methods

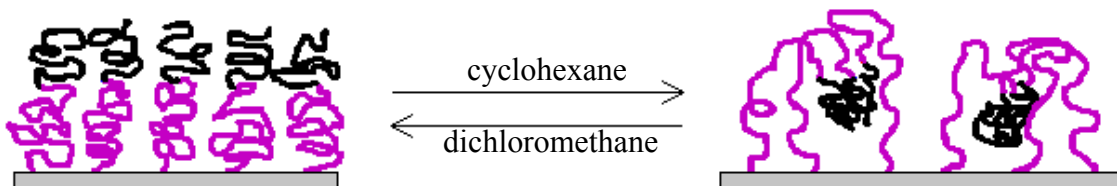
Baum and Brittain<sup>62</sup> deposited the azo initiator developed by Prucker and R  he<sup>17</sup> onto silicon substrates for the RAFT polymerization of PS, PMMA, and poly(*N,N*-dimethylacrylamide) (PDMA) brushes. 2-Phenylprop-2-yl dithiobenzoate was employed

as a chain transfer agent and 2,2'-azobisisobutyronitrile (AIBN) was used as a free initiator in solution. The living nature of the PDMA and PS brushes was confirmed by removal of substrates from polymerization, characterization, and subsequent polymerization of additional blocks which resulted in a linear increase in brush thickness as a function of total polymerization time. Furthermore, a comparison of brushes degrafted from silica gel with polymer simultaneously grown in solution showed similar  $M_n$  and PDI. The living nature of the system also allowed diblock copolymer brushes Si/SiO<sub>2</sub>//PS-*b*-PDMA and Si/SiO<sub>2</sub>//PDMA-*b*-PMMA to be synthesized. These brushes displayed reversible surface properties when exposed to block-selective solvents. Zhai and coworkers<sup>63</sup> also used RAFT to prepare a diblock brush Si/poly[*N,N*-dimethyl(methylmethacryloyl ethyl) ammonium propane sulfonate]-*b*-poly(sodium 4-styrene sulfonate) (Si/PDMA-PS-*b*-PSS) from silicon substrates.

Andruzzi and coworkers<sup>64</sup> used a 2,2,6,6-tetramethylpiperidinyloxy (TEMPO) based initiator anchored to silicon substrates for the NMP of styrene and semifluorinated monomers, producing various homopolymer and diblock copolymer brushes. Some TEMPO-based free initiator was also added to the polymerizations to aid in control of brush growth as well as to produce untethered polymer for GPC analysis. Zhao and coworkers<sup>65</sup> report the deposition of a Y-shaped initiator on a silicon substrate. The initiator contained a TEMPO-based initiating headgroup for NMP and a second bromoisobutyrate-based initiating headgroup for ATRP. After the substrates were placed under ATRP conditions at 75 °C for the SIP of MMA, they were placed under NMP conditions at 115 °C for subsequent SIP of styrene. Treatment of this mixed PMMA/PS brush with acetic acid was found to produce nanodomains, thought to be of micellar

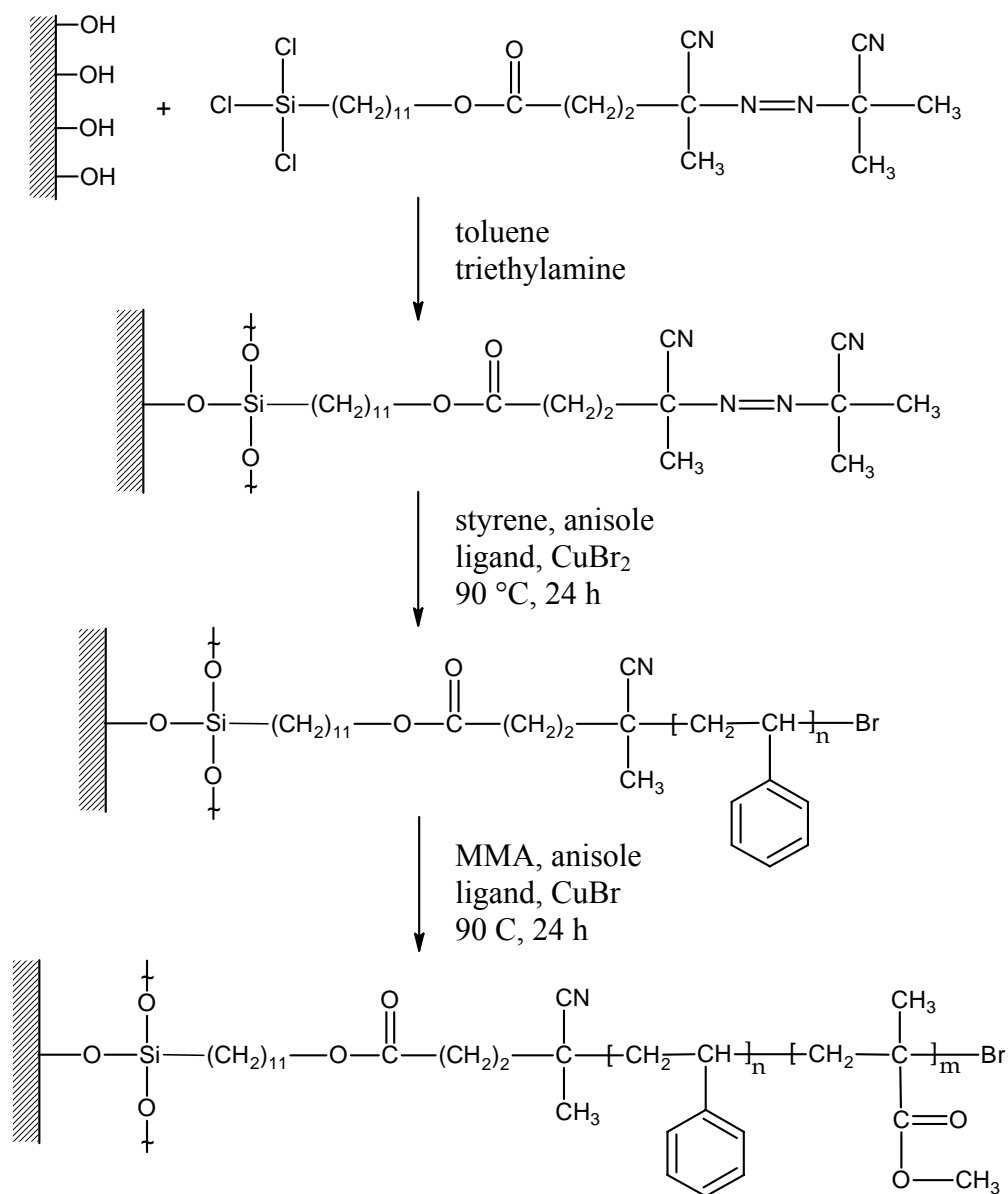
structure with PS cores and PMMA shells. Immersion of the brush in chloroform (a good solvent for both polymers) brought the brush back to a more extended conformation.

Similar reversible solvent-induced morphologies have been produced using diblock polymer brushes synthesized *via* ATRP. Zhao and coworkers<sup>27</sup> report the cationic polymerization of styrene from silicon substrates followed by the ATRP of MMA from the living PS chain ends. The resulting Si/SiO<sub>2</sub>//PS-*b*-PMMA brush had a 23 nm thick PS layer and a 14 nm thick PMMA layer. Treatment with dichloromethane (a good solvent for both blocks) allowed the brush to remain in a somewhat extended conformation. An advancing water contact angle of 74° (characteristic of a PMMA surface) was obtained. An AFM analysis found the surface to be relatively smooth, with an RMS roughness of 0.77 nm. However, upon treatment with cyclohexane at 35 °C (a better solvent for PS than PMMA), the advancing water contact angle increased to 99° (characteristic of a PS surface) and surface RMS roughness increased to 1.79 nm. This change was reversible when the sample was again treated with dichloromethane to promote migration of the PMMA segments to the brush surface. Interestingly, the brush was treated with a solvent mixture of both dichloromethane and cyclohexane, where the percentage of cyclohexane was gradually increased. The RMS roughness became 13.08 nm and an advancing water contact angle of 120° was obtained. Zhao and coworkers<sup>27,66,67</sup> proposed a surface rearrangement mechanism in the presence of block selective solvents (Scheme 2.3)



Scheme 2.3. Proposed Surface Rearrangement Mechanism for Si/SiO<sub>2</sub>//PS-*b*-PMMA

Sedjo and coworkers<sup>68</sup> used an experimentally simpler method to create a Si/SiO<sub>2</sub>//PS-*b*-PMMA brush. The azo initiator developed by Prucker and R  he<sup>17</sup> was used for the reverse ATRP of styrene from a silicon substrate. Conventional ATRP was then used to polymerize MMA from the dormant PS chain ends (Scheme 2.4).



Scheme 2.4. Si/SiO<sub>2</sub>//PS-*b*-PMMA Brush Synthesis Using Reverse ATRP

This brush underwent similar reversible changes in water contact angles when treated with dichloromethane or methylcyclohexane to expose a PMMA or PS surface respectively.

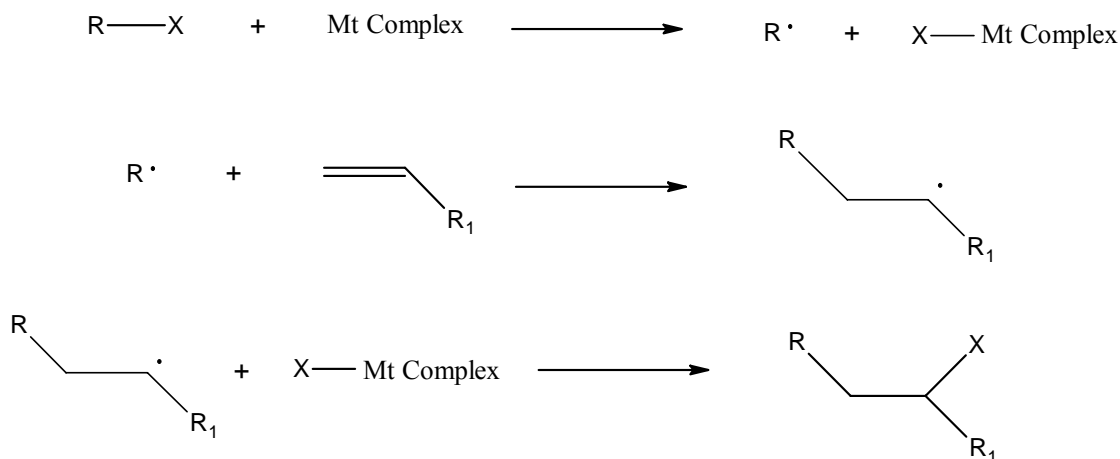
More recently, Granville and coworkers<sup>35</sup> synthesized a variety of semifluorinated polymer brushes *via* ATRP. These brushes consisted of a PS or PMA bottom block, and

had a poly(pentafluorostyrene) (PPFS), poly(trifluoroethyl acrylate) (PTFA), poly(pentafluoropropyl acrylate) (PPFA), or poly(heptadecafluorodecyl acrylate) (PHFA) top block. Reversible solvent-responsive behavior was observed when exposing the diblocks to either a fluorinated or a hydrocarbon solvent. While most systems experienced a noticeable change in contact angles upon exposure to block selective solvents, this work noted that incomplete surface rearrangement may be due to (among other factors) a relatively large difference in solubility parameters of the two polymers, which in turn leads to a large Flory-Huggins interaction parameter ( $\chi$ ) between the two blocks. It was also noted that, in contrast, the  $\chi$  value for PS and PMMA blocks is relatively small.

## 2.3. Atom Transfer Radical Polymerization

### 2.3.1. General Background

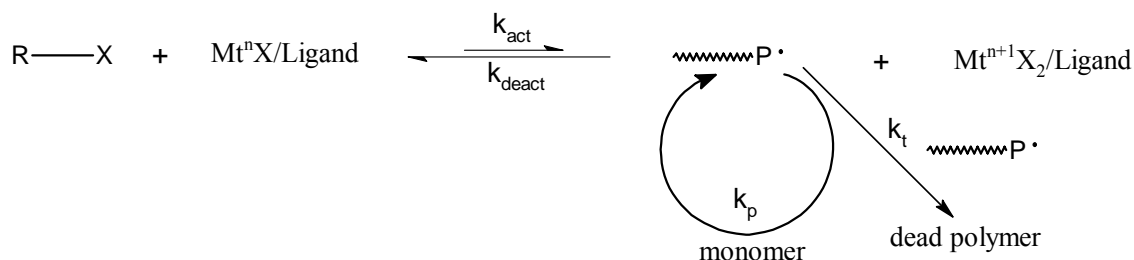
For this research, ATRP was used in the preparation of diblock polymer brushes from a surface immobilized initiator molecule. ATRP has been pioneered by the groups of both Sawamoto<sup>69</sup> and Matyjaszewski.<sup>70,71</sup> ATRP is based on atom transfer radical addition (ATRA)—a modified Kharasch addition in which a transition metal complex catalyzes the addition of an alkyl halide across a carbon-carbon double bond (Scheme 2.5).<sup>72</sup>



Scheme 2.5. General ATRA Scheme

A radical species is generated by the transfer of a halogen atom from the alkyl halide to the transition metal complex. This radical adds to an alkene double bond to form a radical species which is significantly less stable than the original radical. Consequently, the halogen atom is transferred back to the product radical to form the final product. Halogen transfer forming this final product should be irreversible and faster than other competing reactions such as radical termination or telomerization.<sup>72</sup>

The product radical produced in ATRA is typically much less stabilized than the initial radical, causing an irreversible reaction of the product radical with the halogen of the metal halide complex. This halide capping reaction becomes a reversible process in ATRP because the initial radical adds to vinyl monomers which stabilize the product radical, thereby creating a product radical with similar stability to the initial radical.<sup>73</sup> Radicals are generated in ATRP through a reversible redox process catalyzed by a metal-ligand complex which undergoes a one-electron oxidation and abstracts a halogen atom from a dormant species (Scheme 2.6).



Scheme 2.6. General ATRP Scheme

Rate constants  $k_{act}$  and  $k_{deact}$  describe the activation and deactivation, respectively, of the reversible radical generation process, monomer is added to the growing radical (with rate constant  $k_p$ ) in a manner similar to conventional radical polymerization, and growing radicals may terminate (with rate constant  $k_t$ ) by combination or disproportionation to form dead polymer. This irreversible termination can be minimized by shifting the equilibrium of the reaction to the left (dormant state) and lowering the concentration of growing radicals. As in conventional free radical polymerizations, chain transfer can also occur. However, chain transfer is usually only a problem at high or complete conversion. Because ATRP reactions are rarely carried out to complete conversion, chain transfer reactions are negligible.

## 2.3.2. Reaction Components

### 2.3.2.1. Monomers

Initially, ATRP was used to polymerize MMA<sup>69</sup> and styrene.<sup>70</sup> Since then, a wide variety of styrenes, acrylates, and methacrylates, have been successfully polymerized.<sup>23</sup> Perhaps some of the most interesting monomers to be polymerized have been functional monomers such as 2-hydroxyethyl methacrylate,<sup>74,75</sup> 2-(dimethylamino)ethyl

methacrylate,<sup>76</sup> and glycidyl methacrylate.<sup>77</sup> Other monomers such as fluorinated monomers,<sup>35</sup> cationic<sup>78</sup> or anionic<sup>78,79</sup> electrolytes, and acrylonitrile<sup>23</sup> have been polymerized *via* ATRP as well.

For successful control in polymerization, a monomer must stabilize the propagating radical. Under similar conditions, each monomer has its own unique atom transfer equilibrium constant,  $K_{\text{eq}}$ , between the active and dormant species where  $K_{\text{eq}} = k_{\text{act}}/k_{\text{deact}}$ . A small equilibrium constant will lead to slow polymerization because of a low instantaneous radical concentration being present. Conversely, a large equilibrium constant will lead to a higher radical concentration and will result in an increase in termination events. This in turn may shift the polymerization back to the dormant state and result in an apparently slower polymerization.<sup>22</sup>

#### 2.3.2.2. Initiators

Alkyl halides are typically used in ATRP to create the growing radicals. As long as initiation is fast and the system experiences minimal chain transfer or termination, the number of initiator molecules determines the number of growing chains. Alkyl halide initiators have activating substituents on the  $\alpha$ -carbon such as aryl, carbonyl, or allyl groups. Some common examples of these initiators are  $\alpha$ -bromo esters, benzylic halides, and sulfonyl chlorides (Figure 2.5).

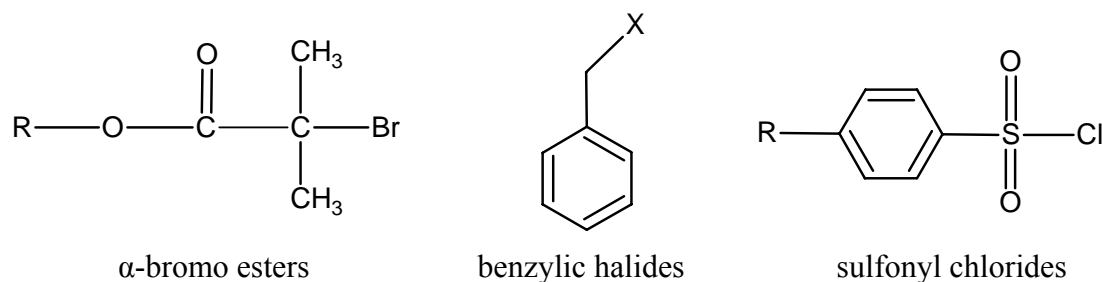


Figure 2.5. Common ATRP Initiators

Bromine and chlorine are typically used as halogens in ATRP. The halogen atom must be able to migrate rapidly and selectively between the metal catalyst complex and the growing polymer chain. A general order of bond strengths for alkyl halides is:

$R-F > R-Cl > R-Br > R-I$ . The C-F bond is too strong to undergo homolytic cleavage and the reactive C-I bond may present a variety of problems.<sup>22</sup> Often the halogen used in the metal salt is the same halogen used in the initiator. However, mixed halogen initiating systems (R-Br/Mt-Cl) have been exploited to increase control over a polymerization.<sup>80,81</sup> Chains initiated from a bromine-terminated initiator will become capped with a chlorine atom due to the greater stability of the R-Cl bond compared to the R-Br bond. In contrast to homogenous halogen systems, this difference in bond strength leads to an increased rate of initiation compared to propagation, thus leading to better control of molecular weight distribution.

### 2.3.2.3. Transition Metal Catalysts

While the position of  $K_{eq}$  depends on the monomer structure, it is also affected by the reactivity of the transition metal complex. Middle to late transition metal complexes have been found to be most efficient for catalyzing ATRP. The metal should have two readily accessible oxidation states that are separated by one electron. The metal should

also have a reasonable affinity toward the halogen and have an expandable coordination sphere upon oxidation to accept the halogen atom. Finally, the metal should be complexed by the ligand relatively strongly.<sup>22</sup> Though a variety of metals such as molybdenum, rhenium, ruthenium, iron, rhodium, nickel, palladium, and copper, have been used in ATRP, copper has probably received the most attention due to its wide versatility and low cost.<sup>23</sup>

#### 2.3.2.4. Ligands

The ligand in ATRP serves to solubilize the transition metal catalyst and adjust the redox potential of the metal complex for suitable reactivity for atom transfer.<sup>22</sup>

Nitrogen-based ligands such as 2,2'-bipyridine (bpy), *N,N,N',N',N''*-pentamethyldiethylenetriamine (PMDETA), 1,1,4,7,10,10-hexamethyltriethylenetetramine (HMTETA), tris[2-(dimethylamino)ethyl]amine (Me<sub>6</sub>TREN), and *N*-alkyl-2-pyridylmethanimine have been popular choices for copper-mediated ATRP (Figure 2.6).

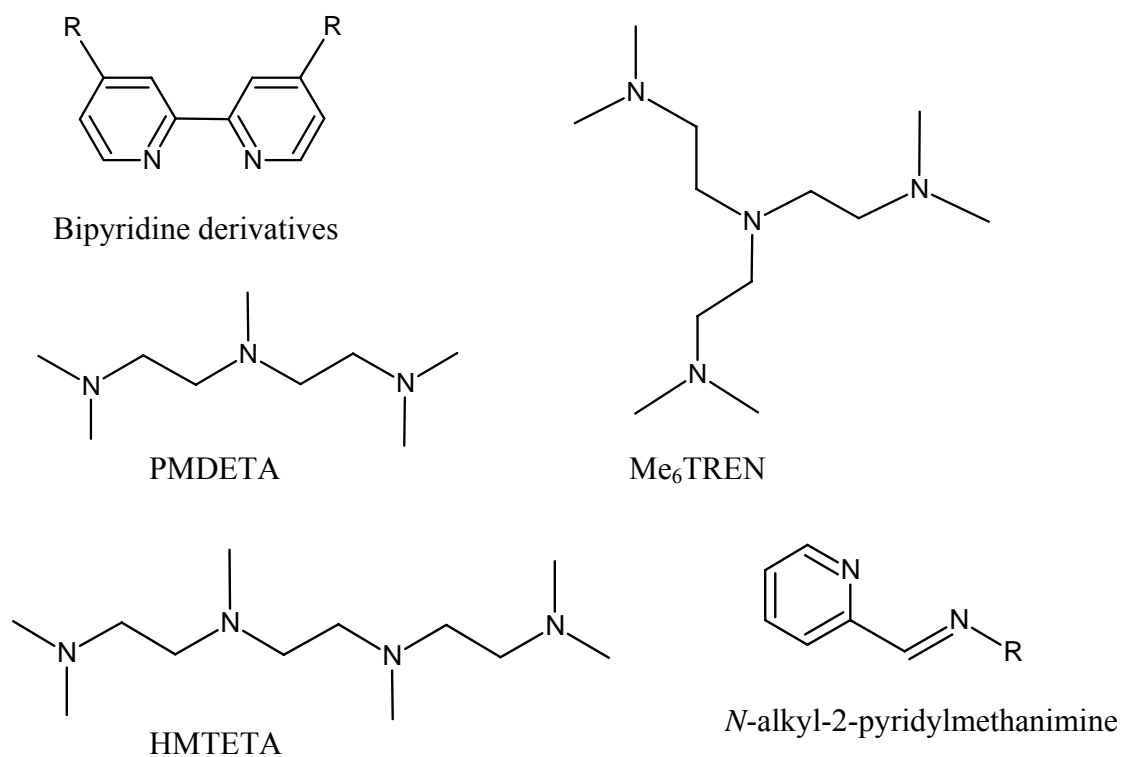


Figure 2.6. Commonly Used ATRP Ligands

The first copper-mediated ATRP of styrene employed bpy as a ligand.<sup>70</sup> Multidentate amines such as PMDETA and HMTETA were later used in the ATRP of styrene, methyl acrylate, and methyl methacrylate.<sup>82</sup> The use of these ligands has resulted in faster polymerization rates—presumably because they formed copper complexes with lower redox potentials than the copper-bpy complex. This lower redox potential allowed for higher activation rates of the dormant alkyl halides. The more strongly coordinating Me<sub>6</sub>TREN ligand has been found to increase polymerization rate<sup>83</sup> as well as prevent competitive coordination of monomer.<sup>84</sup> Derivatives on the 4,4' position of bpy have been used to modify ligand solubility.<sup>85</sup> An alternative to the rather tedious synthetic procedure required to modify the bpy ligand has been developed by the Haddleton research group.<sup>86</sup> This group studied the use of various chain length *N-n*-alkyl-2-

pyridylmethanimine ligands in the ATRP of styrene<sup>87</sup> and methyl methacrylate.<sup>86</sup> These imine-based ligands can be synthesized through a simple one-step procedure which can utilize virtually any primary amine for tuning of ligand solubility.

#### 2.3.2.5. Solvents

ATRP has been carried out in homogenous systems (bulk and solution) as well as heterogenous systems (emulsion and suspension).<sup>22</sup> ATRP is typically performed in solution. A wide variety of solvents such as anisole, dichlorobenzene, toluene, ethylene carbonate, and dimethylformamide (to name a few) have been used.<sup>76,80</sup> ATRP has also been performed in aqueous and alcoholic media. The addition of water to an ATRP has been found to increase polymerization rate,<sup>80</sup> however, possibly at the expense of control of the polymerization.<sup>75,88</sup>

#### 2.3.3. Surface-Initiated ATRP

Grafting polymers from a surface presents a special challenge in maintaining an equilibrium favoring the deactivated radicals. In solution ATRP, a small amount of termination (typically about 5%)<sup>23</sup> occurs during the initial stage of polymerization. This termination allows the buildup of the deactivating  $Mt^{n+1}X_2$  species that shifts the equilibrium towards the dormant state for the remainder of the polymerization. ATRP from a surface (Figure 2.7) is achieved by placing a substrate covered with initiator molecules in a solution of monomer, solvent, and a metal/ligand complex. When polymerization is initiated from the substrate, the persistent radical is free to migrate away from the surface and into the rest of solution.

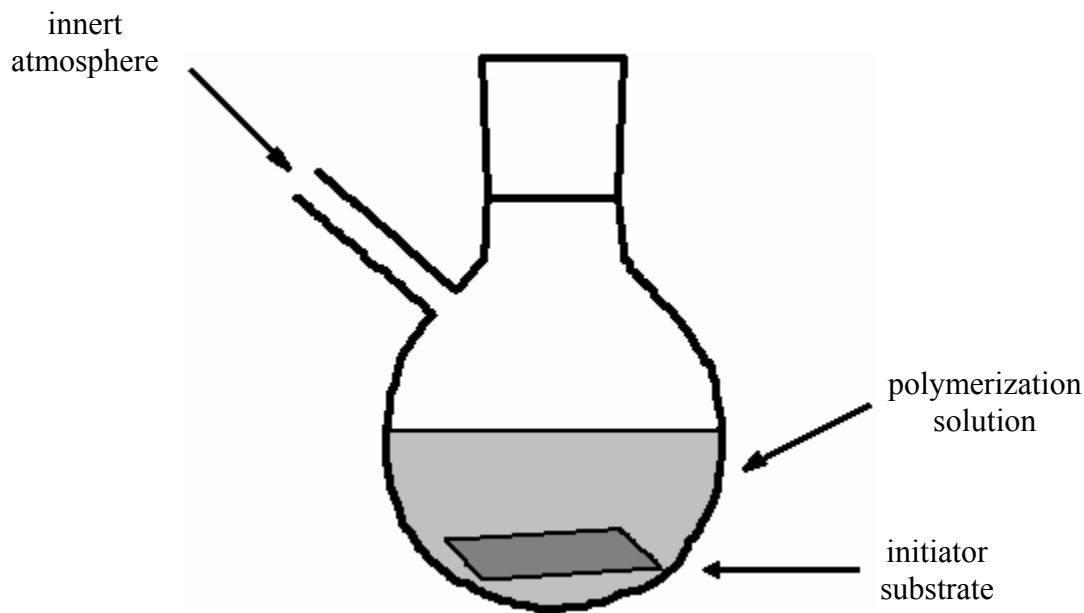


Figure 2.7. Surface-Initiated Polymerization Setup

This migration leaves minimal deactivator concentration near the surface and results in a poorly controlled SIP due to a high concentration of growing radicals on the surface.

Previous research concerning surface initiated ATRP has employed the addition of free initiator to achieve a high enough concentration of deactivating species at the surface as well as throughout the rest of the solution to control brush growth.<sup>3,16,67,89</sup> GPC analysis of brushes cleaved from silica gel has shown good agreement of molecular weight data between polymer grown in solution and polymer grown on a surface.<sup>62,89</sup> Therefore growing polymer in solution has the added benefit of yielding easily obtained GPC results that can approximate molecular weight data for the brush.

While the brush thickness can actually be moderated by free initiator concentration,<sup>67</sup> the addition of free initiator inherently limits the maximum brush thickness because most of the monomer will be consumed by polymer formed in solution.

Another drawback to the addition of free initiator is that free polymer must be removed from the brush when polymerization is finished. This is usually accomplished by extracting the brush in a good solvent.<sup>90</sup> Another approach to controlling brush growth has been to add the deactivating Cu(II) species directly.<sup>80,91,92</sup> Though solution polymer will not be made for molecular weight analysis, the need for tedious solvent extraction is eliminated. In an extreme case, Huang and coworkers<sup>80</sup> were able to produce 700 nm thick poly(2-hydroxyethyl methacrylate) (PHEMA) films by adding deactivating CuBr<sub>2</sub> directly to an aqueous HEMA polymerization.

## CHAPTER III

### EXPERIMENTAL

#### 3.1. Materials

*Monomers:* Styrene (S, Aldrich, 99%), 2-(dimethylamino)ethyl methacrylate (DMAEMA, Aldrich, 98%), 2-hydroxyethyl methacrylate (HEMA, Aldrich, 98%), and glycidyl methacrylate (GMA, Aldrich, 97%) were passed through a column of activated basic alumina (~150 mesh, Aldrich) immediately before use. 2-(Dimethylamino)ethyl acrylate (DMAEA, Aldrich, 98%) was distilled under reduced pressure before use.

*Initiators:* Ethyl 2-bromoisobutyrate (EBiB, Aldrich, 98%) and benzyl chloride (BnzCl, Aldrich, 99%) were passed through a column of activated basic alumina before use. The synthesis of [11-(2-bromo-2-methyl)propionyloxy]undecyltrichlorosilane was adopted from a literature procedure.<sup>91</sup> For the synthesis procedure, anhydrous tetrahydrofuran (Aldrich, 99.9%), anhydrous pyridine (Aldrich, 99.8%),  $\omega$ -undecylenyl alcohol (Aldrich, 98%), 2-bromoisobutyryl bromide (Aldrich, 98%), hexanes (EM Science), hydrochloric acid (EM Science), ethyl acetate (EM Science), silica gel (70-230 mesh, Aldrich), anhydrous sodium sulfate (EM Science), hydrogen hexachloroplatinate (IV) hydrate (Aldrich), trichlorosilane (Aldrich, 99%), absolute ethanol (Pharmco), anhydrous diethyl ether (Fisher), dichloromethane (Fisher), anhydrous toluene (Aldrich, 99.8%), anhydrous magnesium sulfate (Fisher), and activated carbon (Aldrich) were all used as received.

*Copper Halides:* Copper(I) bromide (Aldrich, 98%) and copper(I) chloride (99+%) were

purified before use according to literature procedures.<sup>93</sup> Copper(II) bromide (Aldrich, 99%) and copper(II) chloride (Aldrich, 99.999%) were used as received. For the purification procedures, sulfuric acid (EM Science), sulfurous acid (Aldrich), glacial acetic acid (EM Science), absolute ethanol (Pharmco), and anhydrous diethyl ether (Fisher) were used as received. *Ligands*: 1,1,4,7,10,10-Hexamethyltriethylenetetramine (HMTETA, Aldrich, 97%), *N,N,N',N',N''*-pentamethyldiethylenetriamine (PMDETA, Aldrich, 99%), and 2,2'-dipyridyl (bpy, Aldrich, 99+%) were used as received. *N-n*-pentyl-2-pyridylmethanimine<sup>86</sup> and tris[2-(dimethylamino)ethyl]amine (Me<sub>6</sub>TREN)<sup>94</sup> were synthesized according to literature procedures. For the synthesis procedures, amylamine (Aldrich, 99%), 2-pyridinecarboxaldehyde (Aldrich, 99%), anhydrous diethyl ether (Fisher), anhydrous magnesium sulfate (Fisher), tris(2-aminoethyl)amine (TREN, Aldrich, 96%), formic acid (Aldrich, 88%), formaldehyde (Aldrich, 37 wt% solution in water), sodium hydroxide (EM Science), anhydrous sodium sulfate (EM Science), and dichloromethane (Fisher) were all used as received. *Solvents*: Toluene (EM Science), isopropyl alcohol (EM Science), methanol (EM Science), tetrahydrofuran (EM Science), cyclohexane (Fisher), *N,N*-dimethyl formamide (Fisher), cyclohexane (Fisher), anhydrous 1,2-dichlorobenzene (Aldrich, 99%), methyl alcohol (Aldrich, 99.8+%), anhydrous anisole (Aldrich, 99.7%), and anhydrous acetonitrile (Aldrich, 99.8%) were used as received. House distilled water was used for solvent switching experiments. Water for contact angle measurements was purified by the Millipore Milli-Q system. *Substrates*: Silicon attenuated total reflection (ATR) crystals (25x5x1 mm) were obtained from Harrick Scientific. Silicon wafers were obtained from Polishing Corporation of America. Substrates were cleaned using sulfuric acid (EM Science) and hydrogen

peroxide (Fisher, 30%). *Surface Modification*: 1,2-bis-(2-Iodoethoxy)ethane (Aldrich, 96%), adipoyl chloride (Aldrich, 98%), valeryl chloride (Aldrich, 98%), butyryl chloride (Aldrich, 98%), propionyl chloride (Aldrich, 98%), hexafluoroglutaryl chloride (Ryan Scientific, 98%), 2,2'-(ethylenedioxy)diethylamine (Aldrich, 98%), 1,5-diamino-3-oxapentane (Acros, 98%), and tris(2-aminoethyl)amine (TREN, Aldrich, 96%) were used as received.

### 3.2. Characterization Methods

ATR-FTIR spectra were taken using a Nicolet System 730 spectrometer using a modified 4XF beam condenser (Harrick Scientific). Spectra were recorded at  $2\text{ cm}^{-1}$  resolution and were averaged from 500 scans. Ellipsometric film thickness measurements were obtained using a Gaertner model L116C ellipsometer with a He-Ne laser ( $\lambda = 632.8\text{ nm}$ ) and a fixed angle of incidence of  $70^\circ$ . Refractive indices used for layer thickness calculations were:  $n = 1.455$  for silicon oxide,<sup>95</sup>  $n = 1.508$  for initiator layer,  $n = 1.5894$  for PS,<sup>95</sup>  $n = 1.517$  for PDMAEMA,<sup>95</sup>  $n = 1.512$  for PHEMA,<sup>95</sup> and  $n = 1.500$  for PGMA<sup>96</sup> and PDMAEA. It should be noted that the thickness of a multiple layer system was found using the refractive index for the outermost layer. Contact angle measurements were obtained using a Rame Hart NRL-100 goniometer on a tilting base mounted on a vibrationless table. Advancing and receding contact angles were taken using a  $10\ \mu\text{L}$  drop using the tilting stage method. A Varian Gemini-300 MHz spectrometer was used to collect  $^1\text{H}$  NMR spectra. GPC measurements using DMF as the eluent were taken using a Waters 410 differential refractometer, a Waters 515 pump, and Waters HR2 and HR4 Styragel columns at  $50\ ^\circ\text{C}$  with a flow rate of  $0.7\ \text{mL}/\text{min}$ . PMMA

( $2.9 \times 10^3 - 3.3 \times 10^5$  g/mol) standards (Polymer Laboratories) were used for column calibration and data analysis was performed using a Viscotek software package. GPC measurements using THF as the eluent were taken using a Waters 410 differential refractometer and a Wyatt Technology DAWN EOS multiangle light scattering system, a Waters 510 pump, and Waters HR 1, HR 4E, and HR 5E Styragel columns at 35 °C with a flow rate of 1.0 mL/min. Molecular weights were determined using Universal calibration. AFM images were taken at room temperature in air using a multimode scanning probe microscope (Park Scientific Autoprobe CP) in intermittent-contact with a silicon tip.

### 3.3. Synthesis and Preparation of Reagents

#### 3.3.1. Initiator Synthesis

*Synthesis of 10-undecen-1-yl 2-bromo-2-methylpropionate.*<sup>91</sup> In a round-bottom flask containing a stir bar immersed in an ice bath, 6.8 mL (55.0 mmol) of 2-bromoisobutyryl bromide was added dropwise to a solution containing 50 mL of anhydrous tetrahydrofuran, 4.8 mL (59.3 mmol) of anhydrous pyridine, and 10.0 mL (49.9 mmol) of  $\omega$ -undecylenyl alcohol. The solution was then allowed to warm to room temperature and stirred overnight. The reaction solution was then diluted with 100 mL of hexanes and washed once with 2 N hydrochloric acid and then three times with distilled water (approximately 75 mL per wash). The organic phase was dried over anhydrous sodium sulfate and decanted before removing the solvent under reduced pressure. The crude oil was purified by flash chromatography through a silica gel column using a 25/1, v/v hexane/ethyl acetate solution. Solvent was again removed *via* reduced pressure

and a clear colorless oil resulted.  $^1\text{H}$  NMR (300 MHz,  $\text{CDCl}_3$ )  $\delta$ : 1.22-1.38 (br m, 12H); 1.56-1.67 (m, 2H); 1.86 (s, 6H); 1.97 (q, 2H); 4.1 (t, 2H); 4.84-4.95 (m, 2H); 5.68-5.81 (m, 1H) ppm.

*Synthesis of (11-(2-bromo-2-methyl)propionyloxy)undecyltrichlorosilane.*<sup>91</sup> In a round-bottom flask containing a stir bar, approximately 5 mg of hydrogen hexachloroplatinate (IV) hydrate was dissolved in approximately 0.25 mL of absolute ethanol/anhydrous diethyl ether (1/1, v/v). To this catalyst solution 6.0 g (18.8 mmol) of the initiator intermediate 10-undecen-1-yl 2-bromo-2-methylpropionate was added. Stirring was started before the addition of 20 mL (198 mmol) of trichlorosilane. The flask was equipped with a reflux condenser and the solution was heated under reflux for 4 h. A bulb-to-bulb vacuum distillation was used to remove the excess trichlorosilane before the solution was diluted with 50 mL of dichloromethane. The diluted solution was filtered through columns containing a layer of activated carbon between layers of anhydrous magnesium sulfate. The dichloromethane was removed under reduced pressure to yield a clear colorless oil.  $^1\text{H}$  NMR (300 MHz,  $\text{CDCl}_3$ )  $\delta$ : 1.28-1.44 (br m, 16H); 1.56-1.73 (m, 4H); 1.93 (s, 6H); 4.15-4.19 (t, 2H) ppm. This initiator was then diluted with anhydrous toluene to give a 25% w/w solution and stored in the freezer.

### 3.3.2. Purification of Copper Halides

The copper(I) bromide and copper(I) chloride catalysts were purified following a literature procedure.<sup>93</sup> Several drops of 1 N sulfuric acid was added to approximately 5 g of copper halide to form a paste. In a beaker equipped with a stir bar, 200 mL of 1 N sulfurous acid was added to this paste and the mixture was stirred for 30 minutes at room

temperature. The mixture was passed through a sintered glass frit funnel so that a liquid layer remained above the solid copper halide at all times. The copper halide was washed four times with 25 mL portions of glacial acetic acid, then three times with 25 mL portions of absolute ethanol, and finally five times with 25 mL portions of anhydrous diethyl ether. Each washing was done when the previous liquid layer was barely covering the solids. After the final washing, the copper halide was placed under reduced pressure overnight to remove any residual solvent and then stored in a dessicator until use.

### 3.3.3. Ligand Synthesis

*Synthesis of N-n-pentyl-2-pyridylmethanimine.*<sup>86</sup> In a round-bottom flask containing a stir bar immersed in an ice bath, 14.5 mL (125 mmol) of amylamine was added dropwise to a solution of 10 mL of anhydrous diethyl ether and 10 mL (105 mmol) of 2-pyridinecarboxaldehyde. Approximately 4 g of anhydrous magnesium sulfate was added, and the resulting slurry was stirred at room temperature for 2 hours. The MgSO<sub>4</sub> was then filtered out before the solution was concentrated under reduced pressure to yield a clear yellow oil. <sup>1</sup>H NMR (300 MHz, CDCl<sub>3</sub>) δ: 0.75-0.80 (t, 3H); 1.18-1.25 (m, 4H); 1.55-1.62 (m, 2H); 3.51-3.56 (t, 2H); 7.12-7.16 (t, H); 7.54-7.60 (t, 1H); 7.84-7.87 (d, 1H); 8.25 (s, 1H); 8.49-8.51 (d, 1H) ppm.

*Synthesis of tris[2-(dimethylamino)ethyl]amine (Me<sub>6</sub>TREN).*<sup>94</sup> In a round-bottom flask containing a stir bar immersed in an ice bath, 58.3 mL (1336 mmol) of formic acid was added dropwise to 10.0 mL (66.8 mmol) of tris(2-aminoethyl)amine. After 10 minutes of stirring, 54.7 mL (735 mmol) of formaldehyde was added, and the solution

was heated under reflux for 20 hours. The solution was then concentrated under high vacuum and aqueous 10 M NaOH was added until the solution became approximately pH~11-12. The solution was extracted twice with dichloromethane (approximately 70 mL per wash). The organic phase was dried over anhydrous sodium sulfate and decanted before removing the solvent under reduced pressure. The remaining dark orange liquid was stored in the refrigerator overnight. The light orange liquid (Me<sub>6</sub>TREN) was pipetted off of a dark brown solid precipitate. <sup>1</sup>H NMR (300 MHz, CDCl<sub>3</sub>) δ: 2.07 (s, 18H); 2.19-2.24 (t, 6H); 2.43-2.48 (t, 6H) ppm.

#### 3.4. Substrate Preparation

All silicon wafers and ATR crystals were cleaned by immersion in a freshly prepared “piranha” solution (70/30 v/v sulfuric acid/hydrogen peroxide) for 1 hour at approximately 100 °C. This process generated a hydroxyl-functionalized surface on the silicon substrates. Substrates were then rinsed repeatedly with distilled water and dried in a stream of air. ATR-FTIR and ellipsometry were used to analyze the cleaned substrates. Initiator deposition onto the substrates was performed immediately (within several hours) after cleaning.

#### 3.5. Surface Immobilization of Trichlorosilane ATRP Initiator

In a small flask, 0.3 mL of the diluted initiator solution (25% w/w in anhydrous toluene) was added to 15 mL of anhydrous toluene. Freshly cleaned silicon substrates were placed in the flask so that the substrates were completely covered by the initiator deposition solution. The flask was sealed with a rubber septum and heated to 60 °C for 4 hours. The substrates were then rinsed sequentially with tetrahydrofuran and toluene and

dried in a stream of air. Substrates were then analyzed using ATR-FTIR, ellipsometry, and tensiometry.

### 3.6. Synthesis of Block Copolymer Brushes *via* Surface-Initiated ATRP

#### 3.6.1. Preparation of Si/SiO<sub>2</sub>//PDMAEMA Brushes

For a typical synthesis procedure, a stir bar was placed in a 100 mL Schlenk flask along with 36.5 mg (0.36 mmol) of copper(I) chloride, 9.7 mg (0.072 mmol) of copper(II) chloride and 15 mL of anhydrous 1,2-dichlorobenzene. DMAEMA (15 mL, 89 mmol) was added to a separate 100 mL, round-bottom flask. Both flasks were fitted with rubber septa and sparged with nitrogen for 1 hour. After sparging, 0.20 mL (0.74 mmol) of HMTETA ligand was added to the Schlenk flask. The solution was stirred until a homogenous solution was obtained and the monomer was cannulated from the round-bottom flask to the Schlenk flask. A second Schlenk flask containing initiator substrates was fitted with a rubber septum and then evacuated and backfilled with nitrogen three times. The monomer solution was cannulated into the substrate-containing flask and 22  $\mu$ L (0.15 mmol) of EBiB free initiator was added. The reaction was left to run at room temperature for the desired length of time under a nitrogen atmosphere.

When the reaction was finished, substrates were removed and extracted overnight with isopropyl alcohol in a Soxhlet apparatus. Substrates were then sonicated for 30 minutes in isopropyl alcohol before being rinsed in isopropyl alcohol and dried in a stream of air. Substrates were analyzed using ATR-FTIR, ellipsometry, and tensiometry. A sample of reaction solution was passed through silica gel to remove copper catalyst before being diluted with DMF and analyzed by DMF GPC. A second sample of reaction

solution was used to determine percent conversion *via* NMR. For chain extension experiments, substrates containing previously grown and characterized brushes were subjected to the initial polymerization conditions in a fresh reaction solution.

### 3.6.2. Preparation of Si/SiO<sub>2</sub>//PHEMA Brushes

For a typical synthesis procedure, a stir bar was placed in a 100 mL Schlenk flask along with 35.6 mg (0.36 mmol) of copper(I) chloride. HEMA (15 mL, 124 mmol) and 15 mL of methyl alcohol were added to a separate 100 mL, round-bottom flask. Both flasks were fitted with rubber septa and sparged with nitrogen for 1 hour. After sparging, 0.20 mL (0.74 mmol) of HMTETA ligand was added to the round-bottom flask. The solution was cannulated to the Schlenk flask and stirred until a homogenous liquid was obtained. A second Schlenk flask containing initiator substrates was fitted with a rubber septum and then evacuated and backfilled with nitrogen three times. The monomer solution was cannulated into the substrate containing flask and 22  $\mu$ L (0.15 mmol) of EBiB free initiator was added. The reaction was left to run at room temperature for the desired length of time under a nitrogen atmosphere.

When the reaction was finished, substrates were removed and extracted overnight with methanol in a Soxhlet apparatus. Substrates were then sonicated for 30 minutes in methanol before being sequentially rinsed with methanol and isopropyl alcohol and dried in a stream of air. Substrates were analyzed using ATR-FTIR, ellipsometry, and tensiometry. A sample of reaction solution was passed through silica gel to remove copper catalyst before being diluted with DMF and analyzed by DMF GPC. A second sample of reaction solution was used to determine percent conversion *via* NMR. For

chain extension experiments, substrates containing previously grown and characterized brushes were subjected to the initial polymerization conditions in a fresh reaction solution.

### 3.6.3. Preparation of Si/SiO<sub>2</sub>//PGMA Brushes

For a typical synthesis procedure, a stir bar was placed in a 100 mL Schlenk flask along with 72.8 mg (0.74 mmol) of copper(I) chloride and 7.8 mg (0.035 mmol) of copper(II) bromide. GMA (10 mL, 73 mmol), 0.282 g (1.81 mmol) of bpy, and 10 mL of methanol were added to a separate 100 mL, round-bottom flask. Both flasks were fitted with rubber septa and sparged with nitrogen for 1 hour. After sparging, the monomer solution was cannulated to the Schlenk flask and stirred until a dark brown homogenous liquid was obtained. A second Schlenk flask containing initiator substrates was fitted with a rubber septum and then evacuated and backfilled with nitrogen three times. The monomer solution was cannulated into the substrate-containing flask and the reaction was left to run at room temperature for the desired length of time under a nitrogen atmosphere.

When the reaction was finished, substrates were removed and sonicated in methanol for thirty minutes before being sequentially rinsed with methanol and isopropanol and dried in a stream of air. Substrates were then analyzed using ATR-FTIR, ellipsometry, and tensiometry. For chain extension experiments, substrates containing previously grown and characterized brushes were subjected to the initial polymerization conditions in a fresh reaction solution.

#### 3.6.4. Preparation of Si/SiO<sub>2</sub>//PS Brushes

For a typical synthesis procedure, a stir bar was placed in a 100 mL, round-bottom flask along with 51.6 mg (0.36 mmol) of copper(I) bromide, 13.5 mL (118 mmol) of styrene, and 16.5 mL of anhydrous anisole. The flask was fitted with a rubber septum and immersed in an ice bath before being sparged with nitrogen for 1 hour. After sparging, the flask was allowed to warm to room temperature and 157  $\mu$ L (0.75 mmol) of PMDETA ligand was added. A Schlenk flask containing initiator substrates was fitted with a rubber septum and then evacuated and backfilled with nitrogen three times. The homogenous monomer solution was cannulated into the substrate containing flask and 22  $\mu$ L (0.15 mmol) of EBiB free initiator was added. The reaction was left to run at 100 °C for 22 hours under a nitrogen atmosphere.

When the reaction was finished, substrates were removed and extracted overnight with THF in a Soxhlet apparatus. Substrates were then sonicated for 30 minutes in THF before being sequentially rinsed with THF and toluene and dried in a stream of air. Substrates were analyzed using ATR-FTIR, ellipsometry, and tensiometry. The reaction solution was concentrated under reduced pressure to determine percent monomer conversion gravimetrically before being redissolved in THF and passed through silica gel to remove the copper catalyst. Evaporation of the THF afforded purified PS which was analyzed by THF GPC.

#### 3.6.5. Preparation of PS from Si/SiO<sub>2</sub>//PDMAEMA and Si/SiO<sub>2</sub>//PHEMA Brushes

For a typical synthesis procedure, a stir bar was placed in a 100 mL, round-bottom flask along with 35.6 mg (0.36 mmol) of copper(I) chloride, 15 mL (131 mmol) of

styrene, and 15 mL of anhydrous 1,2-dichlorobenzene. The flask was fitted with a rubber septum and sparged with nitrogen for 1 hour. After sparging, 0.20 mL (0.74 mmol) of HMTETA ligand was added and the solution was stirred until a homogenous liquid was obtained. A Schlenk flask containing Si/SiO<sub>2</sub>//PDMAEMA-Cl or Si/SiO<sub>2</sub>//PHEMA-Cl substrates was fitted with a rubber septum and then evacuated and backfilled with nitrogen three times. The monomer solution was cannulated into the Schlenk flask and 17  $\mu$ L (0.15 mmol) of BnzCl free initiator was added. The reaction was left to run at 90 °C for the desired length of time under a nitrogen atmosphere.

When the reaction was finished, substrates were removed and extracted overnight with tetrahydrofuran in a Soxhlet apparatus. Substrates were then sonicated for 30 minutes in tetrahydrofuran before being sequentially rinsed with tetrahydrofuran and toluene and dried in a stream of air. Substrates were analyzed using ATR-FTIR, ellipsometry, and tensiometry. The reaction solution was concentrated under reduced pressure to determine percent monomer conversion gravimetrically before being redissolved in THF and passed through silica gel to remove the copper catalyst. Evaporation of the THF afforded purified PS which was analyzed by THF GPC.

#### 3.6.6. Preparation of PS from Si/SiO<sub>2</sub>//PGMA Brushes

For a typical synthesis procedure, a stir bar was placed in a 100 mL, round-bottom flask along with 35.6 mg (0.36 mmol) of copper(I) chloride, 15 mL (131 mmol) of styrene, and 15 mL of anhydrous 1,2-dichlorobenzene. The flask was fitted with a rubber septum and sparged with nitrogen for 1 hour. After sparging, 0.14 mL (0.75 mmol) of *N*-*n*-pentyl-2-pyridylmethanimine ligand was added and the solution was stirred until a dark

brown homogenous liquid was obtained. A Schlenk flask containing Si/SiO<sub>2</sub>//PGMA-Cl substrates was fitted with a rubber septum and then evacuated and backfilled with nitrogen three times. The monomer solution was cannulated into the Schlenk flask and 17  $\mu$ L (0.15 mmol) of BnzCl free initiator was added. The reaction was left to run at 100 °C for the desired length of time under a nitrogen atmosphere.

When the reaction was finished, substrates were removed and extracted overnight with tetrahydrofuran in a Soxhlet apparatus. Substrates were then sonicated for 30 minutes in tetrahydrofuran before being sequentially rinsed with tetrahydrofuran and toluene and dried in a stream of air. Substrates were analyzed using ATR-FTIR, ellipsometry, and tensiometry. The reaction solution was concentrated under reduced pressure to determine percent monomer conversion gravimetrically before being redissolved in THF and passed through silica gel to remove the copper catalyst. Evaporation of the THF afforded purified PS which was analyzed by THF GPC.

### 3.6.7. Preparation of PDMAEA from Si/SiO<sub>2</sub>//PS Brushes

A stir bar was placed in a 100 mL Schlenk flask along with 34.4 mg (0.24 mmol) of copper(I) bromide. DMAEA (20 mL, 132 mmol) and 0.13 mL (0.49 mmol) of Me<sub>6</sub>TREN were added to a separate 100 mL, round-bottom flask. Both flasks were fitted with rubber septa and sparged with nitrogen for 1 hour. After sparging, the monomer solution was cannulated to the Schlenk flask and stirred until a homogenous liquid was obtained. A second Schlenk flask containing Si/SiO<sub>2</sub>//PS-Br substrates was fitted with a rubber septum and then evacuated and backfilled with nitrogen three times. The monomer solution was cannulated into the substrate containing flask and 14.5  $\mu$ L

(0.099 mmol) of EBiB free initiator was added. The reaction was left to run at room temperature for the desired length of time under a nitrogen atmosphere.

When the reaction was finished, substrates were removed and extracted overnight with isopropanol in a Soxhlet apparatus. Substrates were then sonicated for 30 minutes in isopropanol before being sequentially rinsed with isopropanol and dried in a stream of air. Substrates were analyzed using ATR-FTIR, ellipsometry, and tensiometry. A sample of reaction solution was passed through silica gel to remove copper catalyst before being diluted with DMF and analyzed by DMF GPC. A second sample of reaction solution was used to determine percent conversion *via* NMR.

### 3.7. Surface Rearrangement and Presumptive Crosslinking of Diblock Copolymer Brushes

#### 3.7.1. Si/SiO<sub>2</sub>//PDMAEMA-*b*-PS

Both thermal annealing at 115 °C for 2 hours and immersion in cyclohexane at 80 °C for 2 hours were used to promote migration of PS segments to the surface of the brush. Immersion in methanol for 2 hours at 60 °C was used to switch the brush by promoting migration of PDMAEMA segments to the surface. It was later found that solvent immersion at 60 °C for 1 hour would produce the same effect as immersion at 60 °C for 2 hours. Presumptive crosslinking was accomplished by immersion of the brush in methanol at 60 °C for 1 hour followed by immersion in a 1% solution of 1,2-bis-(2-iodoethoxy)ethane in methanol at 60 °C for 4 hours. The brush was then rinsed in methanol to remove any unreacted crosslinker from the surface. Immersion in cyclohexane at 60 °C for 1 hour was used to check for rearrangement after presumptive crosslinking.

### 3.7.2. Si/SiO<sub>2</sub>//PS-*b*-PDMAEA

Immersion in isopropyl alcohol at 80 °C for 2 hours was used to promote migration of the more polar PDMAEA segments to the brush surface. Immersion in cyclohexane at 80 °C for 2 hours was used to switch the brush and promote migration of the more non-polar PS segments to the surface. For presumptive crosslinking, the extended brush was first immersed in methanol at 60 °C for 1 hour before being immersed in a 1% solution of 1,2-bis-(2-iodoethoxy)ethane in methanol at 60 °C for 4 hours. The brush was then rinsed in methanol to remove any free crosslinker from the surface. This pre-soak and crosslinking procedure was repeated on different substrates using a 75/25 v/v methanol/water mixture as the solvent. After both crosslinking experiments, the presumptively crosslinked brushes were immersed in cyclohexane at 80 °C for 2 hours to check for rearrangement after presumptive crosslinking.

### 3.7.3. Si/SiO<sub>2</sub>//PHEMA-*b*-PS

Both thermal annealing at 115 °C for 2 hours and immersion in cyclohexane at 80 °C for 2 hours were used to promote migration of the PS segments to the surface of the brush. Switching was attempted by immersion in acetonitrile or water for 2 hours at 80 °C. It was later found that solvent immersion at 60 °C for 1 hour would produce the same effect as solvent immersion at 60 °C for 2 hours. Immersion in a 50/50 v/v H<sub>2</sub>O/DMF mixture at 60 °C for 1 hour was also used to switch the brush. Presumptive crosslinking of the diblock brush was accomplished by immersing the brush in anhydrous acetonitrile for 1 hour at 80 °C prior to immersion in a solution of adipoyl chloride in anhydrous acetonitrile at 80 °C for 1 hour. The brush was then rinsed in THF

and toluene to remove any unreacted crosslinker molecules from the surface. Immersion in cyclohexane or H<sub>2</sub>O/DMF at 60 °C for 1 hour was used to check for rearrangement after presumptive crosslinking. Reactions of mono and difunctional acyl chlorides with homopolymer Si/SiO<sub>2</sub>//PHEMA brushes were carried out in anhydrous acetonitrile at 80 °C for 3.5 days. Brushes were rinsed with THF and toluene to remove any unreacted reagent molecules from the surface before characterization.

#### 3.7.4. Si/SiO<sub>2</sub>//PGMA-*b*-PS

Immersion of the brush in cyclohexane at 60 °C for 1 hour was used to promote migration of the PS chains to the brush surface. Switching was accomplished by immersion in methanol or a 50/50 v/v H<sub>2</sub>O/DMF mixture at 60 °C for 1 hour. Diblock brushes were presumptively crosslinked by immersion in methanol at 60 °C for 1 hour prior to immersion in a 1% solution of primary amine crosslinker in methanol at 60 °C for 12 hours. Alternatively, brushes were pre-soaked and presumptively crosslinked in the H<sub>2</sub>O/DMF solvent mixture under otherwise similar conditions. In both cases, brushes were rinsed with methanol to remove any unreacted reagent molecules from the surface before characterization. Immersion in cyclohexane at 60 °C for 1 hour was used to check for rearrangement after presumptive crosslinking. Reactions of 1% and 100% solutions of 2,2'-(ethylenedioxy)diethylamine with Si/SiO<sub>2</sub>//PGMA homopolymer brushes were carried out at 60 °C for 3 days and 8 hours, respectively. Methanol was used to rinse away any unreacted material before characterization.

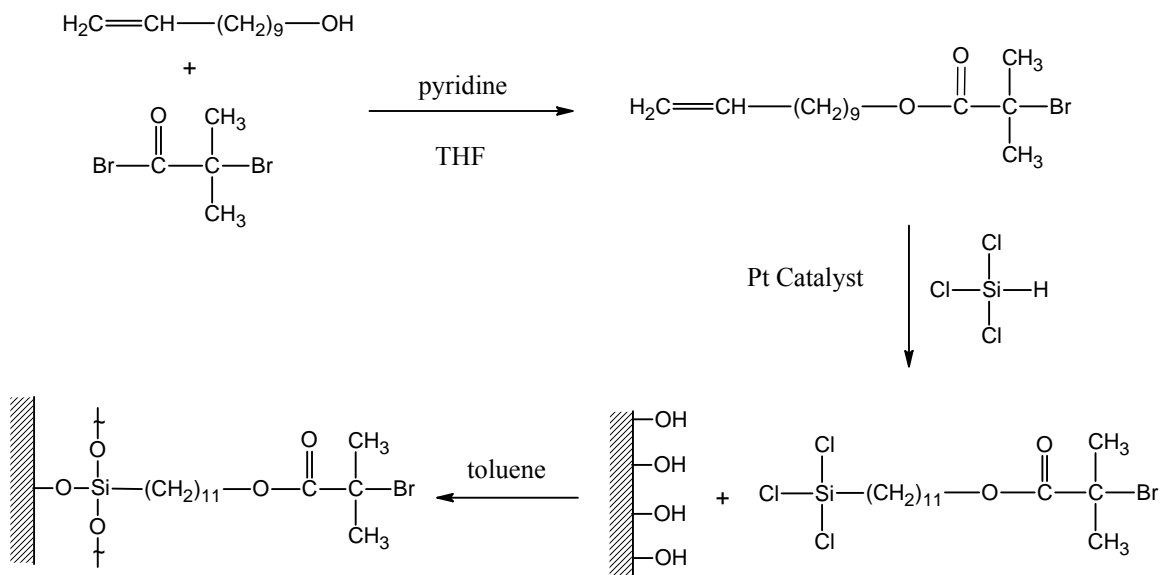
## CHAPTER IV

### RESULTS AND DISCUSSION

#### 4.1. Synthesis and Characterization of ATRP Initiator

For this research, Atom Transfer Radical Polymerization (ATRP) has been selected as the method to produce “grafting from” polymer brushes through a surface-initiated polymerization. An ATRP initiator commonly used with copper halide catalyst systems is an  $\alpha$ -bromo ester type initiator, and this type of initiator has been successfully immobilized on surfaces to prepare a wide range of polymer brushes.<sup>35,80,97,98,99,100</sup>

Matyjaszewski and coworkers<sup>91</sup> reported the synthesis of [11-(2-bromo-2-methyl)propionyloxy]undecyltrichlorosilane, which contains an  $\alpha$ -bromo ester ATRP initiating headgroup, an 11-carbon spacer, and a trichlorosilane end group which can be attached to a surface containing hydroxyl groups through a simple condensation reaction. Due to the proven versatility and facile attachment chemistry, this initiator was selected for surface initiated polymerizations (SIP) in the research reported here. The synthesis and surface deposition are shown in Scheme 4.1.



Scheme 4.1. Synthesis and Surface Immobilization of [11-(2-bromo-2-methyl)propionyloxy]undecyltrichlorosilane

The theoretical thickness of the initiator layer was calculated to be 2.0 nm based on normal bond angles and lengths, and takes into account a  $10^\circ$  tilt of the initiator chain, which has been shown for self-assembled monolayers of trichlorosilanes.<sup>101</sup> The deposited initiator layer thickness was observed to be  $2.0 \pm 0.2$  nm using ellipsometry measurements. This measurement is in good agreement with the theoretical thickness and indicates that the initiator deposited predominantly *via* the horizontal polymerization or covalent attachment mechanisms rather than through a vertical polymerization mechanism (Figure 4.1). The initiator layer was further characterized using water contact angles. The advancing and receding water contact angles were measured to be  $82^\circ \pm 2^\circ$  and  $69^\circ \pm 2^\circ$ , respectively. The value for the advancing contact angle of the  $\alpha$ -bromo ester initiator correlates reasonably well with the value of  $77.1^\circ$  reported by Kong and coworkers;<sup>102</sup> however, no value for a receding angle was given.

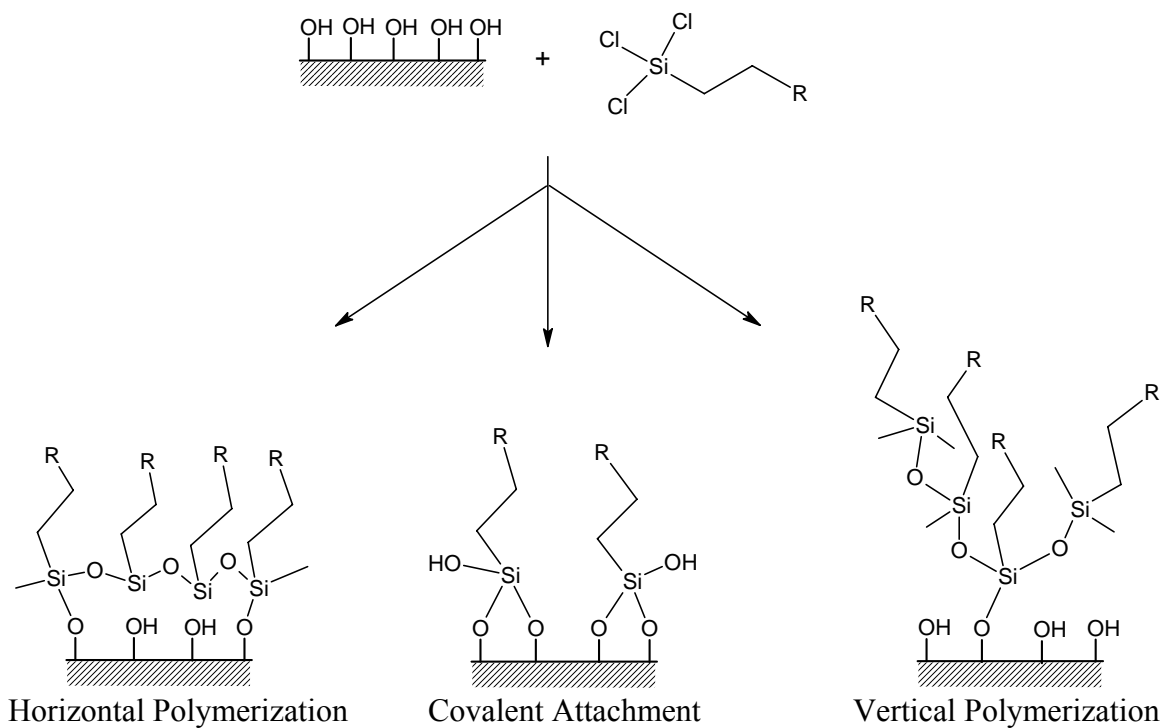


Figure 4.1. Some Reaction Products of Trichlorosilanes with Silicon Substrates<sup>103</sup>

ATR-FTIR was also used to characterize the initiator layer. A typical spectrum of the initiator layer is shown in Figure 4.2. The peaks at 2924 cm<sup>-1</sup> and 2854 cm<sup>-1</sup> are assigned to the asymmetric and symmetric C-H stretching vibrations of the CH<sub>2</sub> groups in the alkyl chain. A peak assigned to the C-H stretching vibrations of the CH<sub>3</sub> groups is barely visible as a shoulder near 3000 cm<sup>-1</sup> and the peak at 1732 cm<sup>-1</sup> is assigned to the carbonyl stretching vibration of the ester group. All of the polymer brushes synthesized in this research were prepared from surface-immobilized layers of this initiator.

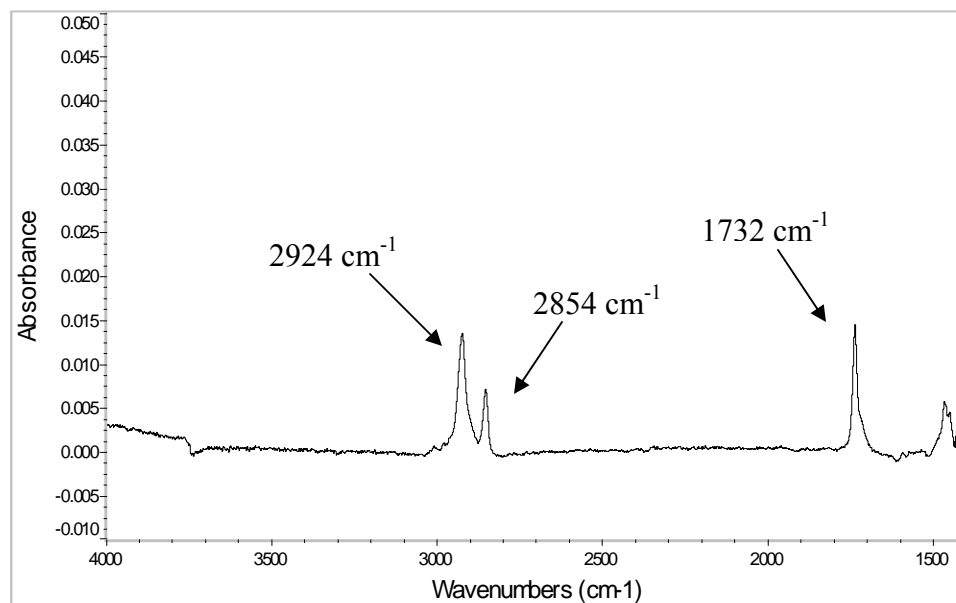
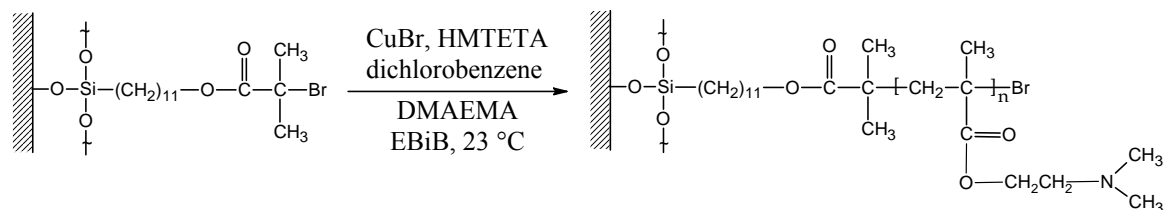


Figure 4.2. ATR-FTIR Spectrum of the Surface Immobilized ATRP Initiator

## 4.2. Synthesis and Presumptive Crosslinking of Si/SiO<sub>2</sub>//PDMAEMA-*b*-PS

### 4.2.1. Si/SiO<sub>2</sub>//PDMAEMA Brushes *via* ATRP

Poly[2-(dimethylamino)ethyl methacrylate] (PDMAEMA) brushes were synthesized according to Scheme 4.2.



Scheme 4.2. Si/SiO<sub>2</sub>//PDMAEMA Brush Synthesis

Anhydrous 1,2-dichlorobenzene was selected as a solvent due to the abundance of literature reporting the ATRP of DMAEMA using this reaction medium.<sup>67,76,104-107</sup> Other solvents such as THF,<sup>97,108,109</sup> methanol,<sup>88</sup> and aqueous solutions<sup>110-112</sup> have previously been used as well. However, a systematic study of a variety of solvents and reaction

temperatures by Zhang and coworkers<sup>76</sup> showed that lowest polydispersities were achieved at room temperature in dichlorobenzene. 1,1,4,7,10,10-Hexamethyltriethylenetetramine (HMTETA) was employed as a ligand because of a similar optimization study<sup>76</sup> and because of an extensive literature precedent.<sup>67,76,97,104,105,108</sup> Ethyl 2-bromoisobutyrate (EBiB) was added as a “free”, soluble, initiator resulting in polymerization occurring in solution as well as from the surface. The addition of EBiB has two advantages. First, molecular weight data of the free polymer has been shown to correlate well with that of the surface-bound polymer, affording important information about the ATRP mediated polymerization.<sup>62,89</sup> A second benefit of added free initiator is that it provides a high enough concentration of the deactivating Cu(II) species to control polymerization both at the surface and throughout the rest of solution.<sup>3,16,67,89</sup> Si/SiO<sub>2</sub>//PDMAEMA brushes were extracted in isopropyl alcohol to remove any free polymer formed in solution. A previous study on the transesterification of tertiary amine methacrylates suggested isopropyl alcohol may be a better solvent than methanol for this solvent extraction.<sup>113</sup>

The conditions in Scheme 4.2 afforded solution PDMAEMA with an  $M_n$  of 15,200 g/mol and PDI of 1.27 after three hours of polymerization. The corresponding Si/SiO<sub>2</sub>//PDMAEMA brush had a film thickness of 16.5 nm from ellipsometry and advancing and receding water contact angles of  $63^\circ \pm 3^\circ$  and  $51^\circ \pm 3^\circ$  respectively. An ATR-FTIR spectrum of the Si/SiO<sub>2</sub>//PDMAEMA brush is shown in Figure 4.3.

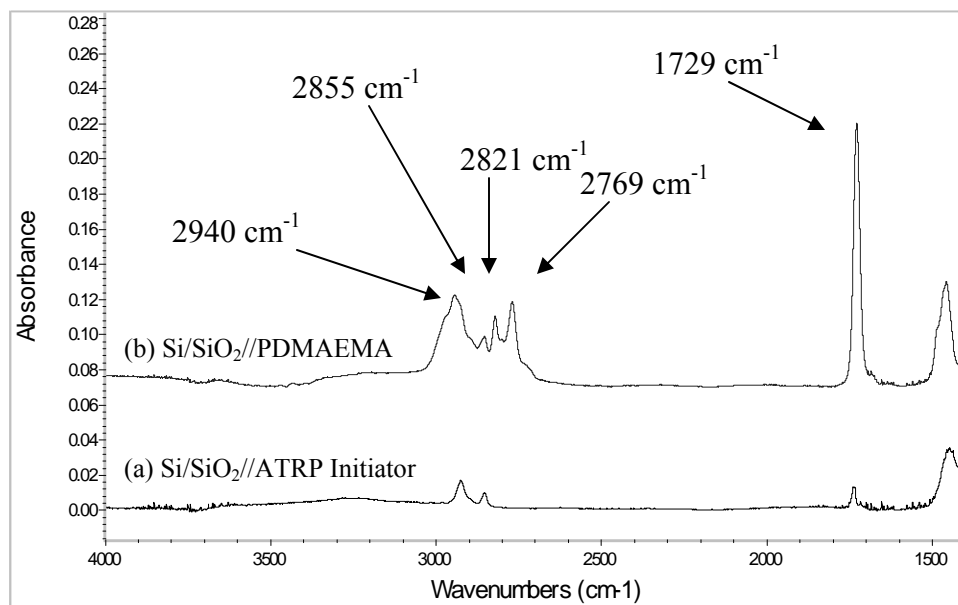


Figure 4.3. ATR-FTIR Spectrum of Si/SiO<sub>2</sub>//PDMAEMA

The peaks at 2940 cm<sup>-1</sup> and 2855 cm<sup>-1</sup> are assigned to the C-H stretching vibrations of the CH<sub>2</sub> groups in the backbone of the polymer chain and the CH<sub>2</sub> group next to the ester group of the repeat unit. A peak assigned to the C-H stretching vibrations of the CH<sub>3</sub> groups is barely visible as a shoulder near 3000 cm<sup>-1</sup>. The peaks at 2821 cm<sup>-1</sup> and 2769 cm<sup>-1</sup> are assigned to the C-H stretching vibrations of the CH<sub>2</sub> and CH<sub>3</sub> groups next to the nitrogen in the repeat unit.<sup>114</sup> The peak at 1729 cm<sup>-1</sup> is assigned to the carbonyl stretching vibration of the ester group.

#### 4.2.2. Sequential Extension of Si/SiO<sub>2</sub>//PDMAEMA Brushes

In order to examine the viability of preparing AB diblock brushes, several chain extension experiments were performed with the Si/SiO<sub>2</sub>//PDMAEMA brushes. In each case, a previously synthesized Si/SiO<sub>2</sub>//PDMAEMA brush was fully characterized before being immersed in a fresh polymerization solution under conditions identical to the first

polymerization. The underlying assumption in this experiment was that if few chain ends of the first block were to reinitiate, and the chains formed in the second block had molecular weights equal to those formed in the first, then a thinner block would result (Figure 4.4a). However, if all chain ends of the first block were to reinitiate, then under identical polymerization conditions a second block of equal thickness should be obtained (Figure 4.4b).

Perhaps the ultimate literature precedent for this kind of experiment comes from Kim and coworkers,<sup>115</sup> who repeatedly removed a PMMA brush from a polymerization, characterized it by ellipsometry, and re-immersed it in a polymerization solution to ultimately prepare a heptablock PMMA brush (Au/S//[PMMA-*b*-]<sub>6</sub>PMMA). Thickness data of each subsequent block was used to get an estimate of the re-initiation efficiency of the brush. Huang and coworkers<sup>107</sup> indirectly investigated initiation efficiency of a PDMAEMA block in the triblock Au/S//PMMA-*b*-PDMAEMA-*b*-PMMA brush by comparing PMMA layer thicknesses (polymerized under similar conditions) for the first and third blocks of the brush. Though polymerization time of the third block was 80% of the first block polymerization time, thickness of the third block was only slightly over half of the thickness of the first block.

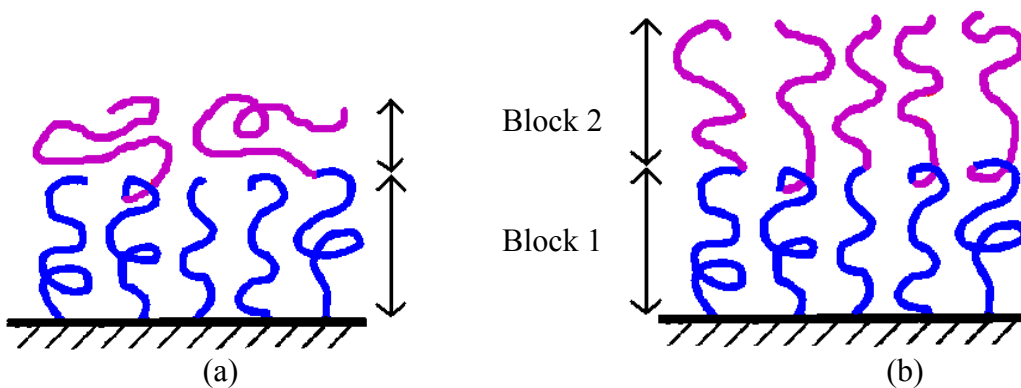


Figure 4.4. Block Extension

It is important to note that this experiment makes the assumption that living chain ends of the bottom PDMAEMA block are accessible to subsequent polymerization and that there is no effect of the initial brush on polymerization kinetics for growth of the subsequent block. Minimal brush extension was observed (Table 4.1) using the reaction conditions outlined in Scheme 4.2. This experiment was carried out to prepare a third block which also had negligible film growth. It was concluded that chain extension experiments failed due to termination events occurring, resulting in “dead” polymer chains in the brush. To circumvent this problem, deactivating  $\text{CuBr}_2$  (20 mol% compared to  $\text{CuBr}$ ) was added to shift the ATRP equilibrium further to the left hand side, lowering the instantaneous radical concentration and leading to fewer termination events. However, the data in Table 4.1 show the addition of  $\text{CuBr}_2$  gave only marginally better results. It should be noted that the error on thickness measurements is  $\pm 0.5$  nm. The negative value for thickness of the third block of the  $\text{CuBr}_2$  system is within experimental error and most likely does not reflect brush degrafting or shrinkage.

Table 4.1. Ellipsometric Measurements of Si/SiO<sub>2</sub>//PDMAEMA Brush Extension With Additional DMAEMA Monomer ( $\pm 0.5$  nm)

System	Block 1	Block 2	Block 3
1 <sup>a</sup>	11.2 nm	1.9 nm	2.4 nm
2 <sup>b</sup>	11.5 nm	3.4 nm	-0.4 nm
3 <sup>c</sup>	14.2 nm	9.5 nm	4.2 nm
4 <sup>d</sup>	7.1 nm	7.0 nm	7.8 nm

<sup>a</sup> [DMAEMA]<sub>0</sub>: [EBiB]<sub>0</sub>: [CuBr]<sub>0</sub>: [HMTETA]<sub>0</sub> = 3000:5:12:25.

<sup>b</sup> [DMAEMA]<sub>0</sub>: [EBiB]<sub>0</sub>: [CuBr]<sub>0</sub>: [CuBr<sub>2</sub>]<sub>0</sub>: [HMTETA]<sub>0</sub> = 3000:5:12:2.4:25.

<sup>c</sup> [DMAEMA]<sub>0</sub>: [EBiB]<sub>0</sub>: [CuCl]<sub>0</sub>: [HMTETA]<sub>0</sub> = 3000:5:12:25.

<sup>d</sup> [DMAEMA]<sub>0</sub>: [EBiB]<sub>0</sub>: [CuCl]<sub>0</sub>: [CuCl<sub>2</sub>]<sub>0</sub>: [HMTETA]<sub>0</sub> = 3000:5:12:2.4:25.

A well known method<sup>23</sup> for increasing the degree of control exhibited by an ATRP system is to use a chlorine based system (i.e., R-Cl and CuCl). The greater strength of the Cu-Cl bond compared to the Cu-Br bond also leads to a shift of the ATRP equilibrium to the left hand side and allows for a lower instantaneous radical concentration. This technique lead to significantly better chain extension results (Table 4.1). Indeed, adding CuCl<sub>2</sub> (20 mol% compared to CuCl) resulted in subsequent preparation of equal thickness PDMAEMA blocks. The sequential addition of PDMAEMA blocks to the brush was also observed by an increase in peak intensities of the ATR-FTIR spectrum of the brush after the preparation of each subsequent block (Figure 4.5).

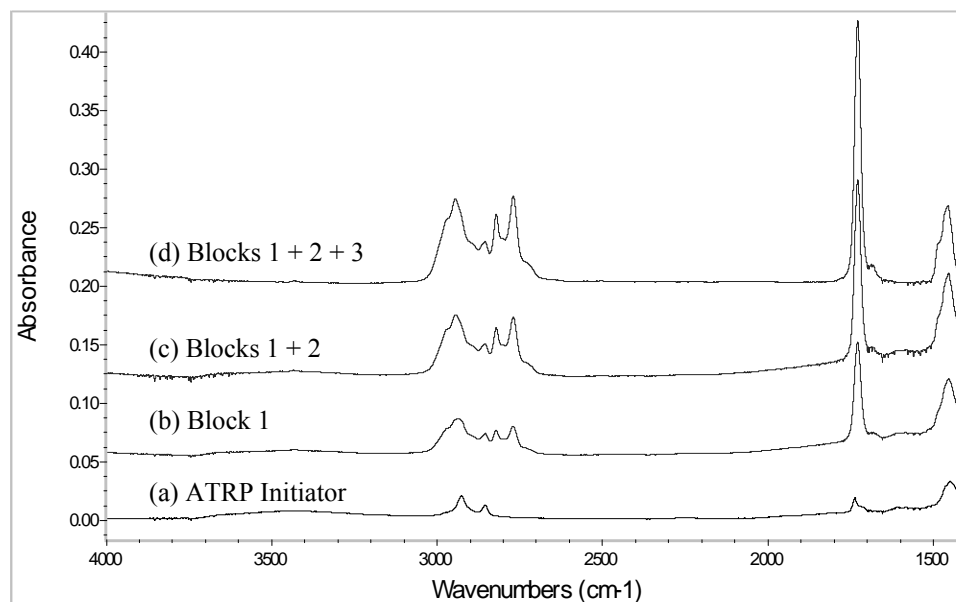
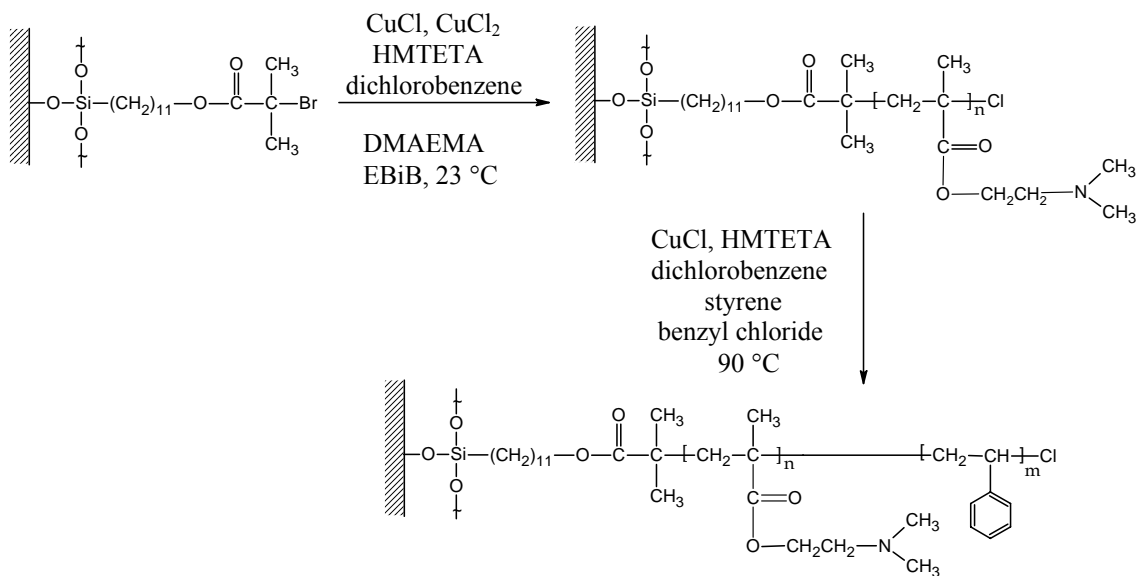


Figure 4.5. ATR-FTIR Spectrum of Si/SiO<sub>2</sub>//PDMAEMA Brush Extension

#### 4.2.3. Preparation of Si/SiO<sub>2</sub>//PDMAEMA-*b*-PS

Styrene was polymerized from a Si/SiO<sub>2</sub>//PDMAEMA brush to create Si/SiO<sub>2</sub>//PDMAEMA-*b*-PS following Scheme 4.3. The Si/SiO<sub>2</sub>//PDMAEMA brush was synthesized using the CuCl/CuCl<sub>2</sub> catalyst system described in Section 4.2.2. Because the Si/SiO<sub>2</sub>//PDMAEMA chains were chlorine-terminated, a CuCl system was also used for the subsequent styrene polymerization. The difference in R-Br and R-Cl bond strengths would dictate that this kind of mixed halogen system (i.e. R-Cl and CuBr) may give a slow initiation and faster propagation—leading to a broadening of molecular weight distribution. Though no deactivating CuCl<sub>2</sub> was directly added to the styrene polymerization, benzyl chloride (BnzCl) free initiator was added to improve control of the polymerization as outlined earlier. After polymerization, the diblock brushes were extracted in THF to remove any untethered PS chains.



Scheme 4.3. Si/SiO<sub>2</sub>//PDMAEMA-*b*-PS Brush Synthesis

The preparation of this diblock brush was monitored using ATR-FTIR (Figure 4.6). In addition to the peaks seen for PDMAEMA, the diblock brush exhibits peaks at 3083 cm<sup>-1</sup>, 3060 cm<sup>-1</sup>, and 3026 cm<sup>-1</sup> assigned to C-H stretching vibrations of the aromatic styrene ring. The appearance of peaks at 1602 cm<sup>-1</sup>, 1490 cm<sup>-1</sup>, and 1450 cm<sup>-1</sup> are assigned to the stretching vibration of the C-C bonds in the aromatic ring. The tip of the broad peak afforded by the C-H stretching vibrations of methyl and methylene groups also moves from 2940 cm<sup>-1</sup> to 2929 cm<sup>-1</sup>, reflecting the C-H bond in the polystyrene backbone.

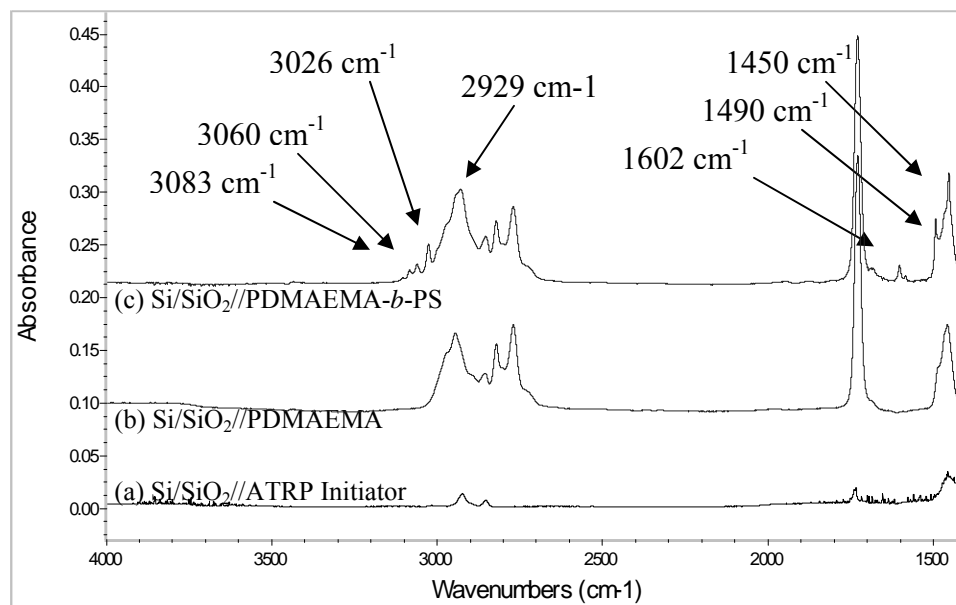


Figure 4.6. ATR-FTIR Spectrum of Si/SiO<sub>2</sub>//PDMAEMA-*b*-PS

Though the CuCl/CuCl<sub>2</sub> catalyst system was observed to afford the highest blocking efficiency for Si/SiO<sub>2</sub>//PDMAEMA brushes, the question remained as to whether a Si/SiO<sub>2</sub>//PDMAEMA brush prepared with the CuCl/CuCl<sub>2</sub> system would exhibit greater reinitiation than a Si/SiO<sub>2</sub>//PDMAEMA brush prepared with the CuBr system in forming a PS block. The goal was to create an AB diblock copolymer brush that contained a minimal amount of homopolymer. In order to answer this question, a Si/SiO<sub>2</sub>//PDMAEMA brush synthesized by each method was placed in the same styrene polymerization. Thus, using a one pot reaction, PS chains of the same molecular weight could be grown from both Si/SiO<sub>2</sub>//PDMAEMA surfaces, and any difference in PS brush thickness would then be a result of grafting density (and therefore relative amount of surface initiation) rather than a result of PS chain length. Unsurprisingly, the thickness of the resulting PS blocks indicates the PDMAEMA brush prepared using the CuCl/CuCl<sub>2</sub>

system indeed gave a much better initiation of styrene (Table 4.2). It is important to note that despite using the CuCl/CuCl<sub>2</sub> catalyst system, some homopolymer PDMAEMA chains may still exist in the optimized Si/SiO<sub>2</sub>//PDMAEMA-*b*-PS brush.

Table 4.2. Thickness of PS Extension from Si/SiO<sub>2</sub>//PDMAEMA ( $\pm 0.5$  nm)

System	PDMAEMA		PS
CuBr	16.5 nm	<div style="border: 1px solid black; padding: 5px; display: inline-block;">                     One Pot Styrene Polymerization                 </div>	4.6 nm
CuCl/CuCl <sub>2</sub>	22.8 nm		12.3 nm

GPC data (Table 4.3) was taken for the solution polymer formed in both PDMAEMA polymerizations and the styrene polymerization described in Table 4.2. Research by Kim and coworkers<sup>115</sup> has shown an approximate relationship between brush thickness and molecular weight to be 1 nm for every 1000 g/mol for an ATRP-initiated PMMA brush. Molecular weight data for the PDMAEMA solution polymer shown here closely resembles that ratio. The thickness of the PS layer initiated from the Si/SiO<sub>2</sub>//PDMAEMA-Cl brush (Table 4.2) also approximates this relationship. The narrower molecular weight distribution of the PDMAEMA-Cl system compared to the PDMAEMA-Br system is indicative of the halogen exchange technique creating a higher ratio of initiation rate to propagation rate.<sup>23</sup> A small peak at shorter elution times in the GPC trace for both PDMAEMA systems indicates some bimolecular coupling to form higher molecular weight polymer.

Table 4.3. Solution GPC Data for Si/SiO<sub>2</sub>//PDMAEMA-*b*-PS Brush Synthesis

System	Block Thickness <sup>a</sup>	Conversion <sup>b</sup>	$M_n^{\text{theo}}$ (g/mol) <sup>c</sup>	$M_n$ (g/mol)	$M_w/M_n$
PDMAEMA-Br	16.5 nm	27%	24,900	15,200 <sup>d</sup>	1.27
PDMAEMA-Cl	22.8 nm	30%	27,600	19,000 <sup>d</sup>	1.15
PS	12.3 nm	7%	6,700	10,800	1.40

<sup>a</sup> PS block thickness extended from Si/SiO<sub>2</sub>//PDMAEMA-Cl

<sup>b</sup> PDMAEMA and PS conversion determined by <sup>1</sup>H NMR and gravimetric analysis, respectively

<sup>c</sup> Theoretical molecular weights based on initiator concentration and percent conversion

<sup>d</sup> See appendix for GPC chromatograms

#### 4.2.4. Surface Rearrangement of Si/SiO<sub>2</sub>//PDMAEMA-*b*-PS

Previous studies have investigated the ability of block copolymer brush systems to undergo stimuli-responsive surface rearrangement through solvent<sup>35,36,67,107</sup> as well as thermal<sup>36</sup> treatment. For example, Zhao and Brittain<sup>67</sup> investigated a Si/SiO<sub>2</sub>//PS-*b*-PDMAEMA brush consisting of a 27 nm PS bottom block and a 3 nm PDMAEMA top block. Treatment of this brush with THF/H<sub>2</sub>O (1/1, v/v) gave an advancing water contact angle of 63° while treatment with cyclohexane gave an advancing water contact angle of 98°. These changes were reversible by immersion of the brush in the opposite solvent. For the present research, the diblock brush is composed of a larger PDMAEMA bottom block and a shorter PS top block. Three different Si/SiO<sub>2</sub>//PDMAEMA-*b*-PS diblocks were synthesized so that the PDMAEMA block thickness was held relatively constant while the thickness of the PS block was varied. Advancing ( $\theta_a$ ) and receding ( $\theta_r$ ) water contact angles were used to probe the surface rearrangement ability of the three diblock brushes (Table 4.4).

Table 4.4. Surface Rearrangement of Si/SiO<sub>2</sub>/PDMAEMA-*b*-PS ( $\theta = \pm 3^\circ$ )

Treatment	PS = 4.7 nm		PS = 11.1 nm		PS = 14.0 nm	
	$\theta_a$	$\theta_r$	$\theta_a$	$\theta_r$	$\theta_a$	$\theta_r$
1 <sup>st</sup> Thermal <sup>a</sup>	85	68	90	75	91	75
1 <sup>st</sup> Methanol	55	46	58	46	60	48
2 <sup>nd</sup> Thermal <sup>a</sup>	86	69	89	72	92	75
2 <sup>nd</sup> Methanol	54	40	56	43	58	44
Cyclohexane	82	63	90	70	90	71

<sup>a</sup> Thermal annealing done at 115 °C

Thermal annealing was used to allow the more hydrophobic PS block to migrate to the surface of the brush due to the relative hydrophobicity of air. It was necessary to anneal the brush at or above the glass transition temperature ( $T_g$ ) of the block with the higher  $T_g$  so that the brush would have sufficient mobility for rearrangement.<sup>36</sup> The reported  $T_g$  values for PDMAEMA and PS are 19 °C and 100 °C, respectively.<sup>95</sup> Reports in literature have varying conclusions about the effect, if any, surface tethering has on  $T_g$  of chains in a brush. Lemieux and coworkers<sup>116</sup> found that 50-90 nm poly(styrene-*co*-2,3,4,5,6-pentafluorostyrene) brushes prepared by a surface-initiated free radical polymerization had an almost identical  $T_g$  as the bulk polymer. However, Prucker and coworkers<sup>117</sup> found that the  $T_g$  for poly(methyl methacrylate) (PMMA) brushes less than 100 nm thick prepared by a surface-initiated free radical polymerization was actually less than the  $T_g$  of the bulk polymer. Interestingly, Yamamoto and coworkers<sup>10</sup> have found that the  $T_g$  for PMMA brushes prepared by surface-initiated ATRP is higher than that of the bulk polymer. Brushes that were 15-25 nm thick exhibited a  $T_g$  increase up to 20 °C.

The  $T_g$  increase was concluded to be due to the restricted mobility of the densely grafted chains. Tate and coworkers<sup>118</sup> also observed a 25 °C  $T_g$  increase for a 43 nm thick PS brush made by grafting end-functionalized chains to a substrate. After reviewing this literature on the  $T_g$  of brushes, it was decided that the Si/SiO<sub>2</sub>//PDMAEMA-*b*-PS diblocks would be annealed at 115 °C—slightly above the  $T_g$  of PS in case of any  $T_g$  increase due to tethering of chains.

Each brush first underwent thermal treatment before contact angle measurements were performed. An advancing water contact angle ( $\theta_a$ ) for a PS homopolymer brush has typically been found to be  $94^\circ \pm 3^\circ$  during this research, which agrees well with other literature values for advancing contact angles of PS brushes:  $91^\circ$ ,<sup>65</sup>  $99 \pm 2^\circ$ ,<sup>99</sup>  $100 \pm 1^\circ$ ,<sup>26</sup> and  $92 \pm 2^\circ$ .<sup>68</sup> The two brushes with thicker PS layers had advancing contact angles near the typical PS value when they were extended by the first thermal annealing treatment. The brush with the thinnest PS layer, however, showed a significantly lower advancing contact angle of  $85^\circ$ . This lower contact angle may be due to incomplete surface coverage or aggregation of the PS chains. The brushes were then immersed in methanol (a good solvent for PDMAEMA but a poor solvent for PS) to draw the PDMAEMA segments to the surface. Methanol has been used previously<sup>107</sup> to promote migration of the PDMAEMA segments of a Au/S//PMMA-*b*-PDMAEMA-*b*-PMMA triblock brush to the brush surface.

Advancing and receding water contact angles for a Si/SiO<sub>2</sub>//PDMAEMA homopolymer brush in this research have been typically found to be  $58^\circ \pm 3^\circ$  and  $48^\circ \pm 3^\circ$  respectively, though other research<sup>3</sup> has found advancing and receding contact angles of PDMAEMA brushes prepared by ATRP to be as low as  $35^\circ$  and  $10^\circ$ ,

respectively. Yu and coworkers<sup>97</sup> found a Si/SiO<sub>2</sub>//PDMAEMA brush prepared by ATRP to have a static water contact angle of  $48^\circ \pm 3^\circ$ ; however, no advancing or receding angles were given. All three diblock brushes exhibited water contact angles characteristic of a PDMAEMA brush after the methanol treatment. This “switching” process was found to be reversible, as demonstrated by contact angles from a second cycle of thermal annealing and subsequent methanol treatment. It is interesting to note that slightly lower contact angles were observed after methanol immersion for the brush with the thinnest PS layer. This effect indicates that the brush with the thinner top block may be able to switch more fully. A proportionally much larger bottom block may migrate to the surface of the brush and better shield chains of the top block from the surrounding solvent. It can easily be envisioned that in an extreme case, a brush with a proportionally large enough top block would not be able to switch at all because the bottom block chains would not be long enough to reach the surface of the brush.

Another method of drawing the PS chains to the surface is by immersion in a good solvent for PS but a poor solvent for PDMAEMA. After “switching” in methanol, the brushes were immersed in cyclohexane to again draw the PS chains to the surface. Contact angles more characteristic of a PS brush ( $\theta_a = 94^\circ \pm 3^\circ$ ) were again obtained. As found with thermal treatment, slightly lower contact angles were observed for the brush with the thinnest PS layer. Again, these lower contact angles may be due to the thin PS block not completely covering the PDMAEMA layer. In this case the water droplet would “see” a small amount of the more hydrophilic PDMAEMA surface and produce a lower contact angle. For a control experiment, homopolymer Si/SiO<sub>2</sub>//PDMAEMA and Si/SiO<sub>2</sub>//PS brushes were subjected to methanol and cyclohexane treatments for one hour

at 60 °C. No experimentally significant change in contact angles was observed after treatment with each solvent.

AFM measurements were taken of Si/SiO<sub>2</sub>//PDMAEMA-*b*-PS (PDMAEMA = 22.7 nm, PS = 3.9 nm) to observe surface Root-Mean-Square (RMS) roughness, which is defined as the root-mean-square of the height deviations taken from the mean data plane. The thermally extended brush (Figure 4.7a) had an RMS roughness of 1.9 nm. After switching in methanol (Figure 4.7b), the RMS roughness was found to be 1.5 nm. Little change in surface roughness occurred after switching. The formation of micellar structures by immersion of tethered diblocks in block selective solvents has previously been observed using AFM to look for any increase in surface roughness due to brushes going from a somewhat extended to switched morphology.<sup>27,35</sup> In fact, instead of seeing the previously observed pattern of “bumps” or pinned micelles,<sup>27</sup> the switched surface seemingly has small pits or holes.

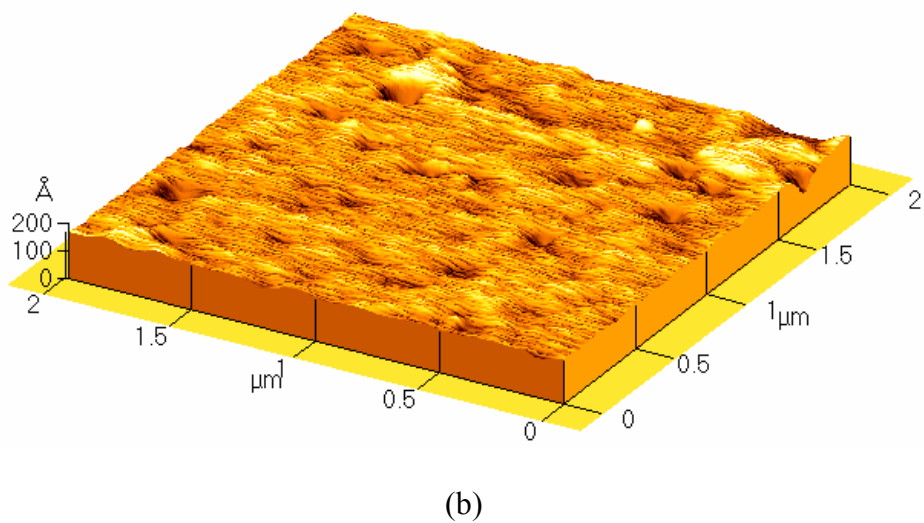
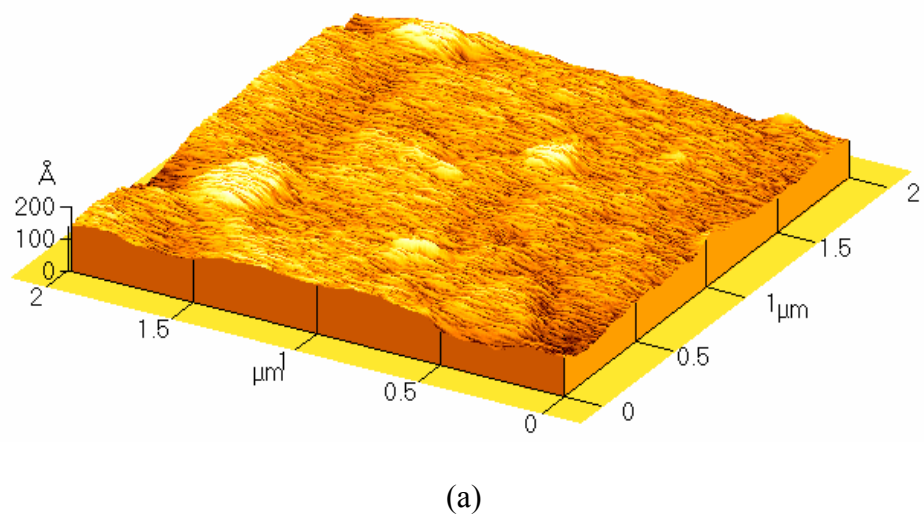


Figure 4.7. AFM Images of Si/SiO<sub>2</sub>//PDMAEMA-*b*-PS After (a) Thermal Annealing and (b) Methanol Treatment

The lack of increase in surface roughness is most likely due to the low  $T_g$  of the PDMAEMA block. As previously stated, the  $T_g$  of bulk PDMAEMA is 19 °C. Because the glass transition temperature of the larger block of the brush is presumably at or below

room temperature, the brush may undergo long range segmental relaxation and prevent rough surface features from being observed with the AFM.

#### 4.2.5. Presumptive Crosslinking of Si/SiO<sub>2</sub>//PDMAEMA-*b*-PS

The goal of this project was to produce diblock brushes that would create a pinned micelle morphology when switched in a solvent which prefers the bottom block. While this effect has previously been observed<sup>27,35</sup> for other diblock systems, the current research seeks to utilize a functional polymer as the bottom block in order to crosslink the switched morphology, thus making any patterning as well as surface composition permanent. The extended brush (Figure 4.8a) is first switched (Figure 4.8b) in a solvent that prefers the bottom block. A crosslinking agent can then be added to the switching solvent to permanently crosslink the switched brush (Figure 4.8c).

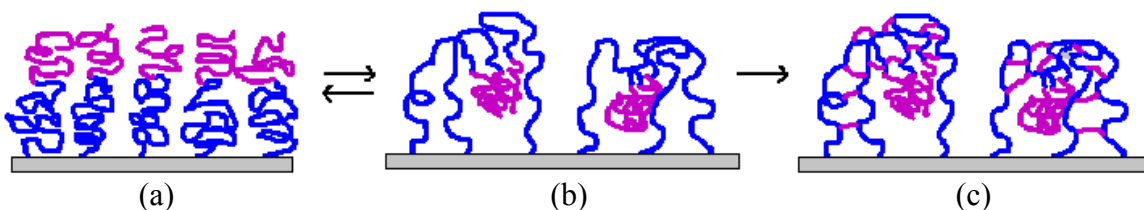


Figure 4.8. Proposed Crosslinking of Pinned Micelles

Various groups have previously crosslinked PDMAEMA shells of polymer micelles in solution. Bütün and coworkers<sup>119</sup> prepared partially quaternized poly[2-(dimethylamino)ethyl methacrylate]-*block*-poly[*N*-(morpholino)ethyl methacrylate] (PDMAEMA-*b*-PMEMA). This diblock formed micelles containing PDMAEMA shells and PMEMA cores in an aqueous solution at 60 °C. The difunctional alkyl halide 1,2-bis-(2-iodoethoxy)ethane was used to crosslink the PDMAEMA shells. Because the PMEMA block exhibited inverse temperature-solubility behavior, the uncrosslinked

micelles would dissociate when cooled to 25 °C as the PMEMA became solubilized. However, the crosslinked core-shell micelles retained their structure when cooled to 25 °C. This crosslinking locked in the micelle structure despite the fact that: the PDMAEMA chains were partially quaternized with methyl iodide to begin with (to improve hydrophilicity), some endgroups of the crosslinking agent probably remained unreacted after crosslinking, and some intrachain reaction was likely. Bütün and coworkers,<sup>120,121</sup> Liu and coworkers,<sup>122</sup> and Zhang and coworkers<sup>123</sup> prepared other core-shell micelles in which a PDMAEMA shell was crosslinked with the same difunctional alkyl iodide.

Though a pinned micelle morphology was not observed with the Si/SiO<sub>2</sub>//PDMAEMA-*b*-PS system in the current research, the brush was still exposed to a solution of difunctional crosslinking agent in an attempt to lock in surface composition and prevent further rearrangement of the brush. A Si/SiO<sub>2</sub>//PDMAEMA-*b*-PS brush was first treated with methanol to switch the brush before being immersed into a 1% solution of 1,2-bis-(2-iodoethoxy)ethane in methanol for crosslinking for 4 hours at 60 °C. Reaction of the PDMAEMA was indicated by a decrease in C-H stretching intensity of the tertiary amine group peaks at 2821 cm<sup>-1</sup> and 2769 cm<sup>-1</sup>, as well as the appearance of broad peaks at 2677 cm<sup>-1</sup> and 2455 cm<sup>-1</sup> assigned to the stretching vibrations of the quaternized amine groups. The change in appearance of the C-H stretching vibration peak at 2929 cm<sup>-1</sup> is most likely due to the addition of CH<sub>2</sub> groups of the crosslinker molecule (Figure 4.9). Interestingly, no significant change in brush thickness was observed after exposure to the crosslinking agent.

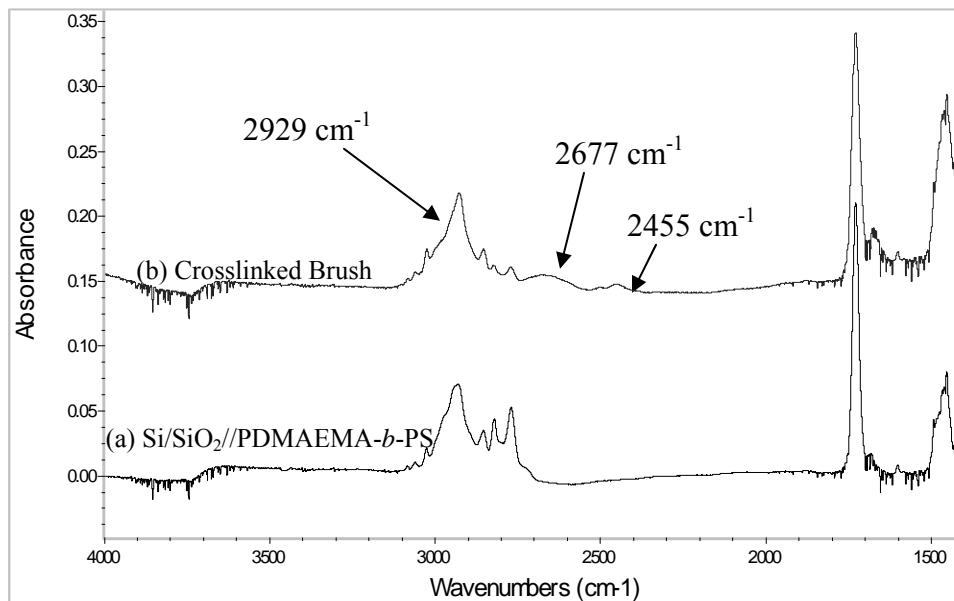


Figure 4.9. ATR-FTIR Spectrum of Si/SiO<sub>2</sub>//PDMAEMA-*b*-PS After Presumptive Crosslinking

While Figure 4.9 shows evidence of reaction of the PDMAEMA with the diiodo crosslinking agent, the spectrum does not provide any information about how many crosslinker molecules reacted at both ends, and whether or not crosslinker molecules reacted with two tertiary amine groups of the same polymer chain or tertiary amine groups on two different chains (Figure 4.10). Overlapping peaks in the IR spectrum also prevent reasonable quantitation of the amount of tertiary amine groups that have reacted.

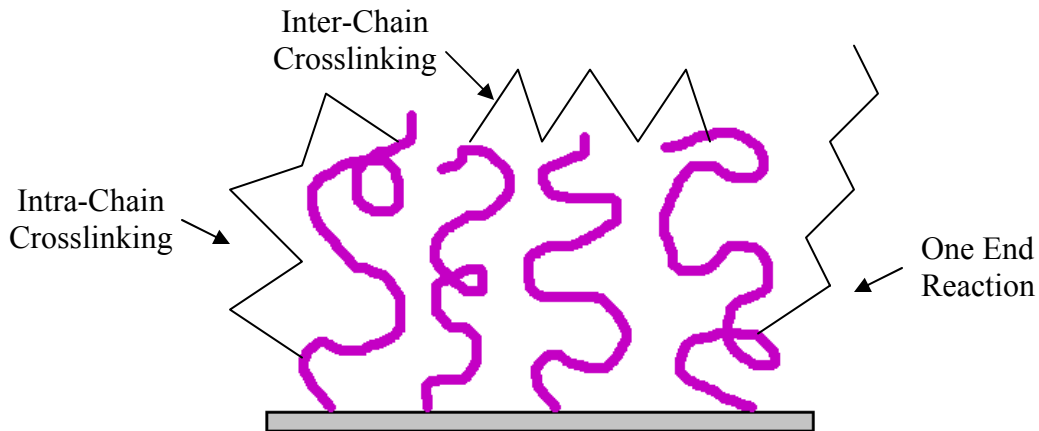


Figure 4.10. Possible Crosslinker Reactions With a Polymer Brush

Water contact angle measurements were used to probe the crosslinking of two diblock brushes with different length PS blocks (Table 4.5).

Table 4.5. Presumptive Crosslinking of Si/SiO<sub>2</sub>//PDMAEMA-*b*-PS ( $\theta = \pm 3^\circ$ )

Treatment	PS = 5.4 nm		PS = 10.7 nm		PS = 15.1 nm	
	$\theta_a$	$\theta_r$	$\theta_a$	$\theta_r$	$\theta_a$	$\theta_r$
Cyclohexane	85	67				
Methanol	59	49				
CROSSLINK (Methanol)	58	49	57	45	62	49
Cyclohexane	60	55	75	61	65	51

As a control, a homopolymer PDMAEMA brush was also exposed to the crosslinking agent. For reference, water contact angle values of the diblock with the thinnest PS layer are given after both cyclohexane and methanol treatment; values for other diblocks can be found in Table 4.4. Though contact angle data for the brush with the thinnest PS layer remains virtually unchanged when the presumptively crosslinked brush is treated with

cyclohexane, the brush with a larger PS layer gives a significantly larger value— indicating that presumptive crosslinking did not make surface composition permanent. As expected, contact angles for the presumptively crosslinked homopolymer brush show little change after cyclohexane treatment.

Several possible explanations exist for why the Si/SiO<sub>2</sub>//PDMAEMA-*b*-PS brush treated with crosslinking agent was still able to undergo surface composition changes in response to solvent treatment. One possibility is that a large amount of the crosslinking molecules only reacted with the brush at one end. Or there may have been a high degree of intra-chain crosslinking, though most likely there would not be any more than in the crosslinking of the shell of a micelle in solution, which was found to be successful.<sup>120-123</sup> One other possibility is that the structure of the switched brush is not fully understood, and the structure is not conducive to locking in surface composition through crosslinking of the PDMAEMA chains. To circumvent this last problem, a diblock brush containing a tertiary amine functional poly[2-(dimethylamino)ethyl acrylate] (PDMAEA) top block and an unreactive PS bottom block was synthesized and crosslinked. This way, the brush could be exposed to the crosslinking agent in a more extended state, a conformation of better-known structure.

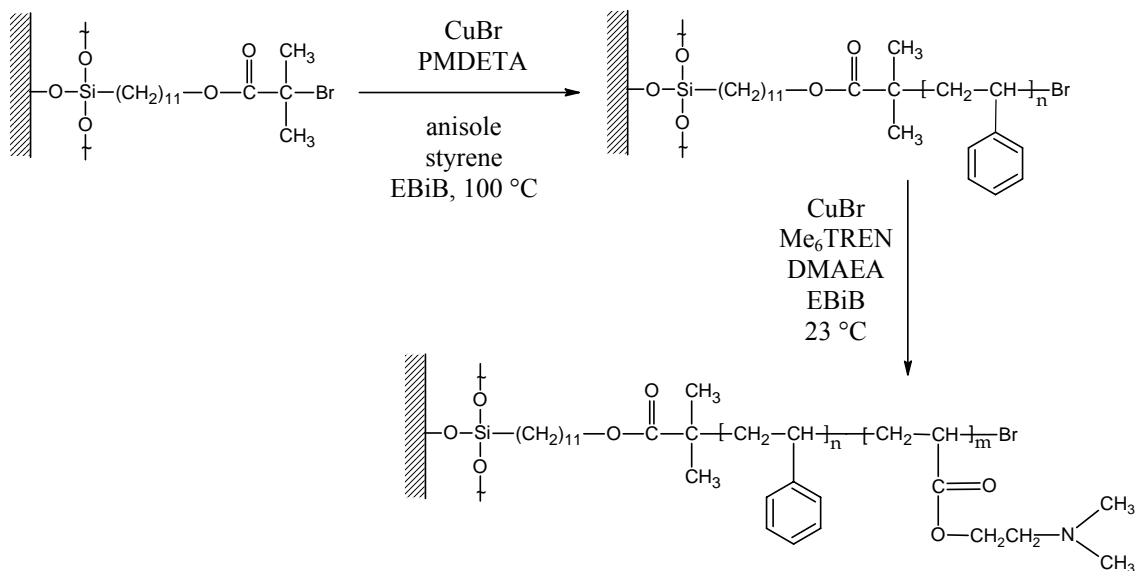
#### 4.3. Synthesis and Presumptive Crosslinking of Si/SiO<sub>2</sub>//PS-*b*-PDMAEA

Si/SiO<sub>2</sub>//PS-*b*-PDMAEA was synthesized to investigate the switching ability of a diblock brush after crosslinking its top block, and observe any relationship with crosslinkable layer thickness. The order of monomer addition in ATRP for efficient chain extension is not important between styrenes and acrylates, but methacrylates should

not follow polystyrene blocks.<sup>23</sup> Therefore, the tertiary amine acrylate DMAEA was used instead of its methacrylate counterpart to extend the Si/SiO<sub>2</sub>//PS brush.

#### 4.3.1. Si/SiO<sub>2</sub>//PS-*b*-PDMAEA Brushes *via* ATRP.

Si/SiO<sub>2</sub>//PS-*b*-PDMAEA brushes were synthesized according to Scheme 4.4.



Scheme 4.4. Si/SiO<sub>2</sub>//PS-*b*-PDMAEA Brush Synthesis

Styrene polymerization conditions were similar to those used previously<sup>35,99,100</sup> for the preparation of Si/SiO<sub>2</sub>//PS brushes which were later chain extended with various monomers. The brushes were extracted in THF to remove any untethered PS chains before being characterized. Conditions used for extending the Si/SiO<sub>2</sub>//PS brushes with DMAEA were similar to those used by Zeng and coworkers,<sup>124</sup> who compared a variety of ligands including PMDETA, HMTETA, bpy, and Me<sub>6</sub>TREN using the CuBr system for the ATRP of DMAEA. Me<sub>6</sub>TREN was found to be the only ligand with which polymerization occurred, albeit with high polydispersities. Quaternization of the tertiary amine group of the monomer or polymer by the carbon-bromine chain end was thought to

play a significant role in chain termination during the polymerization. Untethered PDMAEA was removed from the brush by extraction in isopropanol. The preparation of the Si/SiO<sub>2</sub>//PS-*b*-PDMAEA brush was monitored using ATR-FTIR (Figure 4.11).

Molecular weight data of the polymer formed in solution is shown in Table 4.6. The styrene polymerization appeared to be very well controlled, as evidenced by a very narrow polydispersity and very good agreement between theoretical and experimental molecular weights. The PS data closely matches the correlation of brush thickness to molecular weight as 1 nm for every 1,000 g/mol. The DMAEA polymerization produced solution polymer having high polydispersity and a large peak at shorter elution times in the GPC trace, indicating a significant amount of higher molecular weight material.

Table 4.6. Solution GPC Data for Si/SiO<sub>2</sub>//PS-*b*-PDMAEA Brush Synthesis

System	Block Thickness	Conversion <sup>a</sup>	$M_n^{\text{theo}}$ (g/mol) <sup>b</sup>	$M_n$ (g/mol)	$M_w/M_n$
PS	28.8 nm	35%	28,800	28,900	1.07
PDMAEA	7.0 nm	6%	10,800	14,600 <sup>c</sup>	1.57

<sup>a</sup> PS and PDMAEA conversion determined by gravimetric analysis and <sup>1</sup>H NMR, respectively

<sup>b</sup> Theoretical molecular weights based on initiator concentration and percent conversion

<sup>c</sup> See appendix for GPC chromatograms

#### 4.3.2. Surface Rearrangement and Presumptive Crosslinking of Si/SiO<sub>2</sub>//PS-*b*-PDMAEA

Converse to the previous Si/SiO<sub>2</sub>//PDMAEMA-*b*-PS system, a polar solvent (methanol or isopropanol) was used to order the more polar PDMAEA top block to the surface of the brush and the nonpolar cyclohexane was used to switch the brush. Even for the case of the brush having a very thin PDMAEA top block, cyclohexane treatment was not able to fully switch the brush and give water contact angles characteristic of a PS layer ( $\theta_a = 94^\circ \pm 3^\circ$ ). However, after treatment with isopropanol or methanol, both

brushes gave contact angles characteristic of a Si/SiO<sub>2</sub>//PDMAEA homopolymer brush ( $\theta_a = 53^\circ \pm 3^\circ$ ,  $\theta_r = 40^\circ \pm 3^\circ$ ) (Table 4.7).

After samples of the brushes had been treated with methanol, they were exposed to solutions of the crosslinker 1,2-bis-(2-iodoethoxy)ethane in an attempt to crosslink the PDMAEA chains. This experiment was repeated with a more polar 75/25, v/v methanol/water mixture. In both cases the presumptive crosslinking seemed to have little effect on solvent switching (Table 4.7). Treatment with cyclohexane presumably increased PS character of the surface of the brush, as evidenced by an increase in contact angles. For comparison, a Si/SiO<sub>2</sub>//PDMAEA homopolymer brush was also exposed to the crosslinking agent under the same conditions in methanol. Water contact angles remained unchanged after subsequent treatment with cyclohexane or isopropanol.

Table 4.7. Rearrangement and Presumptive Crosslinking of Si/SiO<sub>2</sub>//PS-*b*-PDMAEA  
( $\theta = \pm 3^\circ$ )

Treatment	PDMAEA = 4.2 nm		PDMAEA = 7.0 nm		PDMAEA = 14.5 nm	
	<u>PS = 24.1 nm</u>		<u>PS = 28.8 nm</u>		<u>PS = 27.5 nm</u>	
	$\theta_a$	$\theta_r$	$\theta_a$	$\theta_r$	$\theta_a$	$\theta_r$
1 <sup>st</sup> Isopropanol	54	44			55	45
1 <sup>st</sup> Cyclohexane	82	69			68	60
2 <sup>nd</sup> Isopropanol	56	46			55	45
2 <sup>nd</sup> Cyclohexane	81	65			67	56
CROSSLINK (Methanol)	55	46	53	40	54	41
Cyclohexane	71	60	66	53	59	46
CROSSLINK (Methanol/H <sub>2</sub> O)	45	35	51	40	50	40
Cyclohexane	73	60	78	64	69	59

Diblock preparation and presumptive crosslinking was monitored with ATR-FTIR (Figure 4.11). Figure 4.11b shows typical peaks for a Si/SiO<sub>2</sub>//PS brush. The addition of a PDMAEA block to the brush (Figure 4.11c) is evidenced by the appearance of C-H stretching vibrations in the 2800 cm<sup>-1</sup> region assigned to the tertiary amine group as well as the carbonyl stretching vibration of the ester group at 1734 cm<sup>-1</sup>. The peaks at 2800 cm<sup>-1</sup> disappear after presumptive crosslinking (Figure 4.11d) (indicating quaternization of the amine), however, the carbonyl stretching peak remains, indicating that loss of the amine peaks was not due to cleavage of the PDMAEA block from the brush. It is interesting to note, as in the case of presumptive crosslinking of Si/SiO<sub>2</sub>//PDMAEMA-*b*-

PS brushes, that no significant increase in brush thickness was observed after crosslinking.

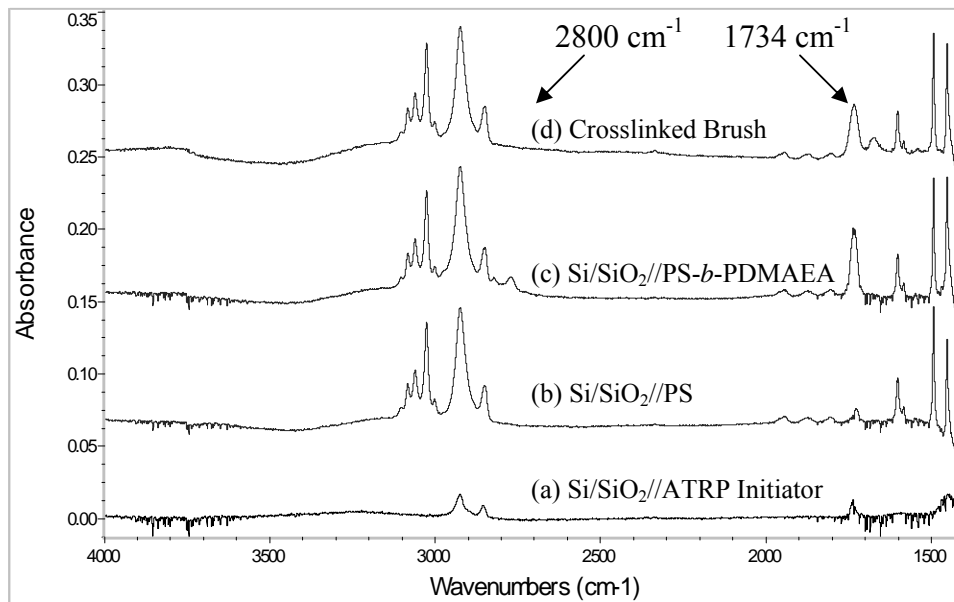
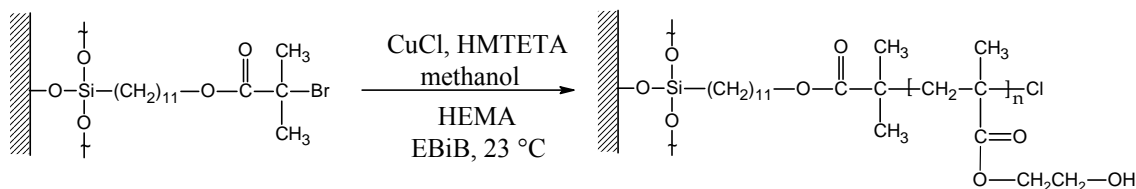


Figure 4.11. ATR-FTIR Spectrum of Si/SiO<sub>2</sub>//PS-*b*-PDMAEA After Presumptive Crosslinking

#### 4.4. Synthesis and Presumptive Crosslinking of Si/SiO<sub>2</sub>//PHEMA-*b*-PS

##### 4.4.1. Si/SiO<sub>2</sub>//PHEMA Brushes *via* ATRP

Poly(2-hydroxyethyl methacrylate) (PHEMA) brushes were synthesized according to Scheme 4.5.



Scheme 4.5. Si/SiO<sub>2</sub>//PHEMA Brush Synthesis

The ATRP of HEMA has primarily been performed in aqueous<sup>75,80,88,125-127</sup> and alcoholic<sup>74,75,88</sup> media at room temperature, and has typically employed bpy as a ligand. Methanol was chosen as a solvent because the addition of water to an ATRP has been found to increase polymerization rate,<sup>80</sup> however, possibly at the expense of control of polymerization.<sup>75,88</sup> This appears to be the first report of the ATRP of HEMA using HMTETA as a ligand. As with previous brush syntheses, EBiB free initiator was added so that polymerization occurred in solution as well as on the surface. Si/SiO<sub>2</sub>//PHEMA brushes were extracted in methanol to remove any untethered polymer from the brush before characterization.

The conditions in Scheme 4.5 afforded solution PHEMA with an  $M_n$  of 57,900 g/mol and PDI of 2.46 after only 35 minutes of polymerization. This extremely high polydispersity was due to a bimodal peak distribution in the GPC chromatogram—presumably the smaller shoulder peak at shorter elution indicates some bimolecular coupling to form higher molecular weight polymer. The corresponding Si/SiO<sub>2</sub>//PHEMA brush had a film thickness of 19.2 nm from ellipsometry and advancing and receding water contact angles of  $54^\circ \pm 3^\circ$  and  $39^\circ \pm 3^\circ$ , respectively. An ATR-FTIR spectrum of the Si/SiO<sub>2</sub>//PHEMA brush is shown in Figure 4.12.

#### 4.4.2. Sequential Extension of Si/SiO<sub>2</sub>//PHEMA Brushes

In order to examine the viability of preparing AB diblock brushes using PHEMA as a bottom block, several chain extension experiments were performed with Si/SiO<sub>2</sub>//PHEMA brushes. As in previous chain extension experiments, a Si/SiO<sub>2</sub>//PHEMA brush was fully characterized before being immersed in a fresh HEMA

polymerization solution under conditions identical to the first polymerization. Block thickness data (Table 4.8) was used to evaluate the re-initiation efficiency of three ATRP catalyst systems.

Table 4.8. Ellipsometric Measurements of Si/SiO<sub>2</sub>//PHEMA Brush Extension With Additional HEMA Monomer ( $\pm 0.5$  nm)

System	Block 1	Block 2	Block 3
1 <sup>a</sup>	18.8 nm	11.9 nm	10.2 nm
2 <sup>b</sup>	8.4 nm	6.6 nm	4.8 nm
3 <sup>c</sup>	7.7 nm	7.0 nm	5.5 nm

<sup>a</sup> [HEMA]<sub>0</sub>: [EBiB]<sub>0</sub>: [CuCl]<sub>0</sub>: [HMTETA]<sub>0</sub> = 4100:5:12:25.

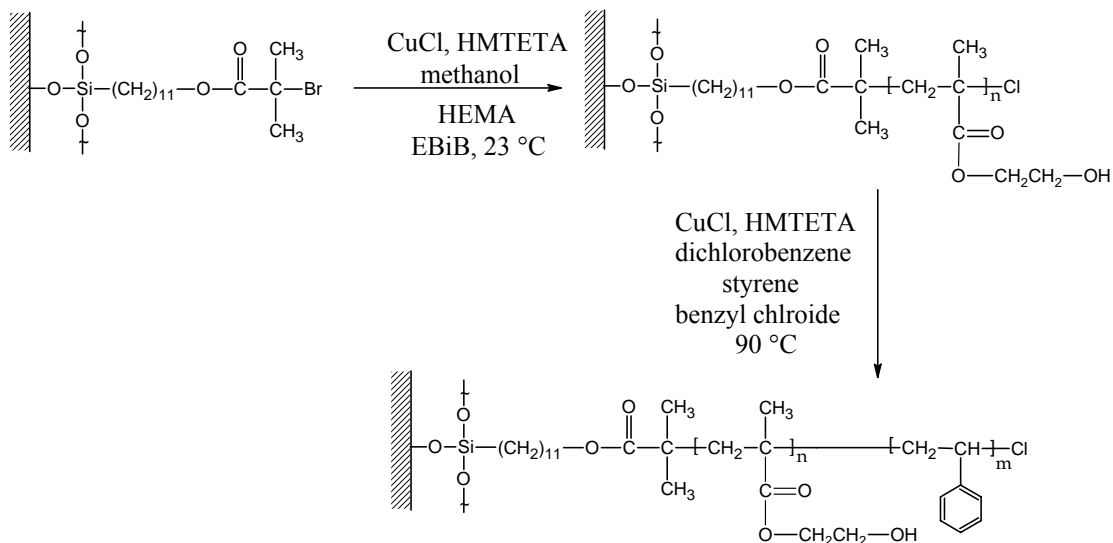
<sup>b</sup> [HEMA]<sub>0</sub>: [EBiB]<sub>0</sub>: [CuCl]<sub>0</sub>: [CuCl<sub>2</sub>]<sub>0</sub>: [HMTETA]<sub>0</sub> = 4100:5:12:2.4:25.

<sup>c</sup> [HEMA]<sub>0</sub>: [EBiB]<sub>0</sub>: [CuCl]<sub>0</sub>: [CuCl<sub>2</sub>]<sub>0</sub>: [HMTETA]<sub>0</sub> = 4100:5:4:8:25.

Reasonable brush extension was observed with CuCl and no extra added deactivating Cu(II) species other than that produced from the addition of free initiator (System 1). In an attempt to optimize the system further, some CuCl<sub>2</sub> (20 mol% compared to CuCl) was added along with the free initiator (system 2). Though a substantial third block was still able to be prepared, the thickness of each successive block still decreased. Even though more CuCl<sub>2</sub> (200% compared to CuCl) was added in System 3, similar chain extension results were obtained. Converse to the PDMAEMA chain extension experiments, it appears that the addition of the deactivating Cu(II) species in this PHEMA system had negligible effect on the ability of Si/SiO<sub>2</sub>//PHEMA brushes to reinitiate HEMA polymerization.

#### 4.4.3. Preparation of Si/SiO<sub>2</sub>//PHEMA-*b*-PS

Styrene was polymerized from PHEMA brushes to create Si/SiO<sub>2</sub>//PHEMA-*b*-PS following Scheme 4.6.



Scheme 4.6. Si/SiO<sub>2</sub>//PHEMA-*b*-PS Brush Synthesis

Because the Si/SiO<sub>2</sub>//PHEMA chains were chloride-terminated, a CuCl system was used for the styrene polymerization. No deactivating CuCl<sub>2</sub> was directly added to the styrene polymerization; however, BnzCl free initiator was added to aid in control of the polymerization. Styrene blocks were polymerized from Si/SiO<sub>2</sub>//PHEMA brushes made by both the CuCl system and the highly deactivating CuCl/CuCl<sub>2</sub> system in a one pot polymerization. The two Si/SiO<sub>2</sub>//PHEMA brushes grew equal thickness PS layers (Table 4.9), confirming the idea that the addition of Cu(II) to the HEMA polymerizations did not increase the ability of Si/SiO<sub>2</sub>//PHEMA brush to reinitiate polymerization.

Table 4.9. Thickness of PS Extension from Si/SiO<sub>2</sub>//PHEMA ( $\pm 0.5$  nm)

System	PHEMA		PS
(1) CuCl	19.2 nm	↘	5.6 nm
(3) CuCl/CuCl <sub>2</sub>	25.6 nm	↗	5.6 nm

One Pot Styrene Polymerization

GPC data (Table 4.10) were taken for the solution polymer formed in each HEMA polymerization and the styrene polymerization described in Table 4.9. Seemingly high values for molecular weight and molecular weight distribution of the PHEMA samples were obtained due to integrating a bimodal peak in the case of the CuCl system and a trimodal peak in the case of the CuCl/CuCl<sub>2</sub> system. The smaller peaks were seen at shorter elution times—presumably due to bimolecular termination occurring during polymerization.

Table 4.10. Solution GPC Data for Si/SiO<sub>2</sub>//PHEMA-*b*-PS Brush Synthesis

System	Block Thickness <sup>c</sup>	Conversion <sup>f</sup>	$M_n^{\text{theo}}$ (g/mol) <sup>g</sup>	$M_n$ (g/mol)	$M_w/M_n$
PHEMA <sup>a</sup>	19.2 nm	41%	43,700	57,900 <sup>h</sup>	2.46 <sup>d</sup>
PHEMA <sup>b</sup>	25.6 nm	36%	38,100	68,000 <sup>h</sup>	2.25 <sup>e</sup>
PS	5.6 nm	6%	5,500	8,200	1.47

<sup>a</sup> Prepared with the CuCl system

<sup>b</sup> Prepared with the CuCl/CuCl<sub>2</sub> (1/2, *mol/mol*) system

<sup>c</sup> PS block thickness was the same for extension from either PHEMA block

<sup>d</sup> Bimodal peak distribution

<sup>e</sup> Trimodal peak distribution

<sup>f</sup> PS and PDMAEA conversion determined by gravimetric analysis and <sup>1</sup>H NMR, respectively

<sup>g</sup> Theoretical molecular weights based on initiator concentration and percent conversion

<sup>h</sup> See appendix for GPC chromatograms

The preparation of the Si/SiO<sub>2</sub>//PHEMA-*b*-PS diblock brush was monitored using ATR-FTIR (Figure 4.12).

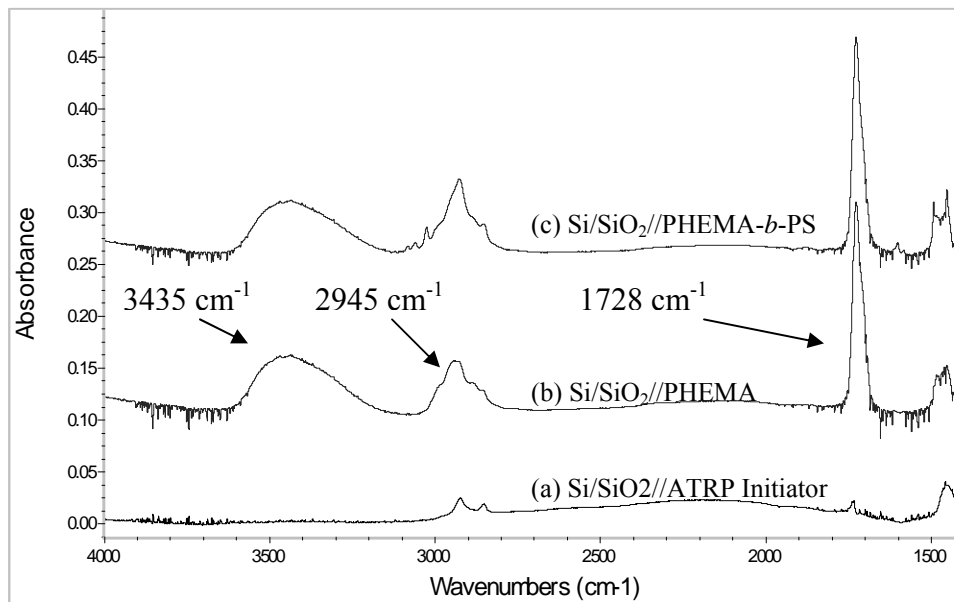


Figure 4.12. ATR-FTIR Spectrum of Si/SiO<sub>2</sub>//PHEMA-*b*-PS

When the Si/SiO<sub>2</sub>//PHEMA brush is prepared, three main sets of peaks appear in the IR spectrum. The broad peak at 3435 cm<sup>-1</sup> is assigned to the O-H stretching vibration. The multiplet at 2945 cm<sup>-1</sup> is assigned to the C-H stretching vibrations of the CH<sub>2</sub> groups in the polymer backbone and the CH<sub>2</sub> groups next to the ester bond in the repeat unit. A barely visible shoulder near 3000 cm<sup>-1</sup> is assigned to the C-H stretching vibrations of the backbone CH<sub>3</sub> groups. The peak at 1728 cm<sup>-1</sup> is assigned to the carbonyl stretching vibration of the ester group. Extension of the brush with PS creates expected peaks at 3081 cm<sup>-1</sup>, 3060 cm<sup>-1</sup>, and 3025 cm<sup>-1</sup> assigned to C-H stretching vibrations of the aromatic styrene ring. The tip of the broad peak that represents C-H stretching vibrations of methyl and methylene groups also moves from 2945 cm<sup>-1</sup> to 2927 cm<sup>-1</sup>, reflecting the

appearance of the new C-H bond in the polystyrene backbone. Also, peaks appear at 1602 cm<sup>-1</sup>, 1493 cm<sup>-1</sup>, and 1453 cm<sup>-1</sup>, which represent the stretching vibrations of the C-C bonds in the aromatic ring.

#### 4.4.4. Surface Rearrangement of Si/SiO<sub>2</sub>//PHEMA-*b*-PS

Advancing and receding water contact angles were used to probe the surface rearrangement ability of three diblock Si/SiO<sub>2</sub>//PHEMA-*b*-PS brushes having slightly different ratios of PS to PHEMA layer thicknesses (Table 4.11).

Table 4.11. Surface Rearrangement of Si/SiO<sub>2</sub>//PHEMA-*b*-PS ( $\theta = \pm 3^\circ$ )

Treatment	PS = 6.4 nm PHEMA = 26.3 nm		PS = 7.9 nm PHEMA = 25.3 nm		PS = 9.1 nm PHEMA = 27.0 nm	
	$\theta_a$	$\theta_r$	$\theta_a$	$\theta_r$	$\theta_a$	$\theta_r$
1 <sup>st</sup> Thermal <sup>a</sup>	90	72	94	75	95	76
1 <sup>st</sup> Acetonitrile	75	62	78	65	85	69
2 <sup>nd</sup> Thermal <sup>a</sup>	91	74	94	72	94	73
2 <sup>nd</sup> Acetonitrile	70	57	78	63	83	67
Cyclohexane	91	74	95	76	93	76
Water	55	41	62	47	62	48

<sup>a</sup> Thermal annealing done at 115 °C

As with the Si/SiO<sub>2</sub>//PDMAEMA-*b*-PS brushes, thermal annealing was used to allow the more hydrophobic PS block to migrate to the surface of the brush. Because the reported  $T_g$  values for PHEMA and PS are 85 °C and 100 °C respectively,<sup>95</sup> the Si/SiO<sub>2</sub>//PHEMA-*b*-PS brushes were annealed at 115 °C so that both blocks would be above their glass transition temperature to have sufficient mobility for rearrangement.<sup>36</sup>

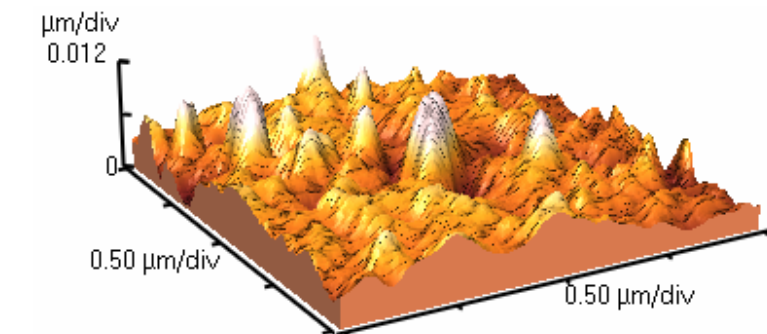
Each brush was thermally extended before beginning contact angle measurements. An advancing water contact angle ( $\theta_a$ ) for a PS homopolymer brush has been found to be  $94^\circ \pm 3^\circ$  during this research. All three extended diblock brushes gave water contact angles close to this value.

To draw the more hydrophilic PHEMA segments to the surface, the brush had to be immersed in a polar solvent. Because the eventual strategy for crosslinking the PHEMA chains was to use a difunctional acyl chloride, the solvent used to switch the brush (and subsequently solvate the crosslinking agent) had to be unreactive with the acyl chloride. Unfortunately, many solvents that would strongly prefer interaction with the PHEMA block such as aqueous, alcoholic, and amine containing media could not be used due to reaction of the solvent with the crosslinking agent. Also, a solvent had to be chosen that would not react with the pendant hydroxyl groups of the brush. Acetonitrile was chosen for its hydrophilicity and its unreactivity to both the acyl chloride and the hydroxyl groups.

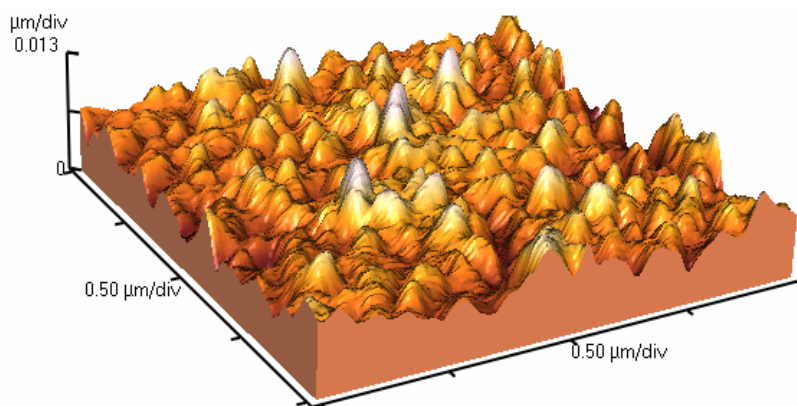
Advancing and receding water contact angles for a Si/SiO<sub>2</sub>//PHEMA homopolymer brush in this research have typically been found to be  $53^\circ \pm 3^\circ$  and  $41^\circ \pm 3^\circ$ , respectively; however, other research has found water contact angles for PHEMA brushes prepared by ATRP to be  $47^\circ$  and  $8^\circ$  for advancing and receding angles, respectively,<sup>3</sup> and  $75^\circ \pm 3^\circ$  and  $23^\circ \pm 2^\circ$  for advancing and receding angles, respectively.<sup>128</sup> It can be seen from Table 4.11 that solvent treatment with acetonitrile lowered contact angles, but not to anywhere close to the  $53^\circ$  and  $41^\circ$  found with PHEMA homopolymer brushes. Acetonitrile may not have a strong enough preference for the PHEMA block to fully switch the brush; however, considerably lower contact angles were obtained from the

brush with the thinnest PS block. Contact angles changes were fully reversible, as demonstrated by a second cycle of thermal annealing followed by acetonitrile treatment. Immersion in non-polar cyclohexane was also used to promote migration of the more hydrophobic PS chains to the surface. After treatment with a very polar solvent (water), the brushes exhibited contact angles very characteristic of a PHEMA surface. Treatment with methanol was able to produce a similar effect. For a control experiment, homopolymer Si/SiO<sub>2</sub>//PHEMA and Si/SiO<sub>2</sub>//PS brushes were subjected to methanol and cyclohexane treatments for one hour at 60 °C. No experimentally significant change in contact angles was observed after treatment with each solvent.

AFM was used to look for any change in surface morphology for the Si/SiO<sub>2</sub>//PHEMA-*b*-PS brush (PHEMA = 27.4 nm, PS = 8.2 nm). The brush extended in cyclohexane (Figure 4.13a) had an RMS roughness of 3.2 nm. After switching in methanol (Figure 4.13b), the RMS roughness was found to be 3.7 nm.



(a)



(b)

Figure 4.13. AFM Images of Si/SiO<sub>2</sub>//PHEMA-*b*-PS After (a) Cyclohexane Treatment and (b) Methanol Treatment

No major noticeable difference in surface morphology was observed for the extended and switched states. For comparison, a Si/SiO<sub>2</sub>//PHEMA homopolymer brush was found to have similar roughness values, though previous research has reported the RMS roughness of a PHEMA brush grown via ATRP to only be 1 nm.<sup>80</sup>

#### 4.4.5. Surface Modification of Si/SiO<sub>2</sub>//PHEMA

Before the Si/SiO<sub>2</sub>//PHEMA-*b*-PS diblock brush was presumptively crosslinked, a homopolymer Si/SiO<sub>2</sub>//PHEMA brush was exposed to varying concentrations of a di-

acyl chloride crosslinker molecule (adipoyl chloride). For crosslinking, the concentration of adipoyl chloride must be low enough so that after the first acyl chloride end reacts with the brush, the second reactive end can react with a nearby hydroxyl group with little competition from other free crosslinking molecules still in solution. However, the crosslinker concentration must be high enough that a significant amount of hydroxyl groups on the brush can react in a reasonable amount of time. The effect of dialkyl iodide crosslinker concentration could not be easily monitored for the previously discussed PDMAEMA and PDMAEA systems because C-I stretching and CH<sub>2</sub> wagging vibrations of the CH<sub>2</sub>I group on any free alkyl iodide endgroups occur at wavenumbers too low to be observed using the FTIR-ATR setup.<sup>114</sup> The acyl chloride crosslinker molecule provides a unique opportunity to observe free acyl chloride groups because the acyl chloride carbonyl stretching frequency is shifted to a slightly higher wavenumber than that observed for the ester group. Figure 4.14 shows IR spectra of a Si/SiO<sub>2</sub>//PHEMA brush reacted with 1%, 5%, and 100% solutions of adipoyl chloride at 80 °C for 3.5 days.

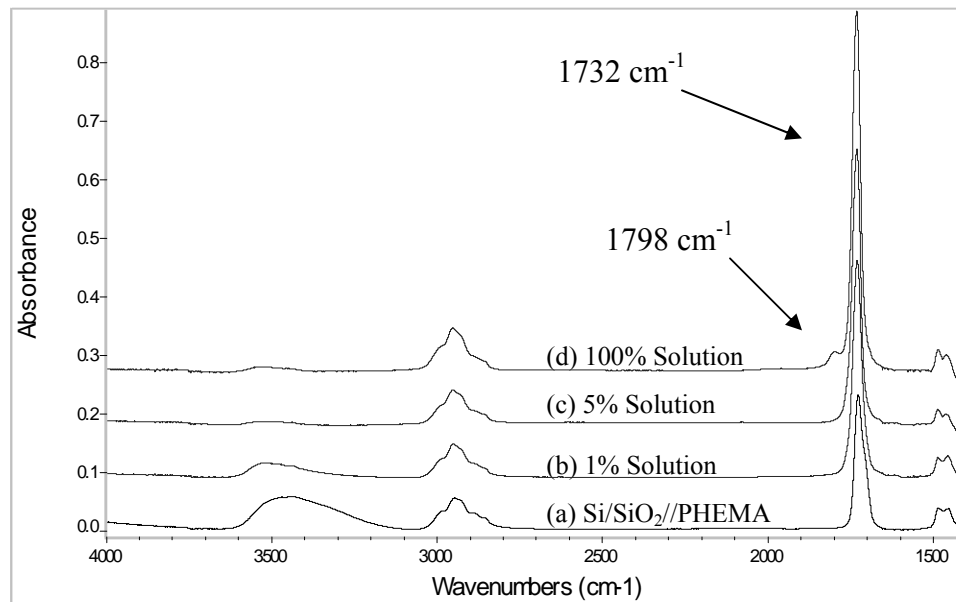


Figure 4.14. ATR-FTIR Spectrum of Si/SiO<sub>2</sub>//PHEMA Reactions

The extent of reaction was monitored by the disappearance of the broad O-H stretching vibration peak near 3435 cm<sup>-1</sup>, as well as the increase in the carbonyl stretching vibration at 1728 cm<sup>-1</sup> due to the formation of new ester bonds *via* the reaction of the acyl chloride crosslinker with the pendant hydroxyl groups of the brush. Assuming that all of the hydroxyl groups react, one would expect to see the complete loss of the O-H peak and an approximate doubling of the carbonyl peak (after taking into account the carbonyl group in the initiator layer), as compared with the original Si/SiO<sub>2</sub>//PHEMA brush. The brush exposed to the 1% crosslinker solution shows a roughly 69% decrease in O-H stretching intensity. The brush exposed to the 5% solution shows almost a complete loss (94% decrease) of the O-H stretching peak. Though ATR-IR data is only semi-quantitative, this data correlates well with the 91% increase in carbonyl stretching intensity for the same sample.

When a Si/SiO<sub>2</sub>/PHEMA brush was exposed to 100% adipoyl chloride, a similar disappearance of the O-H stretching peak and large increase of the carbonyl peak at 1732 cm<sup>-1</sup> was accompanied by the appearance of a new peak at 1798 cm<sup>-1</sup> due to the carbonyl group of the acyl chloride. This peak is formed because the concentration of crosslinker molecules is high enough that only one end of the molecule reacts with the brush and all other surrounding hydroxyl groups have reacted with other molecules so that a free acyl chloride end is tethered to the surface and has no neighboring hydroxyl sites to react with. If this peak were due to completely unreacted adipoyl chloride molecules that were not rinsed off the brush, it would be reasonable to assume that this peak would appear in the IR spectra of other crosslinked brushes as well. This experiment illustrates how a low (1%) concentration of crosslinker molecules may limit the amount of reaction with the brush, given a specified length of time. A high (100%) concentration may force some crosslinker molecules to only react with the brush at one end. It should be noted, however, that the extents of any inter- and intra-chain crosslinking cannot be determined from this experiment. Also, successful crosslinking of a diblock brush (as measured by its inability to switch after crosslinking) may not require most or even many pendant functional groups on a brush to react.

Interestingly, while four methylene groups are added to the brush for every adipoyl chloride molecule that reacts, there is little change in the intensity of the C-H stretching vibration peak near 2950 cm<sup>-1</sup> (Figure 4.14c). Three other monofunctional acyl chlorides (valeryl chloride, butyryl chloride, and propionyl chloride) as well as a fluorinated difunctional acyl chloride (hexafluoroglutaryl chloride) were reacted with

Si/SiO<sub>2</sub>//PHEMA homopolymer brushes to investigate the addition of CH<sub>2</sub> groups (Figure 4.15).

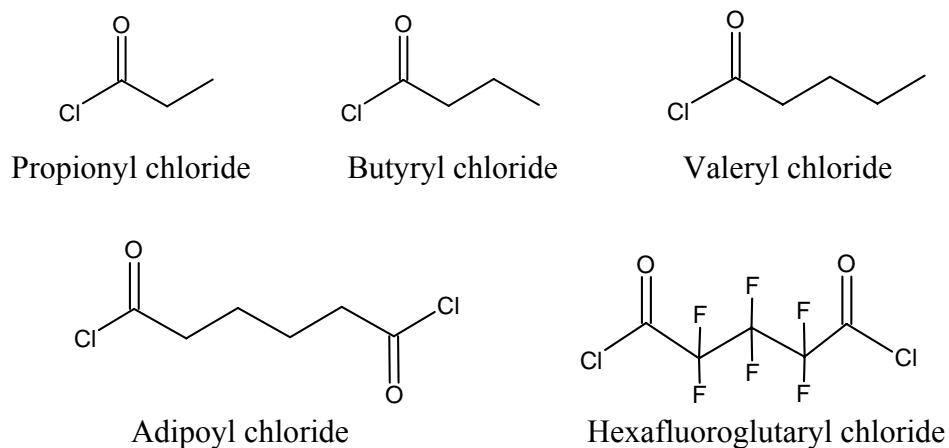


Figure 4.15. Acyl Chlorides

All reactions produced the expected decrease of the O-H stretching peak intensity and increase of the carbonyl stretching peak intensity. In the case of the fluorinated molecule, a new carbonyl peak at  $1784\text{ cm}^{-1}$  corresponding to the ester next to the CF<sub>2</sub> groups appeared next to the original carbonyl peak (Figure 4.16).

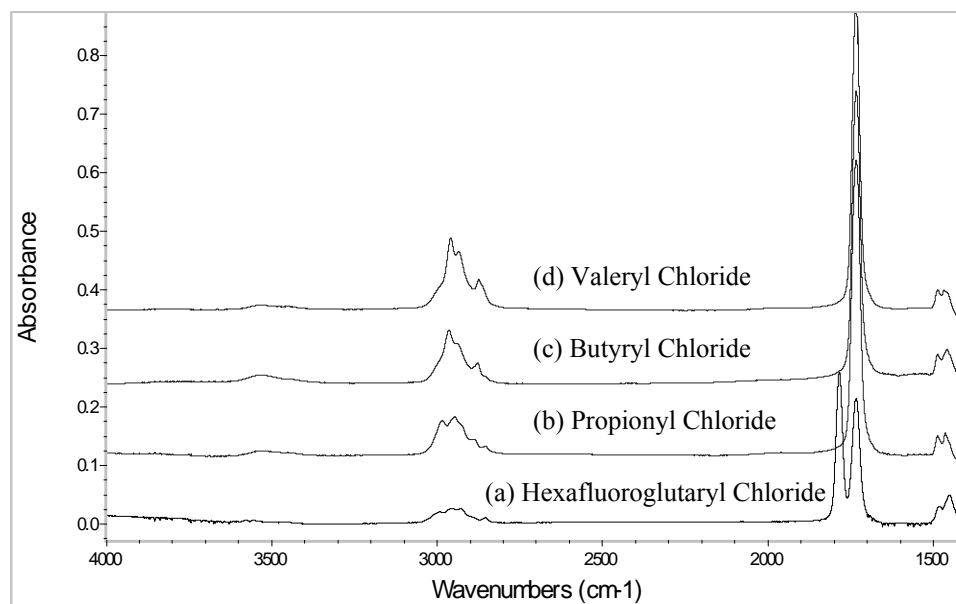


Figure 4.16. ATR-FTIR Spectrum of Modified Si/SiO<sub>2</sub>//PHEMA

Table 4.12 shows a comparison between the change in C-H stretching intensity and the number of new C-H bonds added (per new ester bond formed) when each molecule fully reacts with the brush. In all cases, the decrease in O-H stretching peak intensity suggests that nearly 90% of the hydroxyl groups in the brush have reacted. All numbers have been corrected to account for C-H stretching peak intensity due to the initiator layer.

Table 4.12. C-H Bond Stretching Intensities for Modified Si/SiO<sub>2</sub>//PHEMA

Acyl Chloride	O-H Decrease	New C-H Bonds	C-H Increase
Propionyl Chloride	92%	5	13%
Butyryl Chloride	89%	7	53%
Valeryl Chloride	94%	9	81%
Adipoyl Chloride	94%	4	2%
Hexafluoroglutaryl Chloride	97%	0	-39%

The data shows a striking pattern for the need to add more than four new C-H bonds for every new ester bond formed in order to observe any noticeable increase in C-H stretching intensity. While the exact cause is unknown, it appears that the formation of an ester bond in some way must decrease the observed stretching intensity of neighboring CH<sub>2</sub> groups. For this unexpected reason, the extent of reaction of the acyl chloride crosslinker molecule with the Si/SiO<sub>2</sub>//PHEMA brush was monitored by O-H stretching intensity decrease or carbonyl stretching intensity increase, but not by a change in C-H stretching intensity.

#### 4.4.6. Presumptive Crosslinking of Si/SiO<sub>2</sub>//PHEMA-*b*-PS

Though water contact angle data indicated that acetonitrile did not switch the Si/SiO<sub>2</sub>//PHEMA-*b*-PS brush very well, a diblock was first treated with acetonitrile before treatment with a 5% solution of adipoyl chloride in acetonitrile. This presumptive crosslinking was only performed for one hour (as opposed to the 3.5 days in previous experiments with a HEMA homopolymer brush); however, the 5% solution produced an 80% decrease in the O-H stretching vibration peak intensity. Ellipsometry measurements showed that presumptive crosslinking of a Si/SiO<sub>2</sub>//PHEMA-*b*-PS brush (PHEMA = 27.4 nm, PS = 8.2 nm) produced an approximately 10 nm increase in brush thickness. Some increase in thickness is expected due to addition of material to the brush.

Water contact angle measurements were used to probe the presumptive crosslinking of two diblock brushes as well as a homopolymer PHEMA brush (Table 4.13).

Table 4.13. Presumptive crosslinking of Si/SiO<sub>2</sub>//PHEMA-*b*-PS ( $\theta = \pm 3^\circ$ )

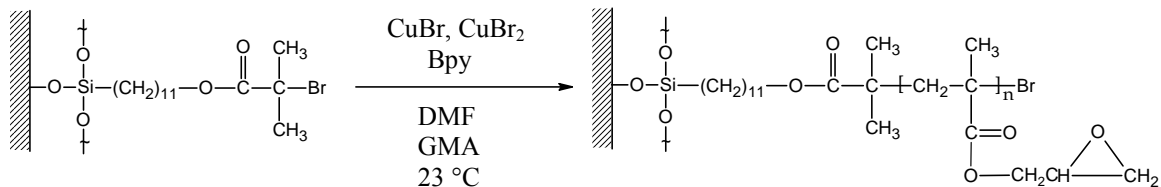
Treatment	PS = 7.3 nm		PS = 8.2 nm		PHEMA = 25.4 nm	
	PHEMA = 25.0 nm		PHEMA = 27.4 nm		$\theta_a$	$\theta_r$
	$\theta_a$	$\theta_r$	$\theta_a$	$\theta_r$	$\theta_a$	$\theta_r$
Cyclohexane	88	70				
H <sub>2</sub> O/DMF	56	44				
Acetonitrile	68	56				
CROSSLINK (Acetonitrile)	71	59	76	64	63	52
Cyclohexane	82	68	89	72	63	49
H <sub>2</sub> O/DMF	71	57	73	59	61	48

For reference, water contact angle values of one of the diblocks are given after cyclohexane, H<sub>2</sub>O/DMF, and acetonitrile treatments; solvent switching values for other diblocks can be found in Table 4.11. After attempted crosslinking, cyclohexane treatment significantly increased the contact angle value of the diblocks. It is interesting to note, however, that solvent treatment in H<sub>2</sub>O/DMF did not decrease the contact angles of the presumptively crosslinked diblocks to values of the presumptively crosslinked homopolymer Si/SiO<sub>2</sub>//PHEMA brush.

#### 4.5. Synthesis and Presumptive Crosslinking of Si/SiO<sub>2</sub>//PGMA-*b*-PS

##### 4.5.1. Si/SiO<sub>2</sub>//PGMA Brushes *via* ATRP

Poly(glycidyl methacrylate) (PGMA) brushes were synthesized according to Scheme 4.7.



Scheme 4.7. Si/SiO<sub>2</sub>//PGMA Brush Synthesis

Polymerization conditions were chosen based on previous research by Yu and coworkers<sup>96</sup> in which Si/SiO<sub>2</sub>//PGMA brushes were found to have a linear increase in thickness with polymerization time and were able to be chain extended with pentafluorostyrene to create diblocks. No free initiator was added for control of the polymerization in this experiment; only the deactivating CuBr<sub>2</sub> was added. While no solution polymer was obtained for molecular weight analysis, Soxhlet extraction of the brush was not necessary to remove any untethered PGMA chains, and brushes were simply sonicated in methanol for 30 minutes before being characterized. After 20 hours of polymerization, the conditions in Scheme 4.7 afforded a 13.0 nm thick brush with advancing and receding water contact angles of 60° ± 3° and 51° ± 3° respectively. These numbers seem to correlate reasonably well with other research<sup>96</sup> that has found static water contact angles for PGMA brushes prepared by ATRP to be 68° ± 3° and 67° ± 3°. An ATR-FTIR spectrum of the Si/SiO<sub>2</sub>//PGMA brush is shown in Figure 4.17.

#### 4.5.2. Sequential Extension of Si/SiO<sub>2</sub>//PGMA Brushes

As with previous brush systems reported in this research, several chain extension experiments were performed with Si/SiO<sub>2</sub>//PGMA brushes to evaluate their viability in forming AB diblocks. Si/SiO<sub>2</sub>//PGMA brushes was fully characterized before being

immersed in a fresh GMA polymerization solution under conditions identical to the first polymerization. Block extension data is presented in Table 4.14.

Table 4.14. Ellipsometric Measurements of Si/SiO<sub>2</sub>//PGMA Brush Extension With Additional GMA Monomer ( $\pm 0.5$  nm)

System	Solvent	Block 1	Block 2
1 <sup>a</sup>	DMF	13.0 nm	3.3 nm
2 <sup>b</sup>	H <sub>2</sub> O, MeOH	12.2 nm	4.7 nm
3 <sup>c</sup>	MeOH	17.5 nm	10.2 nm

<sup>a</sup>[GMA]<sub>0</sub>: [CuBr]<sub>0</sub>: [CuBr<sub>2</sub>]<sub>0</sub>: [bpy]<sub>0</sub> = 2400:12:3:25.

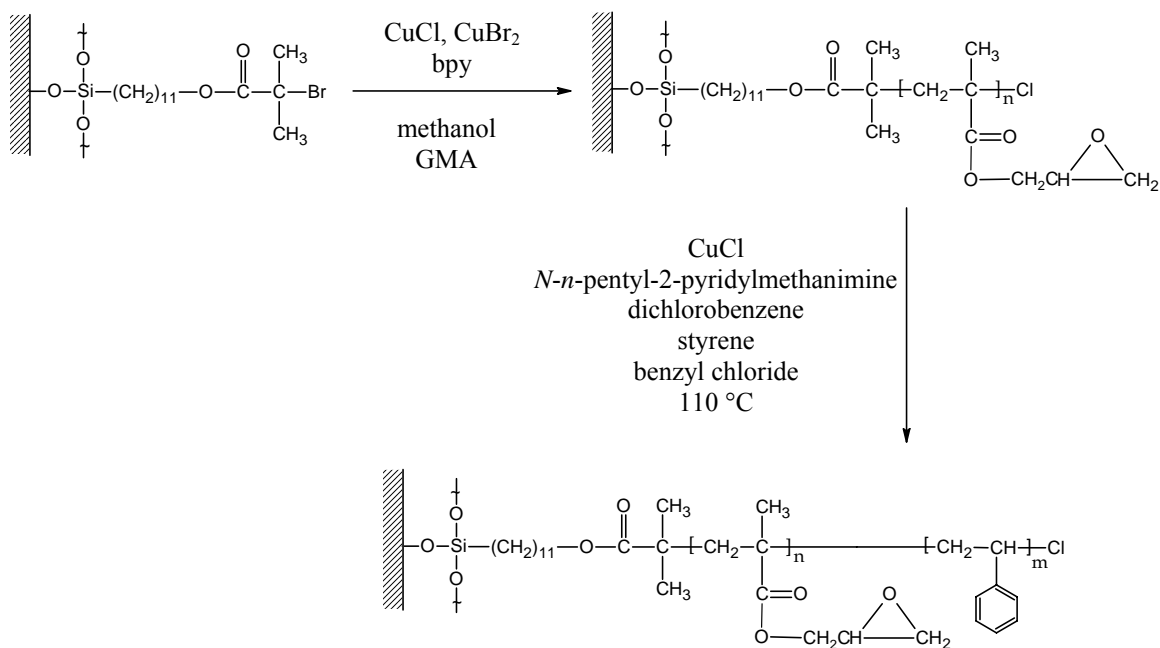
<sup>b</sup>[GMA]<sub>0</sub>: [CuCl]<sub>0</sub>: [CuBr<sub>2</sub>]<sub>0</sub>: [bpy]<sub>0</sub> = 3700:37:1.7:90.

<sup>c</sup>[GMA]<sub>0</sub>: [CuCl]<sub>0</sub>: [CuBr<sub>2</sub>]<sub>0</sub>: [bpy]<sub>0</sub> = 3700:37:1.7:90.

The seemingly living conditions in system 1 reported by Yu and coworkers<sup>96</sup> yielded a second PGMA block with minimal thickness. Marginally better results were found using a CuCl/CuBr<sub>2</sub> catalyst and methanol/water 4/1, v/v solvent system (2) reported reported by Edmondson and Huck<sup>98,129</sup> to give a linear increase in brush thickness with time and the ability to chain extend the brushes. It should be noted that for their brush regrowth experiment, Edmondson and Huck<sup>98</sup> report using a 50% longer polymerization time for the second block of a Si/SiO<sub>2</sub>//PGMA-*b*-PGMA brush to obtain blocks of relatively equal thickness. As previous literature has cited, the addition of water to an ATRP is possibly detrimental to the control of polymerization.<sup>75,88</sup> System 3 employed the CuCl/CuBr<sub>2</sub> catalyst system in a pure methanolic solution. Using pure methanol still could not produce a second PGMA block of equal thickness; however, blocking efficiency of the Si/SiO<sub>2</sub>//PGMA brush was definitely improved and conditions in System 3 were employed for the formation of Si/SiO<sub>2</sub>//PGMA-*b*-PS brushes.

#### 4.5.3. Preparation of Si/SiO<sub>2</sub>//PGMA-*b*-PS

Styrene was polymerized from a PGMA brush to create Si/SiO<sub>2</sub>//PGMA-*b*-PS following Scheme 4.8. Initially, HMTETA was used as a ligand for the styrene polymerization, as had been the case for the extension of Si/SiO<sub>2</sub>//PDMAEMA and Si/SiO<sub>2</sub>//HEMA brushes. However, a significant O-H stretching peak was observed in the IR spectrum of these Si/SiO<sub>2</sub>//PGMA-*b*-PS brushes, presumably due to some ring opening of the pendant epoxy ring of the brush by the amine ligand. To circumvent this problem, the imine ligand *N-n*-pentyl-2-pyridylmethanimine<sup>86</sup> was synthesized and used for ligation of the CuCl and CuBr<sub>2</sub>. The use of this type of ligand for the ATRP of styrene<sup>87</sup> as well as glycidyl methacrylate<sup>77,130</sup> has previously been reported.



Scheme 4.8. Si/SiO<sub>2</sub>//PGMA-*b*-PS Brush Synthesis

Though no polymer was formed in solution during synthesis of the PGMA brush, solution polymer from the styrene polymerization for Si/SiO<sub>2</sub>//PGMA-*b*-PS (PGMA =

26.0 nm, PS = 7.4 nm) showed  $M_n = 48,800$  and  $M_w/M_n = 1.51$  with a monomodal peak. Interestingly, this polymerization gave only an 11% conversion and theoretical molecular weight of  $M_n = 9,700$  g/mol. Poor initiation efficiency may explain why such a large discrepancy exists between the theoretical and experimental molecular weights, and why such a high molecular weight polymer produced such a thin PS block.

The preparation of the Si/SiO<sub>2</sub>//PGMA-*b*-PS diblock brush was monitored using ATR-FTIR (Figure 4.17). Peaks at 3062 cm<sup>-1</sup>, 3000 cm<sup>-1</sup>, 2931 cm<sup>-1</sup>, and 2854 cm<sup>-1</sup> represent C-H stretching vibrations in the Si/SiO<sub>2</sub>//PGMA brush. The large peak at 1730 cm<sup>-1</sup> is assigned to the carbonyl stretching of the methacrylate. Peaks characteristic of a PS layer appear after extension of the brush with styrene. A broad O-H stretching peak appears near 3502 cm<sup>-1</sup>, presumably due to some of the epoxy rings having been opened during the styrene polymerization.

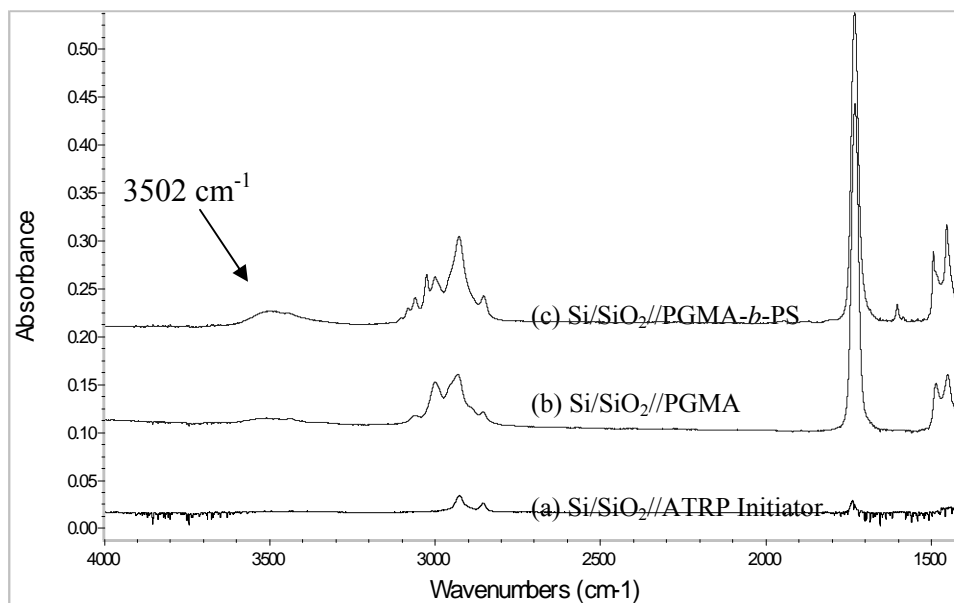


Figure 4.17. ATR-FTIR Spectrum of Si/SiO<sub>2</sub>//PGMA-*b*-PS Reactions

#### 4.5.4. Surface Rearrangement of Si/SiO<sub>2</sub>//PGMA-*b*-PS

Advancing and receding water contact angles were used to probe the surface rearrangement ability of three diblock Si/SiO<sub>2</sub>//PGMA-*b*-PS brushes having widely varying ratios of PS to PGMA layer thickness (Table 4.15). Treatment with cyclohexane was used to order the PS block in all three brushes to the surface of the brush. While treatment of the two brushes with thinner PS blocks with methanol was able to produce water contact angles similar to those obtained with a homopolymer Si/SiO<sub>2</sub>//PGMA brush, the more polar DMF/H<sub>2</sub>O solvent mixture was needed to produce contact angles characteristic of a PGMA surface in the diblock brush with the thickest PS layer.

Table 4.15. Surface Rearrangement of Si/SiO<sub>2</sub>//PGMA-*b*-PS ( $\theta = \pm 3^\circ$ )

Treatment	PS = 2.5 nm PGMA = 25.6 nm		PS = 7.4 nm PGMA = 26.0 nm		PS = 26.9 nm PGMA = 26.4 nm	
	$\theta_a$	$\theta_r$	$\theta_a$	$\theta_r$	$\theta_a$	$\theta_r$
1 <sup>st</sup> Cyclohexane	92	74	95	76	92	77
1 <sup>st</sup> Methanol	63	51	65	53	73	60
2 <sup>nd</sup> Cyclohexane	90	74	89	71		
2 <sup>nd</sup> Methanol	64	54	64	51		
1 <sup>st</sup> DMF/H <sub>2</sub> O					60	47
Cyclohexane					93	75
2 <sup>nd</sup> DMF/H <sub>2</sub> O					63	53

AFM measurements found no significant morphology changes upon solvent treatment for a Si/SiO<sub>2</sub>//PGMA-*b*-PS brush (PGMA = 27.8 nm, PS = 9.5 nm). For a control experiment, homopolymer Si/SiO<sub>2</sub>//PGMA and Si/SiO<sub>2</sub>//PS brushes were subjected to

methanol and cyclohexane treatments for one hour at 60 °C. No experimentally significant change in contact angles was observed after treatment with each solvent.

#### 4.5.5. Presumptive Crosslinking of Si/SiO<sub>2</sub>//PGMA and Si/SiO<sub>2</sub>//PGMA-*b*-PS

Before the Si/SiO<sub>2</sub>//PGMA-*b*-PS diblock brush was presumptively crosslinked, a homopolymer Si/SiO<sub>2</sub>//PGMA brush was exposed to 1% and 100% solutions of the difunctional primary amine crosslinking molecule 2,2'-(ethylenedioxy)diethylamine for 8 hours at 60 °C (Figure 4.18). Any unreacted NH<sub>2</sub> groups would be evident by the asymmetrical and symmetrical N-H stretching vibrations as well as the N-H bending vibration.

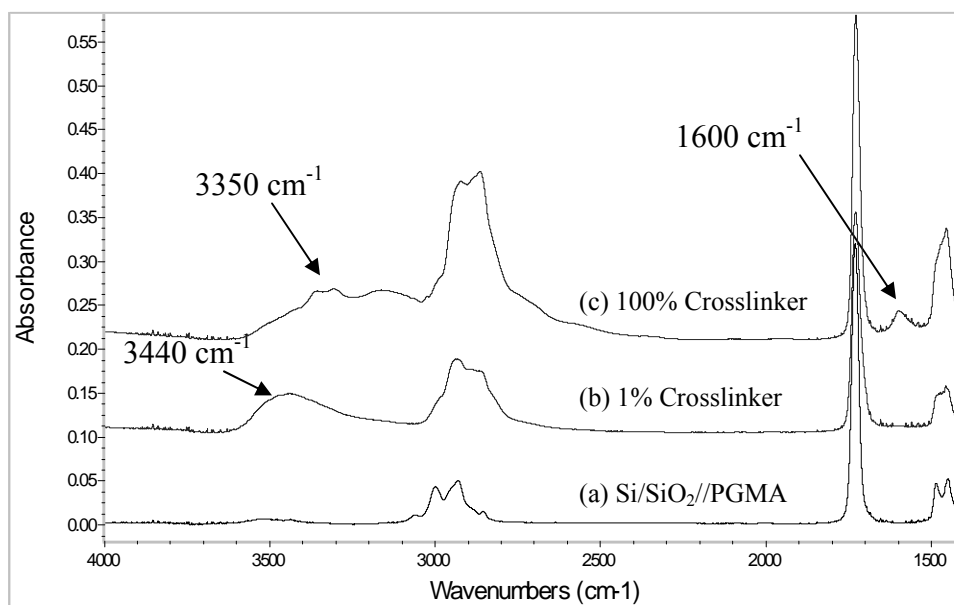


Figure 4.18. ATR-FTIR Spectrum of Si/SiO<sub>2</sub>//PGMA Reactions

The IR spectrum of Si/SiO<sub>2</sub>//PGMA shows the expected C-H stretching vibrations near 3000 cm<sup>-1</sup> and the carbonyl stretching peak at 1730 cm<sup>-1</sup>. An extremely faint broad peak near 3500 cm<sup>-1</sup> indicates a minor amount of hydroxyl groups present, which is

presumably due to a few of the epoxy rings having been opened. When the brush is reacted in the 1% crosslinker solution, a large O-H stretching vibration peak appears at  $3440\text{ cm}^{-1}$  due to hydroxyl groups being formed as the amine opens the epoxy ring. As expected, the addition of  $\text{CH}_2$  groups from the crosslinker molecule increases the intensity of the C-H stretching vibration peaks near  $3000\text{ cm}^{-1}$ . When a Si/SiO<sub>2</sub>//PGMA brush was reacted in 100% crosslinking agent, the appearance of a peak due to the N-H stretching vibration may be visible near  $3350\text{ cm}^{-1}$ , though it is masked by the large O-H stretching vibration peak. The peak at  $1600\text{ cm}^{-1}$  assigned to the N-H bending vibration of unreacted  $\text{NH}_2$  groups was not present after the 1% crosslinker reaction, thus indicating that the 1% solution was dilute enough that most crosslinker molecules presumably reacted with the brush at both ends. Peaks due to  $\text{NH}_2$  groups observed after the brush reaction with the 100% crosslinker solution indicate that a significant number of difunctional crosslinker molecules only reacted with the brush at one end.

A Si/SiO<sub>2</sub>//PGMA-*b*-PS brush was first treated with a polar solvent to switch the brush before being immersed into a 1% solution of 2,2'-(ethylenedioxy)diethylamine for crosslinking at 60 °C for 12 hours. These conditions are similar to those used by Yu and coworkers,<sup>129</sup> who report reacting Si/SiO<sub>2</sub>//PGMA brushes with a 4 M ethylenediamine solution in DMF at room temperature for 10 hours. Switching and presumptive crosslinking were done in methanol for the two brushes with thinner PS layers; a 50/50, *v/v* solution of H<sub>2</sub>O/DMF was used in switching and presumptive crosslinking of the brush with largest PS layer. Water contact angle measurements were used to probe the presumptive crosslinking of three different diblock brushes (Table 4.16). As a control, a homopolymer PGMA brush was also presumptively crosslinked. No change in contact

angles was observed for the presumptively crosslinked homopolymer brush upon cyclohexane treatment; however, all three diblock brushes experienced a significant increase in contact angles upon cyclohexane treatment after presumptive crosslinking had been performed.

Table 4.16. Presumptive Crosslinking of Si/SiO<sub>2</sub>//PGMA-*b*-PS ( $\theta = \pm 3^\circ$ )

Treatment	PS = 2.5 nm PGMA = 25.6 nm		PS = 7.4 nm PGMA = 26.0 nm		PS = 26.9 nm PGMA = 26.4 nm	
	$\theta_a$	$\theta_r$	$\theta_a$	$\theta_r$	$\theta_a$	$\theta_r$
Cyclohexane	92	74	95	76	92	77
Methanol	63	51	65	53		
H <sub>2</sub> O/DMF					63	53
CROSSLINK (solvent)	60	47	66	56	53	42
Cyclohexane	89	73	84	66	94	78

ATR-FTIR was used to monitor the presumptive crosslinking of the diblock brush (Figure 4.19). The expected increase in the O-H stretching peak intensity (indicating opening of the epoxy rings) with no hint of peaks due to the presence of the NH<sub>2</sub> group gives evidence that some crosslinking has occurred. Presumptive crosslinking of the Si/SiO<sub>2</sub>//PGMA-*b*-PS brush (PGMA = 26.0 nm, PS = 7.4 nm) produced an approximately 7 nm increase in brush thickness, presumably due to the addition of material to the brush.

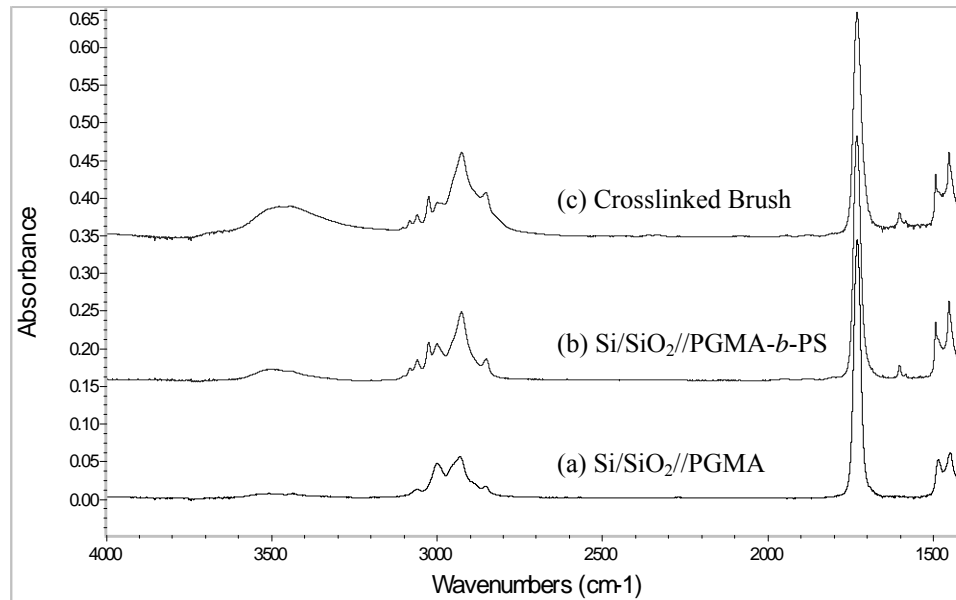


Figure 4.19. ATR-FTIR Spectrum of Si/SiO<sub>2</sub>//PGMA-*b*-PS After Presumptive Crosslinking

A Si/SiO<sub>2</sub>//PGMA-*b*-PS brush (PGMA = 25.6 nm, PS = 2.5 nm) was also switched and reacted with three different crosslinking molecules (Figure 4.20) at 60 °C for 12 hours.

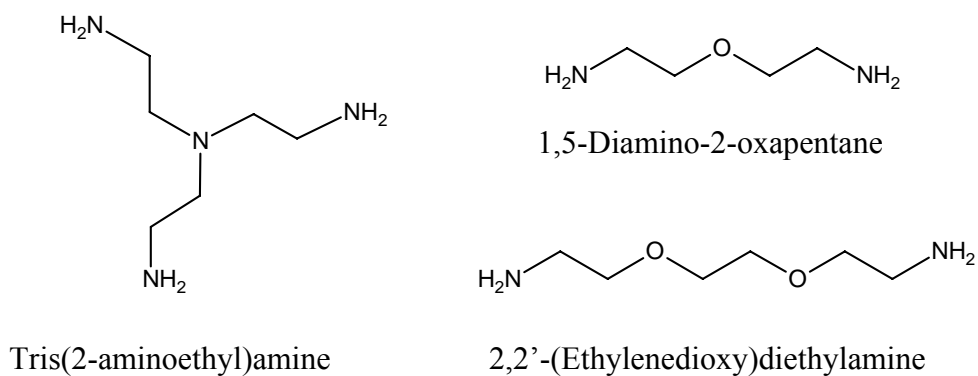
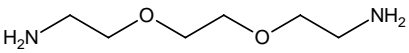


Figure 4.20. Primary Amine Crosslinker Molecules

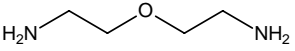
All three molecules proved ineffective in preventing an increase in water contact angles after the brush was again treated with cyclohexane (Table 4.17).

Table 4.17. Presumptive Crosslinking of Si/SiO<sub>2</sub>//PGMA-*b*-PS ( $\theta = \pm 3^\circ$ )

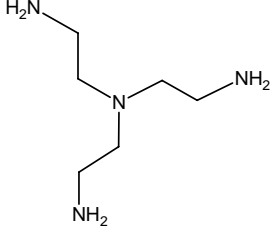
Crosslinker:



NCCOCN



NCCOCN



NCCOCN

Treatment	$\theta_a$	$\theta_r$	$\theta_a$	$\theta_r$	$\theta_a$	$\theta_r$
Cyclohexane	92	74	92	74	92	74
Methanol	63	51	63	51	63	51
CROSSLINK (Methanol)	60	47	55	45	62	52
Cyclohexane	89	73	74	62	76	62

## CHAPTER V

### SUMMARY AND CONCLUSIONS

The purpose of this research was to investigate the surface rearrangement properties of tethered hydrophilic-hydrophobic diblock polymer brushes and their ability to subsequently be crosslinked through the functional hydrophilic block. Atom transfer radical polymerization (ATRP) was used to prepare brushes of controlled thickness from initiators immobilized on the surface of silicon substrates. These brushes were subjected to various solvent and thermal treatments to promote migration of the hydrophilic or hydrophobic blocks to the surface. Brushes were immersed in a solution of crosslinking agent in an attempt to stabilize rearranged surfaces.

Poly(*N,N*-dimethylaminoethyl methacrylate) (PDMAEMA) brushes were synthesized *via* ATRP. Initial reaction conditions employed a CuBr catalyst; however, it was found that using CuCl with the addition of a small amount of the ATRP deactivating CuCl<sub>2</sub> species was necessary to prepare a second PDMAEMA block of equal thickness, suggesting efficient re-initiation of chains. Polymer grown simultaneously in solution was found to have relatively narrow polydispersity (< 1.30) and slightly lower experimental  $M_n$  values than predicted. The solution polymer had molecular weights of approximately 1000 g/mol for every 1 nm of corresponding brush thickness. The Si/SiO<sub>2</sub>//PDMAEMA brushes synthesized from both the CuBr and CuCl/CuCl<sub>2</sub> systems were extended with polystyrene (PS) in a one-pot reaction. Unsurprisingly, styrene

polymerized from the Si/SiO<sub>2</sub>//PDMAEMA-Cl brush gave a PS block almost three times thicker than that from the Si/SiO<sub>2</sub>//PDMAEMA-Br brush. This result suggests that fewer homopolymer PDMAEMA chains exist in the optimized diblock system.

The optimized chlorine-based system was used to prepare Si/SiO<sub>2</sub>//PDMAEMA-*b*-PS brushes with varying ratios of PDMAEMA to PS block thicknesses. Thermal annealing above the glass transition temperature of the block with the higher  $T_g$  or immersion in cyclohexane was used to order the more hydrophobic PS block to the surface of the brush. Advancing water contact angles gave values characteristic of a PS surface ( $94^\circ \pm 3^\circ$ ). The brush with the thinnest PS block (4.7 nm) gave contact angle values slightly lower than expected, presumably due to incomplete surface coverage or aggregation of the PS chains. Immersion in methanol was used to switch the brush and order the more polar PDMAEMA to the surface. Advancing water contact angle values characteristic of a PDMAEMA surface ( $58^\circ \pm 3^\circ$ ) were observed in this switched state. This rearrangement was found to be fully reversible and produced no significant change in surface morphology as observed with atomic force microscopy (AFM). The extended and switched brushes both had a smooth surface—presumably due to the low  $T_g$  of the PDMAEMA block.

An attempt was made to crosslink the switched brushes by exposing them to a solution of a the  $\alpha,\omega$ -dihaloalkane [1,2-bis-(2-iodoethoxy)ethane]. ATR-FTIR evidence for reaction with the brush could not quantitate the amount of difunctional crosslinker molecules that reacted at both ends, and could not distinguish intra- from inter-molecular crosslinking. Subsequent solvent treatment to order the PS block back to the surface gave mixed results. The brush with the thinnest PS block remained virtually unchanged,

while the brush with a larger PS layer showed an increase in water contact angles upon treatment with cyclohexane.

It is possible that the geometry of the switched morphology of the Si/SiO<sub>2</sub>//PDMAEMA-*b*-PS brush prevented any presumed crosslinking from stabilizing the surface composition. Presumptive crosslinking and switching was explored further by synthesizing a Si/SiO<sub>2</sub>//PS-*b*-poly(*N,N*-dimethylaminoethyl acrylate) (PDMAEA) brush. In this system, the top functional block could be crosslinked with the same  $\alpha,\omega$ -dihaloalkane before switching. Interestingly, immersion in cyclohexane to bring the bottom PS block to the surface was still found to increase water contact angle values after presumptive crosslinking in the extended state. Presumptive crosslinking of even a 14.5 nm PDMAEA top block still did not prevent the bottom PS block from being at least partially drawn to the surface.

Another hydrophilic functional monomer, 2-hydroxyethyl methacrylate (HEMA), was used to create Si/SiO<sub>2</sub>//PHEMA-*b*-PS brushes. Optimization studies similar to those for the PDMAEMA system found that the addition of deactivating CuCl<sub>2</sub> had no effect on extension of Si/SiO<sub>2</sub>//PHEMA brushes. Si/SiO<sub>2</sub>//PHEMA-*b*-PS brushes were treated with water to order the PHEMA blocks to the surface. Thermal annealing and treatment with cyclohexane were used to order the top PS block back to the surface. This rearrangement was found to be fully reversible and produced no significant change in surface morphology as observed with atomic force microscopy (AFM).

Using the difunctional acyl chloride crosslinker, adipoyl chloride, provided an opportunity to observe unreacted crosslinker ends in the IR spectrum. A Si/SiO<sub>2</sub>//PHEMA brush was treated with solutions of 1%, 5%, and 100% adipoyl

chloride. The IR spectrum of the brush treated with a 100% solution of crosslinker showed a small acyl chloride carbonyl peak—presumably due to the high concentration of crosslinker molecules reacting with all surrounding hydroxyl groups before the second end of a crosslinker could react with the brush. This experiment gave evidence that both ends of crosslinker molecules would not always react with the brush in high enough concentrations of crosslinker; however, the absence of the acyl chloride carbonyl peak presumably meant that both ends of the difunctional crosslinker react with a brush at reasonably low concentrations. Presumptive crosslinking with adipoyl chloride did not prevent some surface rearrangement upon further exposure to solvent treatment; however, it should be noted that the presumed crosslinking had to be carried out in acetonitrile—a solvent that was not able to fully switch the brush, but was unreactive towards the acyl chloride.

Solvent as well as catalyst were manipulated in optimizing the ATRP of glycidyl methacrylate (GMA) brushes. This polymerization was accomplished without the addition of free initiator to the reaction solution. While no solution polymer was available for analysis, the need for tedious solvent extraction to remove free polymer from the brush was eliminated. Si/SiO<sub>2</sub>//PGMA-*b*-PS brushes with varying ratios of PGMA to PS block thickness were produced. These brushes were switched in methanol or a mixture of DMF and water. Treatment with cyclohexane was used to order the PS block to the surface. Switching and subsequent crosslinking with di- and tri-functional primary amines proved ineffective in preventing water contact angle changes after further solvent treatments.

## REFERENCES

1. Pincus, P. *Macromolecules* **1991**, *24*, 2912.
2. Joanny, J-F. *Langmuir* **1992**, *8*, 989.
3. Shah, R. R.; Merreceyes, D.; Husemann, M.; Rees, I.; Abbott, N. L.; Hawker, C. J.; Hedrick, J. L. *Macromolecules* **2000**, *33*, 597.
4. Tiller, J. C.; Lee, S. B.; Lewis, K.; Klibanov, A. M. *Biotechnol. Bioeng.* **2002**, *79*, 465.
5. Ito, Y.; Park, Y. S. *Polym. Adv. Technol.* **2000**, *11*, 136.
6. Ito, Y.; Ochiai, Y.; Park, Y. S.; Imanishi, Y. *J. Am. Chem. Soc.* **1997**, *119*, 1619.
7. Milner, S. T. *Science* **1991**, *251*, 905.
8. Wu, T.; Efimenko, K.; Vlček, P.; Šubr, V.; Genzer, J. *Macromolecules* **2003**, *36*, 2448.
9. Halperin, A.; Tirrell, M.; Lodge, T. P. *Adv. Polym. Sci.* **1992**, *100*, 31.
10. Yamamoto, S.; Tsujii, Y.; Fukuda, T. *Macromolecules* **2002**, *35*, 6077.
11. Zhao, B.; Brittain, W. J. *Prog. Polym. Sci.* **2000**, *25*, 677.
12. Belder, G. F.; ten Brinke, G.; Hadziioannou, G. *Langmuir* **1997**, *13*, 4102.
13. Mansky, P.; Liu, Y.; Huang, E.; Russell, T. P.; Hawker, C. *Science* **1997**, *275*, 1458.
14. Suzuki, M.; Kishida, A.; Iwata, H.; Ikada, Y. *Macromolecules* **1986**, *19*, 1804.
15. Yamaguchi, T.; Ito, T.; Sato, T.; Shinbo, T.; Nakao, S. *J. Am. Chem. Soc.* **1999**, *121*, 4078.
16. Ejaz, M.; Yamamoto, S.; Ohno, K.; Tsujii, Y.; Fukuda, T. *Macromolecules* **1998**, *31*, 5934.

17. Prucker, O.; R uhe, J. *Macromolecules* **1998**, *31*, 592.
18. Szwarc, M. *Nature* **1956**, *178*, 1168.
19. Szwarc, M.; Levy, M.; Milkovich, R. *J. Am. Chem. Soc.* **1956**, *78*, 2656.
20. Otsu, T.; Yoshida, M.; Tazaki, T. *Makromol. Chem., Rapid Commun.* **1982**, *3*, 133.
21. Fischer, H. *J. Polym. Sci., Part A: Polym. Chem.* **1999**, *37*, 1885.
22. *Handbook of Radical Polymerization*; Matyjaszewski, K., Davis, T. P., Eds.; Wiley & Sons: New York, 2002.
23. Matyjaszewski, K.; Xia, J. *Chem. Rev.* **2001**, *101*, 2921.
24. Chiefari, J.; Chong, Y. K.; Ercole, F.; Krstina, J.; Jeffery, J.; Le, T. P. T.; Mayadunne, R. T. A.; Meijs, G. F.; Moad, C. L.; Moad, G.; Rizzardo, E.; Thang, S. H. *Macromolecules* **1998**, *31*, 5559.
25. Hawker, C. J.; Bosman, A. W.; Harth, E. *Chem. Rev.* **2001**, *101*, 3661.
26. Zhao, B.; Brittain, W. J. *J. Am. Chem. Soc.* **1999**, *121*, 3557.
27. Zhao, B.; Brittain, W. J.; Zhou, W.; Cheng, S. Z. D. *J. Am. Chem. Soc.* **2000**, *122*, 2407.
28. Singhvi, R.; Kumar, A.; Lopez, G. P.; Stephanopoulos, G. N.; Wang, D. I. C.; Whitesides, G. M.; Ingber, D. E. *Science* **1994**, *264*, 696.
29. Chen, C. S.; Mrksich, M.; Huang, S.; Whitesides, G. M.; Ingber, D. E. *Science* **1997**, *276*, 1425.
30. Niu, Q. J.; Fr chet, J. M. J. *Angew. Chem., Int. Ed. Engl.* **1998**, *37*, 667.
31. Aksay, I. A.; Trau, M.; Manne, S.; Honma, I.; Yao, N.; Zhou, L.; Fenter, P.; Eisenberger, P. M.; Gruner, S. M. *Science* **1996**, *273*, 892.
32. Geissler, M.; Xia, Y. *Adv. Mater.* **2004**, *16*, 1249.
33. Zhulina, E. B.; Singh, C.; Balazs, A. C. *Macromolecules* **1996**, *29*, 6338.
34. Zhulina, E. B.; Singh, C.; Balazs, A. C. *Macromolecules* **1996**, *29*, 8254.
35. Granville, A. M.; Boyes, S. G.; Akgun, B.; Foster, M. D.; Brittain, W. J. *Macromolecules* **2004**, *37*, 2790.

36. Granville, A. M.; Boyes, S. G.; Akgun, B.; Foster, M. D.; Brittain, W. J. *Macromolecules* **2005**, *38*, 3263.
37. Bug, A. L. R.; Cates, M. E.; Safran, S. A.; Witten, T. A. *J. Chem. Phys.* **1987**, *87*, 1824.
38. Parsonage, E.; Tirrell, M.; Watanabe, H.; Nuzzo, R. G. *Macromolecules* **1991**, *24*, 1987.
39. Toomey, R.; Mays, J.; Tirrell, M. *Macromolecules* **2004**, *37*, 905.
40. Kelley, T. W.; Schorr, P. A.; Johnson, K. D.; Tirrell, M.; Frisbie, C. D. *Macromolecules* **1998**, *31*, 4297.
41. Guzonas, D.; Boils, D.; Hair, M. L. *Macromolecules* **1991**, *24*, 3383.
42. Field, J. B.; Toprakcioglu, C.; Ball, R. C.; Stanley, H. B.; Dai, L.; Barford, W.; Penfold, J.; Smith, G.; Hamilton, W. *Macromolecules* **1992**, *25*, 434.
43. Fytas, G.; Anastasiadis, S. H.; Seghrouchni, R.; Vlassopoulos, D.; Li, J.; Factor, B. J.; Theobald, W.; Toprakcioglu, C. *Science* **1996**, *274*, 2041.
44. Stöhr, T.; Rühle, J. *Macromolecules* **2000**, *33*, 4501.
45. Koutsos, V.; van der Vegte, E. W.; Hadziioannou, G. *Macromolecules* **1999**, *32*, 1233.
46. Tran, Y. Auroy, P. *J. Am. Chem. Soc.* **2001**, *123*, 3644.
47. Yoshikawa, S.; Tsubokawa, N. *Polym. J.* **1996**, *28*, 317.
48. Prucker, O.; Naumann, C. A.; Rühle, J.; Knoll, W.; Frank, C. W. *J. Am. Chem. Soc.* **1999**, *121*, 8766.
49. Minko, S.; Patil, S.; Datsyuk, V.; Simon, F.; Eichhorn, K.-J.; Motornov, M.; Usov, D.; Tokarev, I.; Stamm, M. *Langmuir* **2002**, *18*, 289.
50. Huang, H.; Penn, L. S.; Quirk, R. P.; Cheong, T. H. *Macromolecules* **2004**, *37*, 516.
51. Wasserman, S. R.; Tao, Y.-T.; Whitesides, G. M. *Langmuir* **1989**, *5*, 1074.
52. Biesalski, M.; Johannsmann, D.; Rühle, J. *J. Chem. Phys.* **2004**, *120*, 8807.
53. Feng, J.; Haasch, R. T.; Dyer, D. J. *Macromolecules* **2004**, *37*, 9525.

54. Juang, A.; Scherman, O. A.; Grubbs, R. H.; Lewis, N. S. *Langmuir* **2001**, *17*, 1321.
55. Detrembleur, C.; Jérôme, C.; Claes, M.; Louette, P.; Jérôme, R. *Angew. Chem., Int. Ed. Engl.* **2001**, *40*, 1268.
56. Liu, X.; Guo, S.; Mirkin, C. A. *Angew. Chem., Int. Ed. Engl.* **2003**, *42*, 4785.
57. Moon, J. H.; Swager, T. M. *Macromolecules* **2002**, *35*, 6086.
58. Harada, Y.; Girolami, G. S.; Nuzzo, R. G. *Langmuir* **2003**, *19*, 5104.
59. Zhou, Q.; Fan, X.; Xia, C.; Mays, J.; Advincula, R. *Chem. Mater.* **2001**, *13*, 2465.
60. Advincula, R.; Zhou, Q.; Park, M.; Wang, S.; Mays, J.; Sakellariou, G.; Pispas, S.; Hadjichristidis, N. *Langmuir* **2002**, *18*, 8672.
61. Quirk, R. P.; Mathers, R. T.; Cregger, T.; Foster, M. D. *Macromolecules* **2002**, *35*, 9964.
62. Baum, M.; Brittain, W. J. *Macromolecules* **2002**, *35*, 610.
63. Zhai, G.; Yu, W. H.; Kang, E. T.; Neoh, K. G.; Huang, C. C.; Liaw, D. J. *Ind. Eng. Chem. Res.* **2004**, *43*, 1673.
64. Andruzzi, L.; Hexemer, A.; Li, X.; Ober, C. K.; Kramer, E. J.; Galli, G.; Chiellini, E.; Fischer, D. A. *Langmuir* **2004**, *20*, 10498.
65. Zhao, B.; Haasch, R. T.; MacLaren, S. *J. Am. Chem. Soc.* **2004**, *126*, 6124.
66. Zhao, B.; Brittain, W. J.; Zhou, W.; Cheng, S. Z. D. *Macromolecules* **2000**, *33*, 8821.
67. Zhao, B.; Brittain, W. J. *Macromolecules* **2000**, *33*, 8813.
68. Sedjo, R. A.; Mirous, B. K.; Brittain, W. J. *Macromolecules* **2000**, *33*, 1492.
69. Kato, M.; Kamigaito, M.; Sawamoto, M.; Higashimura, T. *Macromolecules* **1995**, *28*, 1721.
70. Wang, J.-S.; Matyjaszewski, K. *J. Am. Chem. Soc.* **1995**, *117*, 5614.
71. Wang, J.-S.; Matyjaszewski, K. *Macromolecules* **1995**, *28*, 7901.
72. Curran, D. P. *Synthesis* **1988**, 489.

73. Patten, T. E.; Matyjaszewski, K. *Acc. Chem. Res.* **1999**, *32*, 895.
74. Beers, K. L.; Boo, S.; Gaynor, S. G.; Matyjaszewski, K. *Macromolecules* **1999**, *32*, 5772.
75. Robinson, K. L.; Khan, M. A.; de Paz Banez, M. V.; Wang, X. S.; Armes, S. P. *Macromolecules* **2001**, *34*, 3155.
76. Zhang, X.; Xia, J.; Matyjaszewski, K. *Macromolecules* **1998**, *31*, 5167.
77. Krishnan, R.; Srinivasan, K. S. V. *Macromolecules* **2003**, *36*, 1769.
78. Osborne, V. L.; Jones, D. M.; Huck, W. T. S. *Chem. Commun.* **2002**, 1838.
79. Ashford, E. J.; Naldi, V.; O'Dell, R.; Billingham, N. C.; Armes, S. P. *Chem. Commun.* **1999**, 1285.
80. Huang, W.; Kim, J.-B.; Bruening, M. L.; Baker, G. L. *Macromolecules* **2002**, *35*, 1175.
81. Matyjaszewski, K.; Shipp, D. A.; Wang, J.-L.; Grimaud, T.; Patten, T. E. *Macromolecules* **1998**, *31*, 6836.
82. Xia, J.; Matyjaszewski, K. *Macromolecules* **1997**, *30*, 7697.
83. Xia, J.; Gaynor, S. G.; Matyjaszewski, K. *Macromolecules* **1998**, *31*, 5958.
84. Xia, J.; Zhang, X.; Matyjaszewski, K. *Macromolecules* **1999**, *32*, 3531.
85. Matyjaszewski, K.; Patten, T. E.; Xia, J. *J. Am. Chem. Soc.* **1997**, *119*, 674.
86. Haddleton, D. M.; Crossman, M. C.; Dana, B. H.; Duncalf, D. J.; Heming, A. M.; Kukulj, D.; Shooter, A. J. *Macromolecules* **1999**, *32*, 2110.
87. Perrier, S.; Berthier, D.; Willoughby, I.; Batt-Coutrot, D.; Haddleton, D. M. *Macromolecules* **2002**, *35*, 2941.
88. Jin, X.; Shen, Y.; Zhu, S. *Macromol. Mater. Eng.* **2003**, *288*, 925.
89. Husseman, M.; Malmstrom, E. E.; McNamara, M.; Mate, M.; Mecerreyes, D.; Benoit, D. G.; Hedrick, J. L.; Mansky, P.; Huang, E.; Russell, T. P.; Hawker, C. J. *Macromolecules* **1999**, *32*, 1424.
90. Paul, R.; Schmidt, R.; Feng, J.; Dyer, D. J. *J. Polym. Sci., Part A: Polym. Chem.* **2002**, *40*, 3284.

91. Matyjaszewski, K.; Miller, P. J.; Shukla, N.; Immaraporn, B.; Gelman, A.; Luokala, B. B.; Siclovan, T. M.; Kickelbick, G.; Vallant, T.; Hoffmann, H.; Pakula, T. *Macromolecules* **1999**, *32*, 8716.
92. Jeyaprakash, J. D.; Samuel, S.; Dhamodharan, R.; Rhe, J. *Macromol. Rapid Commun.* **2002**, *23*, 277.
93. Keller, R. N.; Wycoff, H. D. *Inorg. Synth.* **1946**, *2*, 1.
94. Ciampolini, M.; Nardi, N. *Inorg. Chem.* **1966**, *5*, 41.
95. *Polymer Handbook*, 4<sup>th</sup> ed.; Brandrup, J.; Immergut, E. H.; Grulke, E. A., Eds.; Wiley & Sons: New York, 1999.
96. Yu, W. H.; Kang, E. T.; Neoh, K. G. *Langmuir* **2004**, *20*, 8294.
97. Yu, W. H.; Kang, E. T.; Neoh, K. G.; Zhu, S. *J. Phys. Chem. B* **2003**, *107*, 10198.
98. Edmondson, S.; Huck, W. T. S. *J. Mater. Chem.* **2004**, *14*, 730.
99. Boyes, S. G.; Akgun, B.; Brittain, W. J.; Foster, M. D. *Macromolecules* **2003**, *36*, 9539.
100. Boyes, S. G.; Brittain, W. J.; Weng, X.; Cheng, S. Z. D. *Macromolecules* **2002**, *35*, 4960.
101. Ulman, A. *An Introduction to Ultrathin Organic Films from Langmuir-Blodgett to Self-Assembly*; Academic Press: Boston, 1991.
102. Kong, X.; Kawai, T.; Abe, J.; Iyoda, T. *Macromolecules* **2001**, *34*, 1837.
103. Fadeev, A. Y.; McCarthy, T. J. *Langmuir* **2000**, *16*, 7268.
104. Zhang, X.; Matyjaszewski, K. *Macromolecules* **1999**, *32*, 1763.
105. Lu, S.; Fan, Q.-L.; Chua, S.-J. *Macromolecules* **2003**, *36*, 304.
106. Lee, S. B.; Koepsel, R. R.; Morley, S. W.; Matyjaszewski, K.; Sun, Y.; Russell, A. *J. Biomacromolecules* **2004**, *5*, 877.
107. Huang, W.; Kim, J.-B.; Baker, G. L.; Bruening, M. L. *Nanotechnology* **2003**, *14*, 1075.
108. Zeng, F.; Shen, Y.; Zhu, S.; Pelton, R. *Macromolecules* **2000**, *33*, 1628.
109. Zheng, G.; Stver, H. D. H. *Macromolecules* **2003**, *36*, 1808.

110. Zeng, F.; Shen, Y.; Zhu, S.; Pelton, R. *J. Polym. Sci., Part A: Polym. Chem.* **2000**, *38*, 3821.
111. Lee, S. B.; Russell, A. J.; Matyjaszewski, K. *Biomacromolecules* **2003**, *4*, 1386.
112. Kim, D. J.; Lee, K.-B.; Chi, Y. S.; Kim, W.-J.; Paik, H.-J.; Choi, I. S. *Langmuir* **2004**, *20*, 7904.
113. Bories-Azeau, X.; Armes, S. P. *Macromolecules* **2002**, *35*, 10241.
114. Colthup, N. B.; Daly, L. H.; Wiberley, S. E. *Introduction to Infrared and Raman Spectroscopy*; Academic Press: New York, 1990.
115. Kim, J.-B.; Huang, W.; Bruening, M. L.; Baker, G. L. *Macromolecules* **2002**, *35*, 5410.
116. Lemieux, M.; Minko, S.; Usov, D.; Stamm, M.; Tsukruk, V. V. *Langmuir* **2003**, *19*, 6126.
117. Prucker, O.; Christian, S.; Bock, H.; Ruhe, J.; Frank, C. W.; Knoll, W. *Macromol. Chem. Phys.* **1998**, *199*, 1435.
118. Tate, R. S.; Fryer, D. S.; Pasqualini, S.; Montague, M. F.; de Pablo, J. J.; Nealey, P. F. *J. Chem. Phys.* **2001**, *115*, 9982.
119. Butun, V.; Billingham, N. C.; Armes, S. P. *J. Am. Chem. Soc.* **1998**, *120*, 12135.
120. Butun, V.; Lowe, A. B.; Billingham, N. C.; Armes, S. P. *J. Am. Chem. Soc.* **1999**, *121*, 4288.
121. Butun, V.; Wang, X. S.; de Paz Bañez, M. V.; Robinson, K. L.; Billingham, N. C.; Armes, S. P. *Macromolecules* **2000**, *33*, 1.
122. Liu, S.; Weaver, J. V. M.; Tang, Y.; Billingham, N. C.; Armes, S. P.; Tribe, K. *Macromolecules* **2002**, *35*, 6121.
123. Zhang, Z.; Liu, G.; Bell, S. *Macromolecules* **2000**, *33*, 7877.
124. Zeng, F.; Shen, Y.; Zhu, S. *Macromol. Rapid Commun.* **2002**, *23*, 1113.
125. Miller, M. D.; Baker, G. L.; Bruening, M. L. *J. Chromatogr., A* **2004**, *1044*, 323.
126. Ishizu, K.; Satoh, J.; Sogabe, A. *J. Colloid Interface Sci.* **2004**, *274*, 472.
127. Jones, D. M.; Huck, W. T. S. *Adv. Mater.* **2001**, *13*, 1256.

128. Brantley, E. L.; Jennings, G. K. *Macromolecules* **2004**, *37*, 1476.
129. Edmondson, S.; Huck, W. T. S. *Adv. Mater.* **2004**, *16*, 1327.
130. Krishnan, R.; Srinivasan, K. S. V. *Macromolecules* **2004**, *37*, 3622.

APPENDIX

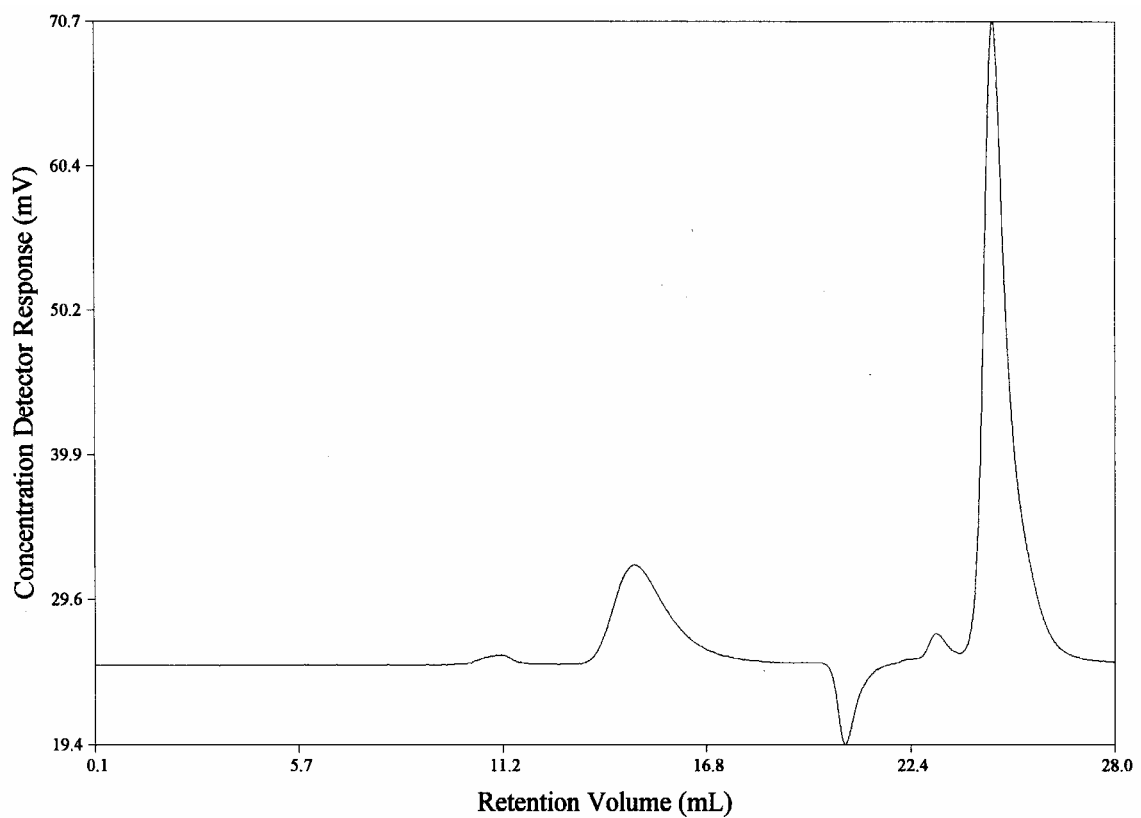


Figure A1. GPC Chromatogram of PDMAEMA Synthesized Using the CuBr Catalyst System

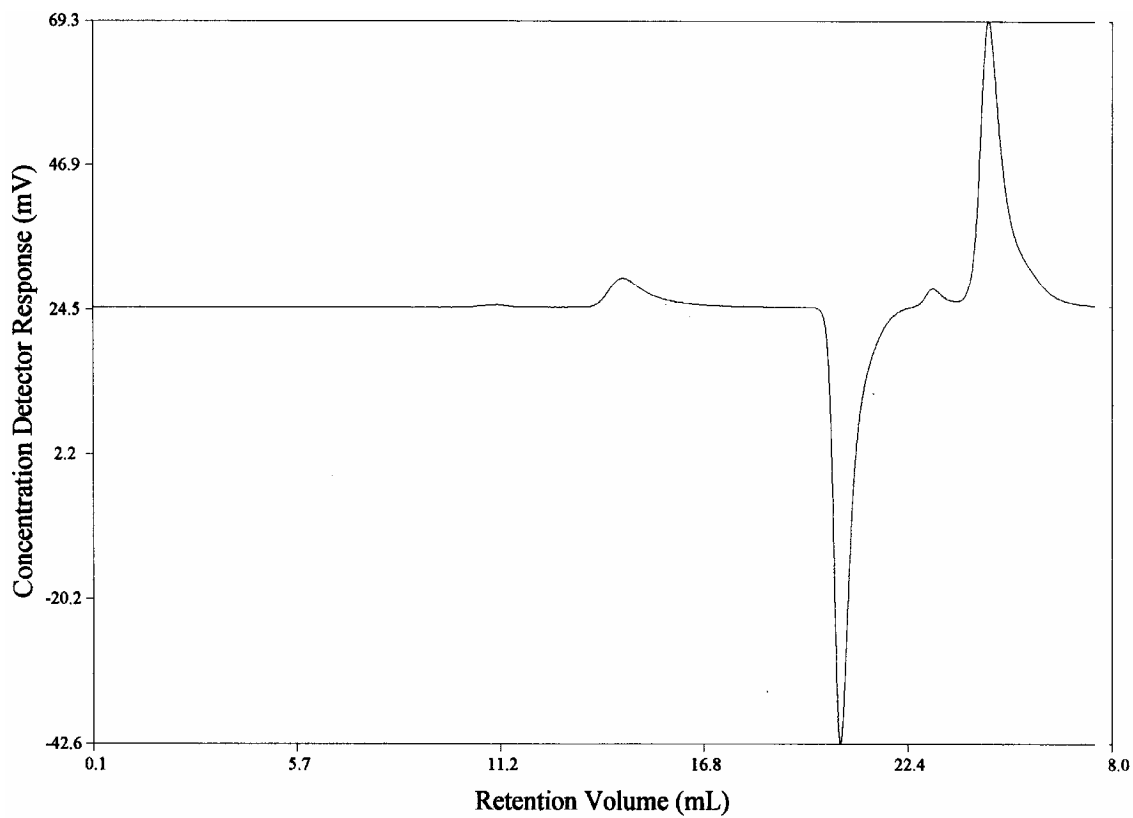


Figure A2. GPC Chromatogram of PDMAEMA Synthesized Using the CuCl/CuCl<sub>2</sub> Catalyst System

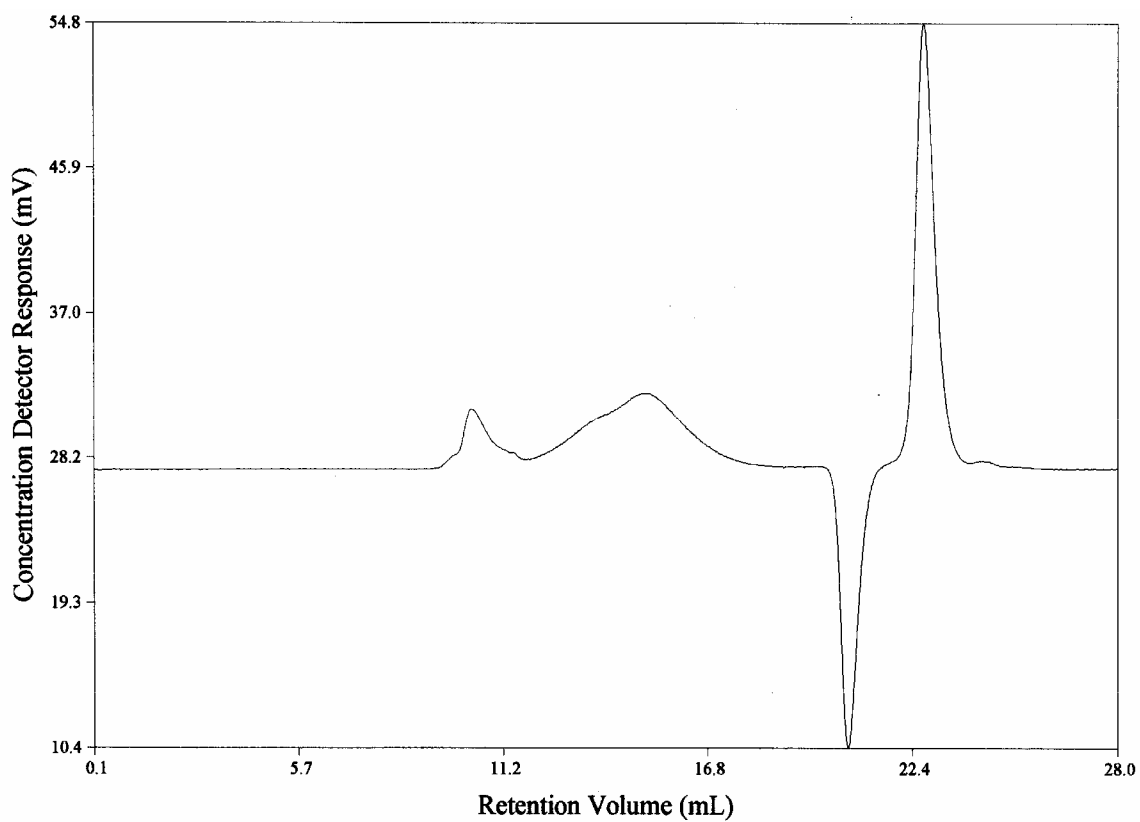


Figure A3. GPC Chromatogram of PDMAEA

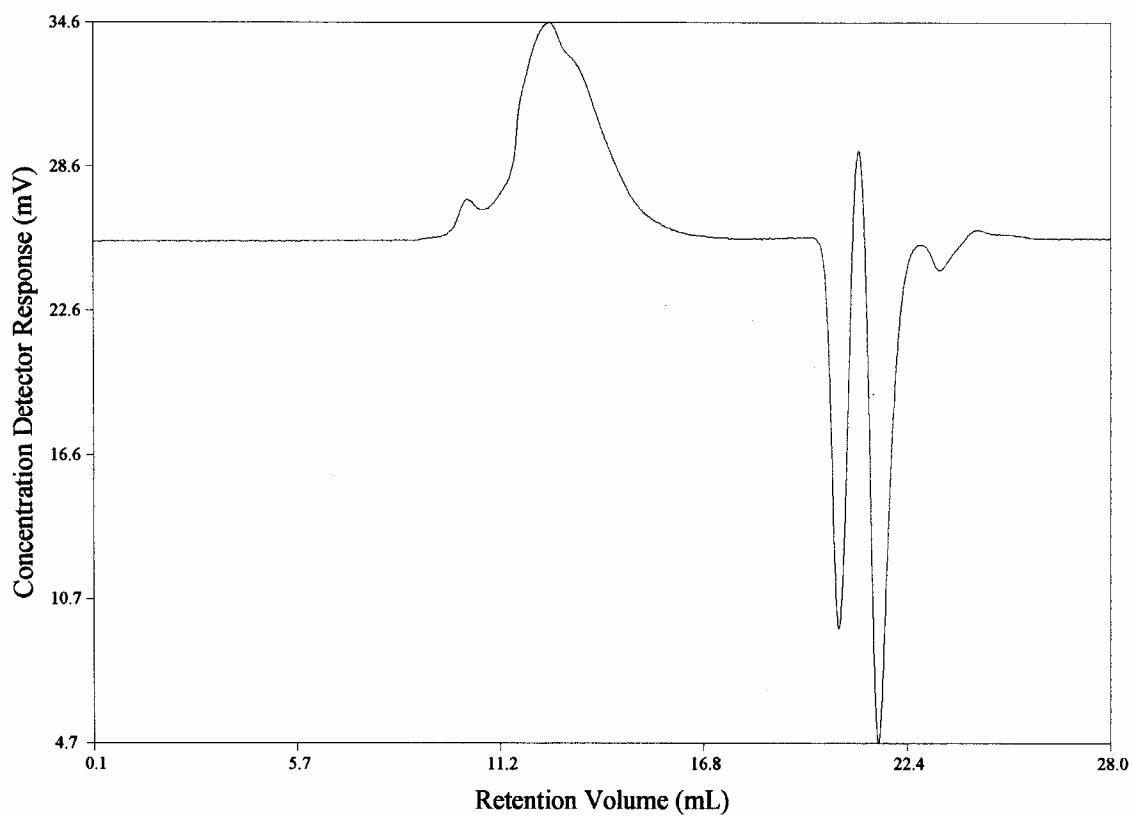


Figure A4. GPC Chromatogram of PHEMA Synthesized Using the CuCl Catalyst System

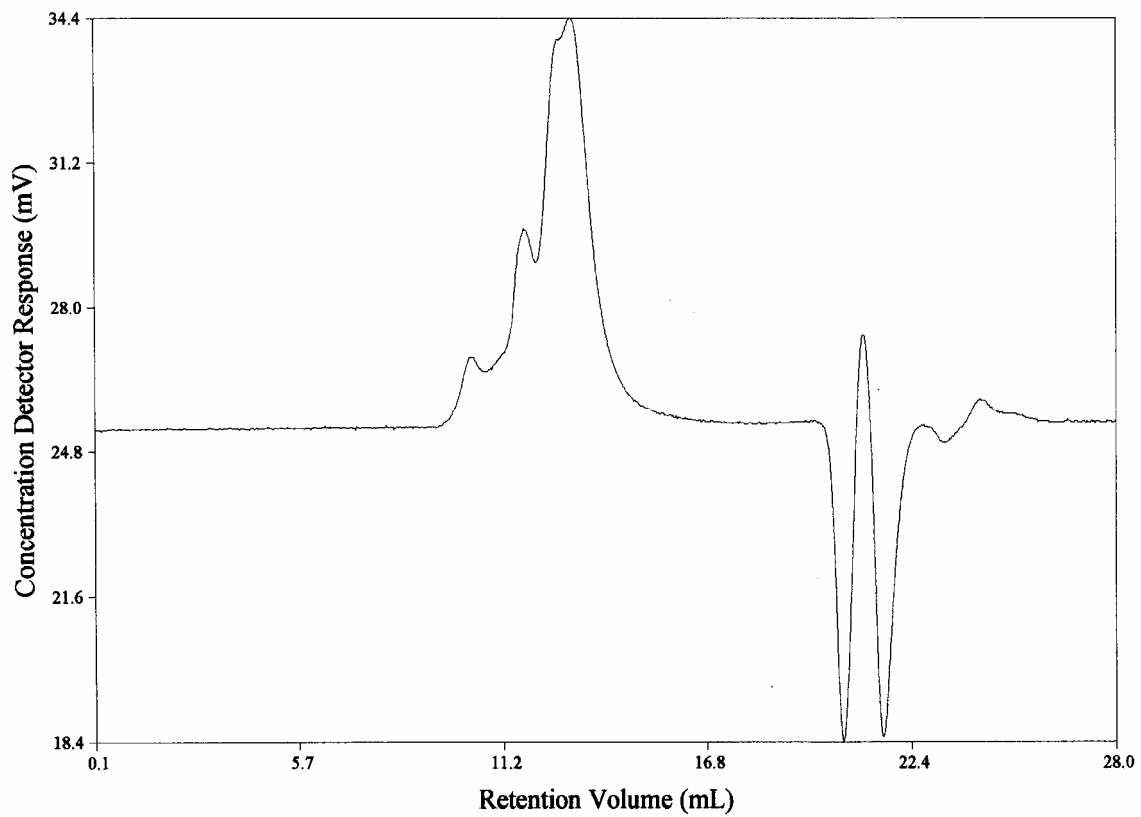


Figure A5. GPC Chromatogram of PHEMA Synthesized Using the CuCl/CuCl<sub>2</sub> Catalyst System